GEOLOGICAL SURVEY OF CANADA

OPEN FILE 1179

CASE FORTRAN IV INTERACTIVE COMPUTER PROGRAM FOR CORRELATION AND SCALING IN TIME OF BIOSTRATIGRAPHIC EVENTS

F.P. Agterberg

J. Oliver

S.N. Lew

F.M. Gradstein

M.A. Williamson

Canada

1988

CASC FORTRAN IV INTERACTIVE COMPUTER PROGRAM FOR CORRELATION AND SCALING IN TIME OF BIOSTRATIGRAPHIC EVENTS*

F.P. Agterberg – Geological Survey of Canada, 601 Booth Street, Ottawa, Ontario K1A 0E8

J. Oliver – Computer Science Department, University of Ottawa, Ottawa, Ontario K1N 6N5

S.N. Lew – Geological Survey of Canada, 601 Booth Street, Ottawa, Ontario K1A 0E8

F.M. Gradstein – Atlantic Geoscience Centre, Bedford Institute of Oceanography, Dartmouth, Nova Scotia B2Y 4A2

M.A. Williamson – Department of Geology, Dalhousie University, Halifax, Nova Scotia B3H 4H6

CONTENTS

CASC FORTRAN IV INTERACTIVE COMPUTER PROGRAM FOR CORRELATION AND SCALING IN TIME OF BIOSTRATIGRAPHIC EVENTS

F.P. Agterberg, J. Oliver, S.N. Lew,
F.M. Gradstein and M.A. Williamson

ABSTRACT

This report provides documentation of the CASC computer program for Correlation And SCaling in time of stratigraphic events. The CASC source code in Fortran IV is provided on a 5¼ inch double sided, double density diskette for reading on an IBM Personal Computer. A data base for Cenozoic foraminiferal stratigraphic events in 24 wells on the Labrador Shelf and Grand Banks is provided on a second diskette together with a Fortran IV version of the RASC computer program for ranking and scaling of stratigraphic events which is needed to generate the complete CASC input.

CASC consists of three parts: (1) Optimum Sequence CASC; (2) Distance CASC; and (3) Multiwell Comparison. Options (1) and (2) use RASC ranking and scaling results respectively, to estimate probable locations of stratigraphic events or isochrons in wells. Results for up to five wells can be shown simultaneously by using Option (3) together with error bars to express the uncertainty in these probable locations.

INTRODUCTION

During the past seven years we have developed several statistical models for the ranking and scaling of biostratigraphic events. This work was largely performed under the auspices of Project 148 (Quantitative Stratigraphic Correlation Techniques) of the International Geological Correlation Programme which will be completed in December, 1985. The resulting computer algorithms: (1) rank fossil events in wells or outcrop sections to arrive at the average sequence in time, (2) scale the average sequence along a relative time scale, (3) test the stratigraphic normality of the individual (well) sequences, and (4) allow participation of rare index fossil events or of a marker horizon occurrence in the scaled optimum sequence. The algorithms for the RASC computer program for RAnking and SCaling were originally written in FORTRAN IV (Agterberg and Nel, 1982a, b). This program also prints the fossil name dictionary and a regional occurrence table of the events. Heller et al. (1983) have published a detailed Syllabus which accompanied a magnetic tape containing the RASC program in Fortran IV with input and output examples. More recently, this computer program was modified and a revised Syllabus accompanying Fortran 77 version of revised RASC will be released in the near future.

The RASC program was originally used to erect the Cenozoic foraminiferal stratigraphy of the Canadian Atlantic Margin (Gradstein and Agterberg, 1982). Detailed theoretical and practical reviews of the method including applications of RASC to 9 data bases constructed by participants in IGCP Project 148 have been documented in the book by Gradstein et al. (in press). The Gradstein-Thomas data for Cenozoic foraminifera on the Labrador Shelf and Grand Banks listed in Appendix I of Gradstein et al. (in press) are used as examples in this report which deals with the CASC program for Correlation And SCaling in time of biostratigraphic events.

The construction of CASC began in 1982, the objective being the development of a system of interactive computer programs to achieve quantitative stratigraphic correlation of sections using the RASC biozonations. Initial methodology and results from this project were described in Agterberg and Gradstein (1983). Recent applications of CASC have been described in Gradstein et al. (in press) and Williamson (in press). The CASC methodology has also been explained elsewhere (Agterberg, in press; Agterberg and Gradstein, in press). CASC operates on RASC output augmented by a file containing the depths of the events as well as an age link file containing the ages of a subgroup of events. For this reason, the CASC source code provided here on diskette is accompanied by a Fortran IV version of revised RASC called RASC-C to generate the complete CASC input.

This report, which is intended for computer programmers as well as users of the program, is organized as follows. First, the RASC method is briefly reviewed and CASC is introduced in comparison with the Shaw (1964) method for stratigraphic correlation of sections or wells. Next, the CASC procedures are presented in a generalized way with selected examples. This section is followed by one on geological applications. A discussion of actual CASC outputs (hard copy for displays on Tektronix screen, see Appendix 2) is given in the next section for the purpose of (a) illustrating how results in previous sections were obtained, and (b) introducing the new options for assigning cluster codes to events and introduction of an unconformity in the sections. Work on the latter two options was completed only recently and these were not available in the versions of CASC used for stratigraphic research during the past two years. In the Appendix the user is also presented with an overview of the options available during an interactive CASC session and brief documentation of all subroutines in CASC is provided to facilitate implementation by computer programmers.

RANKING AND SCALING OF STRATIGRAPHIC EVENTS

In general, the microfossil record obtained from exploratory wells drilled to find hydrocarbons in frontier regions is poor in quality for several reasons. The distances between these wells tend to be large so that facies changes, hiatuses and unconformities can not be studied in detail. Zones of reworking may also be hard to establish due to the isolation of the wells. In most of our applications, the sampling method consisted of obtaining cuttings during drilling and this method is susceptible to cavings. Only the stratigraphically highest occurrences (or 'exits') of the fossil taxa studied can be used for correlation; lowest occurrences (or 'entries') and co-occurrences of fossil species can not be studied because of contamination due to the cavings. In general, the paleontological record is incomplete and taxonomical identification problems are common. The stratigraphically highest occurrences of the taxa show numerous inconsistencies when correlation between wells is attempted. For example, if taxa A and B are observed to coexist in n wells, the exit of A may be seen to occur f_a times above that of B and the exit of B $(n-f_a)$ times above that of A. The relative frequency $P = f_a/n$ can be used as a measure of the inconsistency.

In order to cope with these inconsistencies, Gradstein and Agterberg (1982) developed the RASC method of ranking and scaling. The ranking of the exits consists of determining their optimum sequence. The scaling consists of estimating intervals between successive events in the optimum sequence along a scale based on the relative frequencies (P). These two methods will be briefly reviewed in this section based on a practical example. They result in a quantitative definition of assemblage zones for exits which can be used for correlation.

Although the RASC/CASC method was originally developed for dealing with noisy data consisting of exits only, other data sets, e.g. with entries as well as exits, or with other types of fossil abundance measures (cf. Doeven et al., 1983), can be subjected to it.

The RASC method is illustrated here by means of a simple example from Hay (1972). Figure 1a shows a highest occurrence (HO) and nine lowest occurrences (LO) of Eocene calcareous nannofossils in nine sections from the California Coast Range. The number of levels per sections varies from 2 (section B) to 8 (section E). The names of the 10 biostratigraphic events are shown in Figure 1b. On the lowest level of section A, there are 6 coeval events. Proceeding from left to right in Figure 1a, these are labelled 1 to 6 in Figure 1c. Moving stratigraphically upwards, three other events were observed in A, each on a separate level; these are labelled 7 to 9 in Figure 1c. The triangle Δ which does not occur in A is represented by the number 10. In Figure 1c, the events 1 to 10 have been coded as input for the RASC computer program. Coeval events are preceded by a hyphen or minus sign.

The following method of sequencing the 10 events in this example was proposed by Hay in 1972, before a computer program was available. First a preliminary ranking was carried out with the result shown in column 1 on the right-hand side of Figure 1a. Next, each event was compared with all other events by counting how often it occurred (a) above and (b) below the other events. These counts or frequencies are called f_a and f_b. The positions of events were then changed until the "optimum sequence" of column 2 was found. The positions of the events in column 2 are such that $f_a \geq f_b$ for each event in comparison with all other events. Thus an event that falls below any other event in the optimum sequence never was observed to occur more frequently above the other event in the sections that could be used for comparison. This method was programmed by Agterberg and Nel (1982a) for a digital computer. The optimum sequence obtained by means of the RASC program for the information in Figure 1a is shown in Figure 1d. If $f_a = f_b$ for a pair of successive events in Figure 1d, the events belonging to this pair do not occupy distinct positions in the optimum sequence. Their order as it results from the computer program is then arbitrary. Such uncertainty is shown in Figure 1d by means of a statistical range. For example, the events in positions 1 and 2 both range from 0 to 3. This means that they could occur anywhere between positions 0 (above 1) and 3. These events (10 and 9) are coeval on average. Going back to Figure 1a, it can be seen that Δ and W occur together in 6 sections, each three times above the other.

Other applications of the RASC program have shown that a unique solution to the problem of finding the optimum sequence with $f_a \geq f_b$ for each event compared to all others normally does not exist because of cyclical inconsistencies in the data base involving 3 or more events. For example, if in pairwise comparison an event 1

occurs more frequently above another event 2, 2 above event 3, and 3 above 1, an optimum sequence cannot be obtained without modifications of the preceding method. The method (called 'modified Hay method') used for the RASC program is based on graph theory and provides a solution in situations of this type too.

Agterberg and Nel (1982a) introduced another ranking algorithm (called 'presorting option') to precede the modified Hay method. Harper (1984) has shown that situations exist in which presorting applied on its own produces better results than the modified Hay method without presorting. For this reason, the presorting option, which resembles a method proposed by Rubel (1978, Table 1, p. 244), is now routinely used by us, whether or not it is followed by the modified Hay method. For some data sets the number of cyclical inconsistencies is so large that only the presorting method can be used. The relative position of an event in an optimum sequence is an average of all relative positions encountered. In practice, this may mean that ranges on range charts constructed from an optimum sequence are shorter than those constructed by other methods using stratigraphically highest and lowest occurrences of fossil species.

An example of optimum clustering which may lead to the definition of biostratigraphic assemblage-zones for events (HO and LO) is shown in Figure 1e. (A biostratigraphic assemblage-zone is a body of strata whose content of fossils constitutes a natural association that distinguishes it from adjacent strata). In Figure 1a, the events in the lower parts of the sections are more frequently coeval and show more inconsistencies than those in the upper parts. The cross-over frequency $P = f_a/(f_a + f_b)$ can be computed for each pair of events. Coeval events may be scored as 0.5 toward both f_a and f_b. Note that the cross-over frequency of Δ and W in Figure 1a satisfies $P = 0.5$. By using the Gaussian distribution function, cross-over frequencies can be transformed into "distances" D which can be plotted along a linear scale. For example, if $P = 0.5$, $D = 0$, or if $P = 0.95$, $D = 1.645$. All possible pairwise comparisons can be made and the frequencies weighted according to sample size. Estimates of average distances between successive events obtained by means of the RASC program are shown in Figure 1e. For example, the distance D between events 9 and 10 amounts of 0.4354. Because all possible pairwise comparisons were considered, this distance differs from $D = 0$ resulting from the direct comparison ($f_a = f_b$, see before). The distances in Figure 1e were plotted in the horizontal direction and connected to each other as is commonly done in biometric cluster analysis. Events 1 to 7 cluster relatively strongly while 8 to 10 tend to occur above the others. Clearly, the dendrogram of Figure 1e provides more information than the optimum sequence of Figure 1d. In large-scale applications, the RASC computer program has produced range charts and assemblage zonations which are much more practical to use for geological correlation and superseded micropaleontological resolution previously available.

The scaling algorithms were originally published in Agterberg and Nel (1982b). Figures 1b and 1c show actual RASC input and Figures 1d and 1e RASC output plotted by using a program of Jackson et al. (1984). The transformation from P to D introduced in the preceding paragraph can be written in the form $D = z = \Phi^{-1}(P)$ where $\Phi(z) = P$ represents the fractile (cumulative frequency) of the normal distribution in standard form with ordinate $\pi(z) = (2\pi)^{-\frac{1}{2}}\exp(-z^2/2)$. It can be shown that this is equivalent to assuming that, along the distance scale, the events are normally distributed with variance σ^2 equal to 0.5. The corresponding standard deviation σ satisfies $\sigma = 1/\sqrt{2}$.

The scaling method of RASC results in estimates of distances between successive events. This is equivalent to positioning all events along a relative time scale, measuring them from a common origin. The latter can be chosen at the position of the first exit (e.g., No. 9 in Figure 1e). For isochron construction, the RASC-scale must be transformed into a linear, numerical time scale. Normally, the approximate age is known for only a small fraction of all events used in a study. In our application to Cenozoic foraminifera, dates for 22 exits are used to establish a relationship between RASC distance and age.

Three threshold parameters (k_c, m_{c1} and m_{c2}) have to be chosen at the beginning of a run with the RASC program for ranking and scaling of stratigraphic events. The first parameter (k_c) determines that the events to be considered, all occur in at least k_c wells or sections. The second parameter (m_{c1}) determines that pairs of events compared with one another, all occur in at least m_{c1} wells before the modified Hay method of ranking is applied. Finally, the third parameter (m_{c2}) determines that pairs of events compared with one another occur in at least m_{c2} wells before scaling is performed. Many of the examples in this report are for Cenozoic foraminifera in 24 wells on the Labrador Shelf and Grand Banks with the following threshold parameters $k_c = 5$, $m_{c1} = 2$, and $m_{c2} = 3$. This will be referred to as a 5-2-3 RASC run.

PRINCIPLE OF CORRELATION AND SCALING IN TIME AND COMPARISON WITH COMPOSITE STANDARD METHOD

This section describes the theory and application in geological basin analysis of CASC for Correlation and SCaling in time. The CASC method of quantitative correlation draws on the RASC method and on the philosophical reviews and statistical methodology of several geologists and (geo)mathematicians, for example: Shaw (1964), Hay (1972), Drooger (1974), Blank (1979), Reinsch (1967) and De Boor (1978). The method provides a precise, semi-automated and semi-objective means of correlation of rock sections for which an optimum sequence or a scaled optimum sequence of biostratigraphic events have been determined using the zonation method and computer program RASC. This section as well as the next two sections ('Generalized Description of CASC Method', and 'Geological Applications of CASC') consist of material modified from Gradstein et al. (in press).

The use of RASC and CASC provides the stratigrapher with an integrated biostratigraphic method, particularly suitable for exploiting the considerable amount of micropaleontological data that accumulates during sedimentary basin analysis. The method starts with a data file of the original observations on the distribution in time and in space in wells or outcrop sections of all taxa identified. Next, it will reduce this data file to biozonations that best explain the regional and temporal trends. Finally, it will calculate geologically reasonable correlations of the sections. Segmentation and correlation of the original sections can be achieved by means of fossil events and RASC biozones. Interpolation of the scaled optimum sequence in linear time makes it feasible to correlate isochrons also. Each correlation line carries an uncertainty limit, which is a conservative estimate of various original uncertainties in the data.

Correlation is one of the most widespread, abstract undertakings of the mind and refers to causal linkage of present or past processes and events. Such events

can be inorganic, organic or abstract. Correlation of geological attributes generally expresses the hypothesis that a mutual relation exists between stratigraphic units. In a more narrow stratigraphic sense it means that samples (or imaginary samples) from two separate rock sections occupy the same level in the known sequence of stratigraphic events. Without correlation, successions of strata or events in time derived in one area, are unique and contribute nothing to understanding the earth history elsewhere (McLaren, 1978).

Geological correlation traditionally is expressed in terms of:

1. rock units, like formations or well log intervals = lithostratigraphic correlation;
2. fossil units, like zones = biostratigraphic correlation.
3. relative age units or stages = chronostratigraphic correlation;
4. linear time units or ages = geochronologic correlation.

Instead of units with a certain thickness or a duration in time, it is events that are frequently correlated. Events or datum planes refer to the fossilized physical or organic occurrences of supposedly irreducible resolution along the geological scale.

An important contention of geological correlation is that once the events or rock-, fossil-, or relative age units have been properly determined and defined, these units can indeed be used for correlation. This statement, which might seem to be trivial and redundant, is made here because existing stratigraphic codes show how to define stratigraphic units, but they do not define how to correlate them. The latter is the subjective domain of experts. Procedures for correlation or stratigraphic equivalence depend on subjective judgement of the unique relationship of each individual record to the derived and accepted standard.

It follows that correlation as practised in geology cannot be readily verified without a detailed review of all the underlying facts. It also follows that traditionally there is no expression of the uncertainty in fixation of the individual record to the standard. Or, as Riedel (1981) wryly wrote: "Biostratigraphy will be continued to be regarded as an art rather than a science, until it is possible to attach confidence limits to suggested correlations". An improvement in definition of the zonation through increased numbers of observations and taxa may increase the number of correlation tiepoints, but still leaves the question of uncertainty unanswered. Such an uncertainty will generally be couched in qualitative terms only. For many geological investigations such a subjective procedure yields satisfactory results, correlation being only a part of the scientific objectives. Situations do arise, however, where the quality of correlations determines the outcome of the study. This is particularly true in the field of operational biostratigraphy, where large and complex data sets may have to be reduced before they can be of assistance in deciphering basin history.

Let us assume that the stratigraphic distributions of hundreds of fossils have been sampled in dozens of cored wells or outcrop sections. Following a detailed analysis, which lasted many months or even several years, a range chart is proposed. The range of each fossil taxon divides geological time into three segments by its entry (first occurrence) and exit (last occurrence). The range chart synthesizes the information on all observed ranges to arrive at average or total (maximum) ranges for each species. The range chart is then segmented, using co-existence of taxa and discrete taxon events, to establish time-successive intervals. Each segment is called a zone. When only last occurrences of fossils are known, such a chart portrays a succession of events or partial ranges.

The critical and least understood step in the practice of correlation is to actually tie the zones back to the individual (well) sections. This may be a difficult undertaking when the individual stratigraphic record shows frequent inconsistencies, due to sampling problems, reworking, unfilled ranges due to facies changes, and other problems (cf. Gradstein et al., in press).

Ideally, the individual fossil record as observed in each rock section, should be normalized prior to actual correlation. By doing this insight should be gained in the probability that the observed events occur where the standard suggests they should be found. In our hypothetical example, the paleontologist will make a judgement on the outliers, of events to be rejected or moved up and down the section. Such normalization is based upon geological or paleontological experience. Next, the paleontologist will in each rock section, define the successive zones in such a manner that a minimum number of (key) taxa for each of the zones are observed outside the zonal limit. Mismatch of the zones and the individual record is explained by poor data or unfilled ranges due to facies changes.

The problem with the hypothetical case history is not so much that it leads to right or wrong stratigraphy, but that a single solution is proposed. What is a reasonable criterion for successful correlation, if there is no insight into the actual uncertainty in correlation, either in millions of years or in depth in meters? In the regional correlations there frequently is limited or no understanding of how much (in depth or in relative time units) the solution differs from alternate solutions, using the same data. In all likelihood it is difficult to propose or compare two alternative correlations, without a major review or analysis of all underlying facts.

Biostratigraphic correlation depends on the probability that:

(a) in each rock section the events defining a biostratigraphic increment have been detected and properly taxonomically determined; and

(b) the true (or natural) sequence of events is known.

This principle was succinctly stated by Hay (1972), who then went on to propose the principle of matrix permutation for construction of the most likely sequence of (nannofossil) events in time, (see previous section). In the ranked sequence each event position is an average of all the relative positions, but no direct insight is available into the uncertainty of rank.

As early as 1964, Shaw not only proposed a simple ranking method for biostratigraphic events, but also a method for correlating the sections in which the events occur. The original method runs as follows: From a number of individual geological sections (A, B, C, D, etc.), one (for example A) is selected that shows a more complete and reasonable "normal" order and spacing of events. This particular sequence of entries and exits of taxa is plotted along one axis and that of a reasonable comparable sequence B along the other axis of a conventional two-axis graph. Scale units are in feet or meters, as found in each section, but in a simplified procedure, order only can be used. The best fit of the resulting scattergram is called the line of correlation. Shaw (1964) advocates regression

analysis as a linear trend-fitting technique, although A and B are probably both subject to uncertainty. There are two regression lines, one for A over B and one for B over A. Spline fitting, as now available (see later) may be more suitable, particularly if a straight-line fit is not possible due to changes in sedimentation rate.

The order and spacing of first and last occurrence events along the A-axis is now updated through projection of the homologous B-axis events, via the best fit line, on the A-axis. If the first occurrence of an event in B occurs relatively lower than in A, the range of this event in A is appropriately extended downward. If a last occurrence of an event in B occurs relatively higher than in A, the range of the event is appropriately extended upward. Attempts are generally made to maximize the stratigraphic ranges. Next, the updated A-axis (composite section) is compared to section C, etc. In the final composite section the scale of the successive events has become a composite of all spacing values between successive events.

Actual correlation of events, clusters of events, etc. are achieved by making new bivariate plots for each individual section as a function of the final composite one. For each bivariate scattergram a new best fit line or best fit channel is calculated which serves to project the composite events on the individual section scale. In a mathematical sense, each value in the composite standard can be expressed as a function of its correlative (depth) value in the individual sections. Miller (1977) provides a good description of use of the composite standard method.

One might also choose to hand-fit the scatter of points to arrive at some kind of composite standard (Shaw, 1964; Edwards, 1984), particularly so if scatter is limited. In variation of the basic technique, the best fit line of the scattergram can become the standard section, to arrive at some kind of average event positions. When a third section is added this standard section becomes one of the axes of the scattergram.

An important difference between Hay (1972) and Shaw (1964) is that the latter tries to find the highest and lowest possible occurrences in all individual records. Shaw maximizes possible stratigraphic ranges, but as a result no uncertainty limits can be attached to the range end points. In the Hay and RASC methods, average ranges are calculated, which allows an expression of sampling error. The CASC method of quantitative correlation combines average sequence methodology with bivariate correlation technique.

Input for CASC is the RASC input file that shows the original sequence of events in each of the sections. In addition, the program requires a depth file, that shows the observed depth in feet or in metres for all the events in the original sequence file.

The correlation and scaling in time (CASC) program first computes the RASC optimum sequence and RASC scaled optimum sequence of events. Using the three normality testing techniques in the RASC method, bivariate graphs, stepmodel and normality testing, outliers in the individual sections may be eliminated. Based on the filtered data file, a new optimum sequence may be calculated, after which each individual sequence of events is compared to the (scaled) optimum one, and best fit curves (splines, see later) are calculated. A spline fit yields a function such that, for each optimum sequence position, the most likely stratigraphic equivalent position can be found in the individual sequences. These normalized tiepoints are then correlated.

Figure 2 graphically depicts the principal steps, executed for the correlation of event 29 (top of **Cyclammina amplectens**) in wells Adolphus D-50 (left graph) and Flying Foam I-13 (right graph), Grand Banks. The y-axis is the optimum sequence in 21 of the wells (k_c = 7, m_{c1} = 2; see previous section). Instead of the optimum sequence, the scaled optimum sequence can be used. The x-axis is the observed sequence of events, whereas the z-axis is the common depth scale of the well.

The lower scattergram expresses mismatch of the individual sequence and the optimum one. The best fit line for the graph (here visually estimated) is the line of correlation. Working with event scales initially has the advantage that complications due to different rates of sedimentation in different places which may be hundreds of km apart are avoided. Moreover, equal spacing of values for the independent (x-axis) variable in spline-curve fitting has the considerable advantage that the possibility of unrealistic oscillations of the fitted curve between irregularly spaced control points is avoided. However, the number of levels in the event scale differs from section to section in a 'random' manner. For correlation between wells it is necessary to replace the levels of the event scales with depths (in km). This replacement is shown in the upper part of the scattergram of Figure 2. The individual sequence x is a function of the depth z at which the events were observed. This function is shown here as the 'line of observation'. The most likely position of event 29 in the Adolphus well is found by projecting its optimum position via the line of correlation to the individual sequence and from there via the line of observation to the depth scale. Thus all optimum sequence events are scaled in (well) depth. In a multiwell comparison, the most likely depth value (z-axis) in each well is calculated for selected y-axis values (event positions) in the optimum sequence.

In our example, event 29 in Flying Foam should occur at 4850' (observed 5300') and in Adolphus at 6050' (observed 6200'). These depths then are the most likely correlation tiepoints.

The standard deviation (SD) of the events relative to the line of correlation (and the line of observation) in the y direction (and parallel z direction, which is the depth-axis in the well) provides an estimate of the mismatch of each event. Further on this is called the local error. When it is geologically unreasonable to expect a continuous sedimentation rate in the vicinity of a certain depth, the local SD can be modified so that it is restricted to shorter time increments.

The same procedures as shown in Figure 2, using the RASC optimum sequence, are applied when the scaled optimum sequence is chosen instead. The interfossil distances in the scaled optimum sequence reflect the average relative distance of the events in relative time. If it is possible to estimate the numerical geological ages of some of the events in the scaled optimum sequence, the relative distance estimates can be used to stretch the scaled sequence in linear time. This way the scaled optimum sequence becomes a (local) biochronology and hence isochrons can be traced through the wells or outcrop sections. For paleontologists this is a valuable method for finding the numerical age of the most likely position of principal zone boundaries in each well. Such boundaries, as argued in Gradstein et al. (in press), can delineate sedimentary cycles. The original standard deviations for the interfossil distances in the scaled optimum sequence now reflect the uncertainty in linear time between the events. This uncertainty is named the global error bar.

As a first test of the validity and use of this numerical time interpolation for geological analysis, Figures 3 and 4 were constructed. Along the y-axis of Figure 3 are plotted the interfossil distances for the Cenozoic foraminiferal events in the scaled optimum sequence in 21 wells. For some events, listed later in the section on 'Geological Applications of CASC', which are the (regionally averaged) last occurrences of key planktonic and a few benthic foraminifera, numerical ages can be estimated. This involves comparison of the regional to standard Atlantic zonations, details of which follow later. The horizontal scale is linear time in Ma, for the Cenozoic period.

The calibrated events are used to form a nomogram or line of correlation, such that all events in the scaled optimum sequence can be dated. In Figure 4 this new RASC biochronology (horizontal axis) is used to estimate the rate of sediment accumulation (dashed line) in one of the wells – Adolphus D50.

Several years earlier, prior to development of RASC and CASC an approximate chronostratigraphy of this well section was given, in system units, Paleocene, Eocene, etc. As shown in Figure 4, there is a close approximation of the two, independently arrived at, sediment accumulations. The earlier interpretation obscures a possible late Oligocene-early Miocene hiatus. Scaling in time of the scaled optimum sequence is a pragmatic way of erecting a local time scale.

In summary, the CASC method of correlation is based on three conditions:

1. each individual stratigraphic sequence of events is a sample of the optimum sequence;
2. the observed depths of the events in a stratigraphic section are estimates of the true depths;
3. the calculated relative interfossil distances of events in the scaled optimum sequence can be used to stretch this sequence along the numerical geological scale; known ages for index fossils in this sequence provide the necessary tiepoints.

Input for (semi-)automated correlation of fossil events (or zones) with confidence limits in depth – or in time units are:

a. depth in feet or in meters for all fossil events in all wells or outcrop sections. The events are the same as used in the RASC method;
b. ages of index fossils to stretch the scaled optimum sequence in linear time;
c. events, clusters of events (zones) or ages to be correlated;
d. wells or outcrop sections to be correlated.

GENERALIZED DESCRIPTION OF CASC METHOD

The CASC program was developed, using a CDC Cyber 730 computer with a Tektronix 4014 terminal and is coded in Fortran Extended Version 4. Two computer libraries are required to use CASC: IMSL Library and Tektronix Advanced Graphing Library. Also, mass storage facilities are used (see later). To obtain the geologically most satisfactory bivariate fits, the program is best used interactively.

One of two different routes may be selected at the beginning of an interactive CASC session. The first route uses as a starting point the RASC optimum sequence, plotted against the so-called event scale. The latter has entries for the original sequence data in each stratigraphic section. Instead of the optimum sequence, the RASC scaled optimum sequence may be used. The latter combines average order and relative distance. The optimum sequence option is simpler than the so-called distance option based on the scaled optimum sequence, but not principally different. As an additional illustration the distance method is applied to results using RASC on the distribution of Cenozoic foraminifers in 21 and 24 wells on the Grand Banks and Labrador Shelf. The same data file is used in the next section of this report that deals with applications of CASC.

If RASC distances are used as input, it is necessary to replace them by ages (in Ma). The procedure for this is schematically shown in Figure 5. Assuming approximate ages are known for a subgroup of events in the scaled optimum sequence shown in Figure 5a, the objective is to fit a curve to these data in order to be able to replace any RASC distance by its age (see Figure 5d). First, RASC distances with the same age are averaged (see Figure 5a). Then a cubic spline curve is fitted to the age-distance pairs minimizing the sum of squares of deviations between points and curve in the vertical (age-) direction of Figure 5b. The smoothing factor SF can be chosen beforehand by the user of the interactive CASC computer program. It is equal to the square root of the mean square deviation between points and curve. Because this standard error is normally not known beforehand, the user can determine it by trial and error while experimenting with different plots on the screen of the monitor. In Figure 5b a curve was fitted to 5 original values (o) and 2 averages of two values (+). The standard deviation of the original data in relation to this curve is also shown on the screen (SD in Figure 5c). The fitted curve does not extrapolate outside the range of the RASC distances used for the curve fitting. Consequently, the circle with the highest RASC value is not considered for estimating SD in this example. It is noted that a curve could also be fitted directly through the 8 circles in Figures 5a and 5c. Then SD would be equal to SF.

Next, the CASC user can display and edit the RASC distances for any well from the set of the wells used. Editing options are schematically shown in Figure 6, which displays preliminary data analysis. The scale in the vertical direction is relative. It shows successive levels for the stratigraphic events in the well considered. RASC distances of 2 or more coeval events are averaged (see Figure 6a) before cubic spline fitting (Figure 6b). The user has the option of omitting events for which the second-order differences were anomalously high (i.e. shown by two asterisks in the RASC normality test). Such anomalous events are then displayed by use of a special symbol (single asterisk in Figure 6a) and are not employed for curve fitting. The deviations are measured in the horizontal direction. SF and SD serve the same purpose as in Figure 5. The user may wish to remove other events considered to be anomalous, for example, those labelled R in Figure 6c. Then a new cubic spline-curve will be fitted for the reduced data set (Figure 6d). If extreme values are deleted, SD will probably be decreased in value. The original RASC model is based on the assumption that positions of events in a well are distributed around their expected value, according to a normal probability distribution, with standard deviaiton set equal to $1/\sqrt{2} = 0.7071$. We, therefore, would expect SD to be approximately equal to 0.7 if the number of events in the stratigraphic section is sufficiently large.

For further analysis in preparation of automated correlation, RASC distance is replaced by age (see Figure 7a) using the earlier derived relationship between RASC distance and age (see Figure 5d). In the following discussion, the variables for event level, age and depth are denoted as x, y and z, respectively. A spline curve can be fitted to express y as a function of x, as was done for distance in Figure 6d. It is also possible to replace the levels by their depths and fit a spline curve to express y as a function of z using depth as the independent variable. This leads directly to a plot similar to Figure 7f.

However, the rate of sedimentation may have changed significantly during geologic time at a well site and this can result in irregular distribution of the points along the z-axis. This, in turn, may make it difficult to obtain a spline curve that extrapolates in a satisfactory manner across data gaps along the z-axis corresponding to short periods with high sedimentation rates. For this reason, the indirect method given in Figure 7 can be employed instead. Assume that the spline-curve of Figure 7a is written as $y = f(\underline{x}) + e_y$ where e_y represents a random deviation in the y-direction. The bar under x indicates that y is regressed on x using data points which are regularly spaced along the x-axis. Depth (z) is plotted against x in Figure 6b, and a separate spline-curve with $z = g(\underline{x}) + e_z$ is obtained, using the same set of regularly spaced data points along the x-axis. The deviation e_z points in the z-direction. Obviously, the curve $g(\underline{x})$ cannot decrease in the x-direction.

The curve for z in Figure 7b is shown again in Figure 7c. It has been rewritten in the form $\hat{x} = g^{-1}(\underline{z})$, to indicate that estimates $\hat{x}$ were obtained at points which are regularly spaced along the z-axis. Assume that $\hat{y}$ is obtained for the irregularly spaced values of x in Figure 7c using f(x) shown in Figure 7a. This results in a set of $\hat{y}_{xz} = f(g^{-1}(z))$ for regularly spaced points along the z-axis (see Figure 7d). The function $f(g^{-1}(\underline{z}))$ is not a simple mathematical expression. For example, its first derivative is not readily available. A cubic spline $\hat{y} = h(\underline{z})$ can be fitted to the values $\hat{y}_{xz}$ (see Figure 7e). In Figure 7e, $\hat{y}$ is considerably smoother than $\hat{y}_{xz}$. By using a smaller smoothing factor (SF), the difference between $\hat{y}$ and $\hat{y}_{xz}$ may be kept negligibly small (see curve to be used for example in Figure 8a). The standard deviation SD for points used for fitting in Figure 7a with respect to the curve $\hat{y}$ is provided in Figure 7f. The deviations from $\hat{y}$ are measured in the y-direction. A similar age-depth diagram is shown in Figure 8a where less smoothing was applied. The spline-curve $\hat{y} = h(z)$ can be used to assign a probable age to any point along the well.

Figure 9 shows a so-called multiwell comparison for five wells. It is based on a 7-2-4 RASC run on 21 wells. Points with estimated ages of 10, 30, and 50 Ma along the five wells are connected by lines of correlation in Figure 9. The uncertainty in the position of these isochron contours is indicated by error bars, constructed according to one of three methods further explained in Figures 8 and 10. The displays of Figures 9a and 9c were redrafted from displays on the Tektronix terminal obtained during an interactive CASC session; the error bars in Figure 9b were obtained from age-depth plots according to the method explained in Figure 8d.

The local error bar in Figure 9a is obtained by multiplying s(y) (=SD) along the y-axis by rate of sedimentation to obtain a modified error s(z) along the z-axis, as shown in Figure 8b. The rate of sedimentation (Figure 8c) is the first derivative

between the 18 average RASC distances and the fitted spline curve. The standard deviation of residuals (=0.5664) representing differences between original RASC distances and fitted spline curve is also given in Figure 11b. It is noted that this value is only slightly less than $\sigma = 0.7$ representing the theoretical standard deviation along the RASC scale.

Figure 11c shows a new default result, obtained after replacing RASC distance by age. It is possible to inspect the first derivative dx/dy of this graph (Figure 11d). If the slope in the direction of increasing age for the curve in Figure 11c exceeds 10, its values are not displayed in Figure 11d. Because the default yields the first monotonically increasing spline curve, normally at least one interval with very high sedimentation rate is introduced with this option. By increasing SF, the user can remove artificially high sedimentation rates.

Figure 11e shows the relationship between depth and event level with fitted spline curve for SF = 0.02. It passes almost exactly through the observed values. After display of this plot, the CASC user has the option of either using this spline curve in conjunction with the age-event level plot of Figure 11b, or of bypassing the indirect procedure by directly fitting a curve to the age-depth diagram in which event levels have been replaced by their depths. The default result for the direct method is shown in Figure 11f.

The result obtained by following the indirect method is shown in Figure 12a for small SF(=0.1). The first derivative corresponding to Figure 12a is given in Figure 12b. The irregularity between 2.2 and 2.3 km in this diagram is due to lack of precision of the approximations, used in the indirect method, to obtain new values on the spline curve (see Figures 7c and 7d). The regular spacing along the depth scale, used for this purpose in CASC, is 50 m. Consequently, irregularities due to lack of precision will not extend for more than 100 m along the depth scale.

Figures 12c to 12f show new results for the indirect method, obtained after changing the value of SF from the default (SF = 3.5751 in Figure 11c) to SF = 4.0 in Figure 12c. During a CASC session, the user is also shown the unsmoothed values of $f\{g^{-1}(\underline{z})\}$ (cf. Figure 7d) connected by straight lines. An example of the latter type of display is Figure 13a which originally appeared during the CASC session just before Figure 12e where SF = 0.1. It is not possible to see differences between the curves of Figures 12e and 13a. However, when SF is enlarged to 1.0, the smoother curve in Figure 13b is generated from Figure 13a. The rate of sedimentation for Figure 13b is shown in Figure 13c.

Figure 13d represents the depth versus event level curve that replaces Figure 11e, when SF = 0.00 instead of SF = 0.02 is selected. The difference between these two curves is small and when the curve of Figure 13d is combined with that of Figure 12c, the resulting plot (Figure 13e) does not differ significantly from Figure 12e. However, the first derivative of Figure 13e which is shown in Figure 13f differs significantly from Figure 12f. It shows many 100 m irregularities, which are due to lack of precision as also discussed before (see Figure 12b). In general, the final age-depth curve is less sensitive than the sedimentation rate curve to small changes in the choice of smoothing factors for successive curves during an interactive CASC session.

As a final example, Figure 14 contains various CASC displays for Adolphus D-50. The input for this CASC run was output from a 5-2-3 RASC run on 24 wells. As shown in Figure 14a there are as many as 39 events on 28 levels in this well so that there is good control in the vertical direction. The first derivative of the

spline-curve for SF = 2.2 (Figure 14a) remains fairly constant. It has its largest value at event level 14 (see Figure 14b). This indicates that place where the spline-curve in Figure 14a has its steepest dip. The pattern of Figure 14c suggests that rate of sedimentation was above average between events 6 and 7 and also between events 21 and 22. These two maxima also occur in Figure 14e which is the first derivative of the age-depth curve (Figure 14d), obtained by combining the spline-curves of Figures 14a and 14c with one another using the indirect method. The smaller peak in Figure 14e, which occurs at a depth of about 1600 m, represents the place (level 14) where the curve of Figure 14a has its steepest dip. The same three intervals with relatively steep slopes in the age-depth spline-curve can be observed in Figure 14f, which resulted from applying the direct method to the age-depth values. Without corroboration from other wells drilled in the immediate vicinity it may not be possible to decide with certainty whether or not small fluctuations in the rate of sedimentation, as shown in Figure 14e, are significant. Increased smoothing in the age-depth diagram (Figure 14d) would change the pattern of Figure 14e much more drastically than the pattern of Figure 14d itself.

As was illustrated in more detail for Indian Harbour M-52 in Figures 11 to 13, minor smoothing in Figure 14a for Adolphus D-50 would, in a multiwell comparison, only slightly change the position of isochrons in Adolphus D-50. However, the widths of the error bars are proportional to rate of sedimentation in both local and global error bar estimation and these widths would change drastically if smoothing is increased. This is because rate of sedimentation does depend strongly on choice of smoothing factors.

GEOLOGICAL APPLICATIONS OF CASC

The geological use of the CASC method and its value in sedimentary basin analysis are illustrated by means of examples drawn from exploration micropaleontology. The examples are based on the original distribution of 168 Cenozoic foraminifera in 21 Grand Banks and Labrador wells, and of 116 taxa of Mesozoic foraminifers in 16 Grand Banks wells. The latter file was largely prepared by Williamson (in press). The Cenozoic file accompanies this report on diskette as an example for running RASC and CASC, with the one difference that in well Bjarni H-81, taxa 54 and 55 (**Gavelinella beccariiformis** zone, Paleocene) have now been added. Both taxa were observed at a depth of 6660'.

The discussion touches on the following questions:

(1) What is the stratigraphical meaning of CASC-type of correlation?

(2) What is the degree of confidence, expressed in depth and in linear time units of CASC correlation, and to what extent is the error bar useful for geological interpretation?

A third question concerning the difference between subsidence and sedimentation models that rely on subjective age-depth data, or more objective RASC-CASC types of age-depth interpretations, is discussed elsewhere (Gradstein et al., in press).

dz/dy for z in $\hat{y} = h(z)$. In general, a cubic spline curve y, fitted to n data points, consists of (n-1) successive cubic polynominals

$$y = y_i + c_{1i}d + c_{2i}d^2 + c_{3i}d^3$$

with $d = z - z_i$, $z_i \leq z < z_{i+1}$, where z_i and z_{i+1} ($i = 1, 2, \ldots, n-1$) represent the n depths used to convert $\hat{y}_x = f(x)$ into $\hat{y} = h(z)$. The coefficients c_{1i}, c_{2i} and c_{3i} can be used to calculate

$$dy/dz = c_{1i} + 2c_{2i}d + 3c_{3i}d^2$$

at any point. Inversion of this expression gives dz/dy. The new standard error $s(z) = (dz/dy)\, s(y)$ can be displayed for any z as the local error bar $z \pm s(z)$ (see Figure 9a). This propagation of error is based on the local rate of sedimentation, which is assumed to remain approximately constant over the interval $y \pm s(y)$. The latter condition is frequently not satisfied, especially when $\hat{y}$ has many inflection points (between local maxima and minima in sedimentation rate). Curvature of $\hat{y}$ is considered in the construction of a modified local error bar as illustrated in Figure 9d. For any point $z = h^{-1}(y)$, this bar extends from the point $h^{-1}\{y - s(y)\}$ to $h^{-1}\{y + s(y)\}$. It is asymmetrical with respect to z and is significantly shorter at places where the rate of sedimentation is high.

Finally, a global error bar (Figure 9c) can be constructed as illustrated in Figure 10. The standard deviation $\sigma = 1/\sqrt{2}$ of events along the RASC linear scale for distance is changed into a variable standard error s(y) along the age scale. This new, variable standard error is changed into s(z) according to the method used for SD in Figure 8b. In global error bar estimation, it is assumed that a single RASC distance error σ can be applied to all wells. On the other hand, in local error bar estimation, use is made of a constant SD value along the age scale which was estimated from the deviations between the points used for spline fitting and the spline curve itself (cf. Figure 7e). Because of possible elimination of anomalous events and averaging of ages for events at the same levels, the local error bar is likely to be narrower than the global error bar.

The purpose of the error bar is to quantify the uncertainty of the observed depths of events with respect to their estimated depths in the wells. Each local or global error bar extends from the estimated depth minus one standard deviation to estimated depth plus one standard deviation. If the observed depth is normally distributed about the estimated depth, the error bar can be interpreted as a 68 percent confidence interval for single events. Then there is a 68 percent probability that the observed event falls within the range outlined by the error bar. Likewise, there is 95 percent probability that the observed event falls within an extended error bar, which is 1.96 times as wide as the error bar shown.

The actual precision of the estimated depth of an event in a well is probably much higher than that indicated by the error bar for single events. If a value on the spline-curve would be interpreted as the arithmetic average of all (n) values used for its estimation in a well, the standard deviation of this mean would be equal to the standard deviation of the single events, divided by $\sqrt{n}$. For example, in a well with 16 event levels, the standard deviation of the difference between estimated depth and 'true' depth would be one-fourth the standard deviation of the 16 single events used to construct the error bar. The degree of validity of the assumption that a value on the spline-curve can be interpreted as an arithmetic

mean of all values used for estimation is not precisely known, except when the smoothing factor is large. In the limit, which is reached when SF exceeds an upper threshold value, the spline-curve reduces to the best fitting straight line of least squares. Then the preceding assumption is known to hold approximately true. Further research would be needed to estimate the standard deviation of the difference between an estimated value on the spline-curve and its corresponding 'true' depth when the smoothing factor is smaller.

Output from a 7-2-4 RASC run on 21 wells and a 5-2-3 run on 24 wells were used as input for examples of actual CASC runs in the remainder of this section.

Table 1 shows the optimum sequence, modified optimum sequence (after final reordering) and RASC distances for the 7-2-4 run on 21 wells. Several events, occurring in fewer than seven wells, were later inserted as unique events. Table 2 shows estimated ages of 22 events, including these unique events. Average RASC distances for events with the same age are shown in the last column of Table 2. Figure 11a shows the ages plotted against the RASC distances. The displays in Figure 11 (and Figures 12-14) were redrafted from hard copy of displays on a Tektronix terminal. A cubic spline function with smoothing factor SF = 2.0 was fitted to the 15 ages, using the average distances shown in the last column of Table 2. The smoothing factor SF is the standard deviation of differences between the 15 ages and corresponding estimated ages on the spline-curve for the same RASC distance values. The standard deviation of the 22 original ages before averaging of some RASC distances is also shown in Figure 11a.

The original sequence of events occurring in 7 or more wells is shown in Table 3 for Indian Harbour M-52 (Well No. 5), which will be used for further analysis.

As mentioned earlier, one of two different routes can be selected at the beginning of CASC. These consist of using either optimum sequence data or RASC distances for the events. In both subprograms, event levels for successive, non-coeval events are defined, as illustrated for Indian Harbour M-52, in the second column of Table 3. In the second subprogram, the RASC distances in a well are transformed into ages using the spline curve fitted in Figure 11a (see last column in Table 3). The methods used in the two subprograms are identical, except that sequence position numbers instead of ages are used in the first subprogram. Only the option that uses the ages (in Ma) will be illustrated in detail here.

CASC produces a number of successive plots. For each of these plots the user is required to answer one or more questions. The plot that comes after Figure 11a during a CASC session is shown in Figure 11b. It shows the RASC distances of Table 3 plotted against their event levels. Before this plot is actually shown on the Tektronix screen, the user is asked if he wishes to exercise the option of deleting anomalous events which are out of place with a probability of 99 percent according to the RASC normality test. Moreover, points can be deleted from Figure 12 itself by positioning the Tektronix cursor on top of them. No points were omitted in this example. Next a cubic spline curve is fitted to the average RASC distance values in the third column of Table 4. First the user is shown the default smoothng factor (SF = 0.5146 for Figure 11b) and asked if this value should be used. This default was obtained automatically, by fitting spline curves with SF increasing from 0.0 until the first curve is found for which the distance does not anywhere decrease with increasing depth. The default solution is shown in Figure 11b. The smoothing factor is the standard deviation of the differences

In order to find answers to these questions, we show conventional and subjective and more objective CASC-type correlation of wells based on three related stratigraphic criteria:

(a) selected zone markers;

(b) assemblage zones; and

(c) isochrons in Ma.

In all cases, the underlying biostratigraphical zonations were defined with the RASC method, but in principle CASC can be applied to non-RASC zonations based on biostratigraphical events.

Firstly, we trace ten selected zone markers through six wells. Starting point is the Cenozoic optimum sequence (Figure 15; 21 wells, 7-2-4 run). For the interactive spline fitting of the bivariate plots, all defaults were accepted, unless otherwise specified.

The default is the smoothing factor (SF) that defines the spline curve for which an increase in position or depth along one axis does not anywhere correpond to a decrease in position (or time) along the other axis. The default is obtained by means of an algorithm that calculates spline curve fits with SF increasing or decreasing according to a binary search method. The default satisfies the condition that the observed sedimentation rate is never negative.

In three wells the cursor option was used to delete aberrantly positioned events, including:

Well 21 - Hibernia P-15

one point was deleted on level 12.

Well 11 - Bonavista C-99

three points were deleted at levels 4, 11 and 5 and SF for the events versus depth graph was changed from 0.02 to 0.15.

Well 9 - Snorri J-90

one point was deleted at level 6.

The results of the so-called multiwell comparison are shown in Table 5, listing both the observed and the most likely depth of the ten Paleocene through Miocene zone markers 50 (56), 90, 32, 29, 261 (260), 259, 24, 26(15), 18 and 16. In two wells substitute taxa were correlated rather than the three designated events 50, 261, and 26. The substitutes 56, 260, and 15 are neighbours of the original events in the optimum sequence.

In most instances, the observed and the most likely depth values are within half the length of the error bar (68% probability) around the most likely value. As pointed out in the previous section, the actual precision of the estimated depth of an event in a well is probably much higher than that indicated by the local error bar for single event positions along the spline curve. Also, the local error bar at any depth is initially calculated over the time interval along the (scaled) optimum sequence scale (y), as defined by twice the standard devition (SD) in that (y) direction. It is directly proportional to the fitted average sedimentation rate for each point (Figure 8).

Because this average sedimentation rate may frequently change through time, significant curvature may occur over the span of the original 2SD in the scaled optimum sequence (y) direction. It may therefore be better to use the so-called modified local error bar that does not, like the local error bar, calculate uncertainty by extrapolating a constant average sedimentation rate across the entire length of the error bar. Strictly speaking, the slope of the spline fit in the optimum sequence versus event depth does not represent sedimentation rate in a well, but the principle of this discussion on the modified local error bar stays valid. This new error bar estimate is not automatically obtainable in the interactive version of CASC; and only the total and global error bar options of the CASC program were used for the applications discussed below.

Figure 16 grapically correlates the ten events through the six wells. The conventional chronostratigraphic segmentation, which is shown for comparison, only uses the observed depth of events. The new, most likely, zone marker depths would lead to slight up or down adjustments of the age boundaries. It could be assumed that such a change might violate stratigraphic boundaries as adjusted for major lithology changes as determined from well logs. However, using sonic and gamma logs, no evidence for this was found. In the Snorri well there is no direct micropaleontological evidence for the presence of events 259, 24 and 26, associated with Oligocene-Early Miocene strata, although the CASC method predicts their likely depth in this well. These depths are not unreasonable given that Oligocene strata were thought to be present at that depth, based on palynology.

The next example, shown in Table 6 and in Figure 17, correlates the RASC zones of **Spiroplectammina carinata** (events 18, 71, 21, and 20) and of **Turborotalia pomeroli – Cyclammina amplectens** (events 260, 261, 263, 32 and 29 only), Late Eocene. The six wells are as in the previous example, but now the distance CASC option is employed for 21 wells (7-2-4 run; Figure 15).

A summary of the run is as follows:

Well Hibernia P-15

deleted one point at level 12;
SF in RASC distance versus event scale plot is 0.35;
SF in RASC distance converted into age versus depth scale plot is 0.15 (default is 0.10)

Well Bonavista C-99

SF in events versus depth plot is 0.10 (default is 0.02);
SF in age versus depth plot is 0.15 (default is 0.10).

Well Indian Harbour M-52

SF in age versus depth plot is 0.15 (default 0.10).

Well Bjarni H-81

SF in age versus depth plot is 0.15 (default 0.10).

Well Snorri J-90

deleted one point at level 6.

Table 6 is a listing of the most likely depths in the six wells of taxa that characterize the two RASC zones. The error bar is the local one and with few exceptions it shows that there is limited uncertainty in depth. The global error bar combines error in relative time of the events in the scaled optimum sequence (RASC distance scale) with the error in position of the events along the well (depth) scale. In a few cases, shown with (*) this error approaches 20-30% or more of the actual depth value, particularly in Hibernia P-15.

Tracing the two zones through the well sections (Figure 17) determines the most likely intervals of Upper Eocene and Middle Miocene strata. The same figure displays subjectively estimated thicknesses of these strata. In the Indian Harbour and Bjarni wells, the subjective analysis was not able to differentiate between the **Uvigerina dumblei** and **Spiroplectammina carinata** zones; hence, Lower and Middle Miocene were lumped. This explains why the objective thickness of Middle Miocene may seem thin. We also determined in the six wells the most likely depth of **Ammodiscus latus** (A) which occurs in the 7-2-4 run (Figure 15) at the base of the **Turrilina alsatica** zone (Oligocene). The top Eocene is below the level of A, and above the level of event 260 (**Haplophragmoides kirki**). The CASC results are entirely reasonable and define depth intervals in which the two zones are most likely to occur. The use of CASC for the tracing of zones and for stratigraphic segmentation of exploration wells, will lead to correlation of intervals in which a stratigraphic boundary is most likely to fall. The latter may then be compared to discrete wireline log parameters reflecting physical changes in the sediments.

The conversion of the scaled optimum sequence to a (local) biochronology enables the stratigrapher familiar with CASC to trace isochrons in the same way as zones were traced. The exercise starts with the designation of numerical ages in Ma to those events in the scaled optimum sequence for which literature based ages are available. In all, 23 events were dated this way, as explained below. The time scale is that of Berggren et al. (in press). The regional use of the standard planktonic zonation follows Gradstein and Srivastava (1980), and Gradstein and Agterberg (1982):

(1) 63 Ma – events 253 and 61 – **Subbotina triloculinoides** and **S. pseudobulloides** – two rare events that mark approximately the end of Danian time.

(2) 58 – event 55 – **Gavelinella beccariiformis;** occurs up to standard zone P5 (Tjalsma and Lohman, 1983), which fits well with its disappearance in the Adolphus well together with **Aragonia velascoensis** (Paleocene) and below the appearance of **Pseudohastigerina** (post P5).

(3) 57 Ma – event 194 – **Planorotalites chapmani;** disappears in standard zone P6. Specimens are often transitional between **P. chapmani** and **Pseudohastigerina.** The latter is thought to appear at the boundary of P5 and P6, or ±57 Ma ago.

(4) 55 Ma – event 50 – **Subbotina patagonica;** is frequent in the Ypresian of Belgium (Muller and Willems, 1981), in the Moe Clay of Denmark and in the Lower Eocene of the North Sea and Labrador Sea. The end of the **S. patagonica** peak occurs at the boundary of NP11/NP12, which coincides with the boundary of the **Morozovella formosa formosa** Zone, at the time of Anomaly 24, just after 55 Ma.

(5) 52 Ma – event 93 – **Acarinina broedermanni;** the species has its top well below **A. densa,** probably in the **A. pentacamerata – Hantkenina aragonensis** Zone, near the Early-Middle Eocene boundary at 52 Ma. In some RASC runs, **A. broedermanni** falls between Early and Middle Eocene zones.

(6) 49 Ma – event 90 – **Acarinina densa;** this is the time of the optimum climatic warming in the Labrador Sea, in early Middle Eocene time. Less common at this time are **A. senni, A. aff. pentacamerata, A. aff. broedermanni, Morozovella caucasica, M. spinulosa,** and **M. aff. aragonensis.** The event probably falls in the **Hantkenina aragonensis – Globigerinatheka subconglobata** Zone at Anomaly 21 time or 52-46 Ma, (average 49 Ma).

(7) 40 Ma – event 29 – **Cyclammina amplectens;** in RASC runs this event falls below **Turborotalia pomeroli** and **Globigerina yeguaensis** and above **Acarinina densa.** In Poland its peak occurrence is so-called Middle Eocene; it is less frequent in upper Eocene strata (Gradstein and Berggren, 1981). The event is tentatively placed at 40 Ma.

(8) 38 Ma – event 85 – **Pseudodhastigerina micra;** same reasoning as for **Turborotalia pomeroli** (see below), but often disappears in slighty older beds, as shown also in scaling (Figure 15).

(9) 37 Ma – event 33 – **Turborotalia pomeroli;** co-occurs in southern wells with **Subbotina linaperta, Globigerina yeguaensis** and **Pseudohastigerina micra,** of the **Turbortalia cerroazulensis** Zone, late Late Eocene. The top is placed just below the inferred Eocene/Oligocene boundary.

(10) 28 Ma – event 24 – **Turrilina alsatica;** the top of this distinctive Oligocene taxon roughly equates with the top of the Boom Clay in Belgium and the top of the **Globorotalia opima opima** Zone, at ±28 Ma.

(11) ±20 Ma – event 26 – Uvigerina dumblei; slightly older than **Globigerina praebulloides** (see later).

(12) 20 Ma – event 137 – **Globigerinoides primordius trilobus;** rare Early Miocene event.

(13) 17 Ma – event 15 – **Globigerina praebulloides;** disappears locally with **Sphaeroidinella seminula** and with or just below **Globorotalia scitula praescitula,** which may equate with the **G. fohsi peripheroronda** Zone, early Middle Miocene of Scotian Shelf wells (Gradstein and Agterberg, 1982). The RASC runs (7-2-4) indicate an average disappearance in the **Uvigerina dumblei** zone. Its local extinction is placed between 14 and 20 Ma (average 17 Ma).

(14) 15 Ma – event 179 – **Globorotalia scitula praescitula;** probably occurs in the late Early to early Middle Miocene warming event, as observed from the northern incursion of warmer water planktonic taxa.

(15) 3.5 Ma – events 266, 4, 269 and 5 – Both **Globorotalia puncticulata, G. inflata, G. crassaformis, and Neogloboquadrina atlantica** are thought to disappear with the onset of major glaciation in the Labrador Sea, dated at approximately 3.5 Ma.

Four other events occur at or near significant breaks in the 5-2-3 and 7-2-4 scaling solutions for 21 and 24 wells. These breaks were equated with zonal boundaries and series breaks as follows:

58 Ma – event 56 – **Glomospira corona;** Paleocene-Eocene boundary on (upper) continental margin wells.

52 Ma – event 57 – **Spiroplectammina spectabilis** LCO; Early-Middle Eocene boundary; LCO = Last Common Occurrence.

37 Ma – event 259 – **Ammodiscus latus;** Eocene – Oligocene boundary.

11 Ma – event 17 – **Asterigerina gurichi;** Middle-Late Miocene boundary.

Figure 11a is a plot of the ages of the previously listed events in a RASC distance scale (21 wells, 7-2-4 run) versus linear time scale. Smoothing of the spline curve function diminishes some of the uncertainty in subjective assignment. The spline function can now be used to convert the RASC distance scale in an age scale.

Next, the question can be asked what is the most likely depth in the wells of the principal boundaries between RASC zones, expressed in Ma. We have traced the boundaries between the successive Cenozoic RASC zones (Figure 15), which are close approximations to the boundaries between Paleocene and Eocene (≈56 Ma), Early Eocene and early Middle Eocene (≈52 Ma), early Middle Eocene and Middle Eocene (≈49 Ma), Middle and Late Eocene (≈44 Ma), late Eocene and Oligocene (≈36 Ma) Oligocene and Miocene (≈24 Ma), Early and Middle Miocene (≈16 Ma) and top of Middle Miocene (≈12 Ma).

Table 7 lists most likely and subjectively determined (as far as known) depths for these isochrons. The same results are plotted in Figure 18, with the wells arranged latitudinally, (48° - 58°N). The CASC depths are from a batch run that accepted all SF defaults. Although it yields more crude results than interactive runs, this procedure takes less time and the actual depth estimates are not influenced much. As explained in the previous section, the choice of SF has much more influence on the average rate of sedimentation and hence on the error estimation, than on the actual depth of the isochrons. In a few instances, default smoothing yielded unacceptably steep spline fits, and the local error bar estimate was deleted. In one well, Karlsefni H-13, both foraminifers and palynomorphs agree on the absence of Oligocene beds (**Turrilina alsatica** Zone). Batch CASC calculates a thin Oligocene interval (24-36 Ma), where in an interactive version of CASC the recently developed unconformity option (see next section) should have been used. However, above the Eocene the well has only a few data points and results are crude.

The local error estimates of the most likely depths for the isochrons are within 1 to 10% of the actual depth values, and more frequently 2 to 5%. In about ten cases the subjectively assigned depths for the zonal boundaries as converted to isochrons are outside the 68% confidence limits (±1 SD). For geological interpretations, it should be borne in mind that the error in most likely depth is an upper limit, and the SD is probably smaller by a factor that, amongst others, is related to the number of observations per spline curve, as explained earlier. Palynologically determined depths for these stage boundaries often are outside the depth interval (most likely depth ±1 SD), calculated by CASC. The errors in this independent biostratigraphic exercise are unknown, but the comparison suggests that multiple biostratigraphy uncertainties exceed the CASC-type of errors using one fossil

discipline only. The conclusion may be drawn that the CASC program is able to predict reliable and objective well to well isochrons. The error expression, that hitherto was mysteriously vague in conventional, subjective correlation schemes, is conservatively large when one fossil discipline only is used.

As a further test of the use of CASC for subsurface correlation, Williamson (in press) applied RASC and CASC to Mesozoic strata of the northern Grand Banks. This author edited existing micropaleontological data and considerably expanded the file to include close to 20 wells, centered on the Hibernia oil field. Williamson determined that eleven RASC zones of Kimmeridgian through Cenomanian age are able to account for most of the biostratigraphic signal. The results are based on last occurrences of over 50 foraminiferal taxa that occur in more than four wells (4-2-3 run). Eleven taxa were defined as unique events. The eleven RASC zones supersede conventional biostratigrapical analysis based on limited data. Figure 19 presents Early Cretaceous CASC isochrons for the wells on and around the oil field. Solid lines represent subjective age interpretation; the dashed lines are the CASC ages. Both interactive and batch runs were made to arrive at the best possible results. The closeness of the subjective and the objective tielines provides another example of model verification.

Observed fossil event sequences in wells or in outcrop sections, for which an RASC (scaled) optimum sequence has been calculated, can be subjected to CASC analysis. The CASC method computes the most likely depth in the wells for events or zones in this (scaled) optimum sequence. The method involves estimation of three or four best fit (spline) functions per well, including:

(1) (scaled) optimum sequence versus event sequence;

(2) this event sequence versus its observed depth; and

(3) (scaled) optimum sequence versus depth.

The combination of the functions for (1) and (2) yields function 3.

If the age is known for some of the events in the scaled optimum sequence, the interfossil distance values can be used as interpolators between these tiepoints in the time scale to make a RASC biochronology. This bivariate function of the RASC distance scale versus linear time can also be smoothed to reduce scatter in the original age data.

Error analysis in the three bivariate functions (under 1, 2, and 3) makes it possible to attach confidence limits to the most likely depth values. This gives the local error bar. The standard deviation of the RASC interfossil distances in the scaled optimum sequence can be converted to a global error bar, applied in all wells. Smoothing of the three bivariate fits under 1, 2, and 3 affects the error values much more than the most likely depths values.

Examples of objective correlation involved Cenozoic foraminiferal events, zones and isochrons based on the RASC zonation in Labrador and Grand Banks wells, and Early Cretaceous isochrons based on the RASC zonation in the Hibernia oilfield, off Newfoundland. Previous analysis based on subjective age-depth data consistently confirms results obtained by the CASC model. The error for the most likely depths of the correlation lines rarely exceeds 10%; it commonly is 2 to 5%. Further research in the methods of error analysis may show the values to be relatively large. CASC-type of age/depth data offer the potential for significant

contributions to analytical error analysis in tectonic subsidence and sedimentation calculations. RASC and CASC make subsidence analysis more objective and accurate, and easier to perform by non-paleontologists.

The version of CASC presented in this report is interactive. It leaves the responsibility of selecting appropriate age-depth curves for individual wells largely with the user who retains considerable flexibility in choosing smoothing factors in a subjective manner. Future research on CASC will concentrate on efforts to estimate the smoothing factor automatically and to refine the error analysis. We are planning to develop a version of CASC which is not interactive. This batch version of CASC will be comparable with RASC in that a limited number of parameters will be set at the beginning of each run while different types of output are produced simultaneously for many wells. The interactive version presented here will retain the advantage that the user can modify results during a session by using outside knowledge not included in the data base.

The combination of the RASC method for biozonations and the CASC method for the most likely segmentation and correlation of well sections is an objective and powerful stratigraphic tool in geological basin analysis.

EXAMPLES OF DISPLAYS GENERATED DURING A CASC INTERACTIVE SESSION

A 5-2-3 run with RASC-C on the familiar Gradstein-Thomas data base provided input for all examples in this section. The 52 displays to be discussed are contained in Appendix 2. The first six displays (numbered 1 to 6) for Adolphus D-50 were previously shown in redrafted form in Figure 14 (a to e). The next 9 displays (7 to 15) were obtained during the same interactive session for Adolphus D-50 which led to Figure 14. Displays 7 to 9 were produced at the beginning of this session to transform the RASC distances for the 5-2-3 run into numerical geologic time. Display 10 represents a table produced on the screen each time a new well is to be selected. Display 11 provides an example of the first display for a well selected. It ends with the prompt: 'Do you want to consider anomalous events'. The latter are events with two asterisks in the RASC normality test output. If the answer to this prompt is: 'Yes', these events will be eliminated from further analysis of the well considered. Editing capabilities of CASC were previously illustrated in this report by means of Figure 6.

Display 12 shows RASC distances for the events of Display 11 converted into ages using the spline curve of Display 9. These ages were averaged for coeval events. The default smoothing factor of 1.8164 is for the first spline-curve, obtained by increasing the smoothing factor from zero, without any segment dipping in the direction of the negative age axis. Keeping this default value will lead to Display 16 which is to be discussed later. Changing it to 2.2 gave Display 1. A similar display (no. 13) preceded Display 6 with SF = 2.1 in which the points separating successive cubic polynominals are irregularly spaced in the vertical direction which is the procedure followed in the direct method of spline-curve fitting. As previously explained in Figure 7, the indirect method of spline-curve fitting initially results in a combination of two spline-curves which itself is not a spline-curve. Display 14 shows this combination which consists of discrete values connected by straight line segments for Adolphus D-50. Smoothing it with the default SF = 0.1 gave Display 4. The differences between the curves of Displays 4 and 14 are minimal. They cannot be seen by eye because the default (SF = 0.1) is very small. The fitted values on the spline-curve of Display 4 are shown in Display 15.

Display 16 followed Display 9 during the session using the default smoothing factor of 1.8164. This spline-curve is much more irregular than the curve for SF = 2.2 in Display 1. Its first derivative is shown in Display 16. Nevertheless, further use of the curve in Display 16 and other defaults yields a final age-depth curve which is not much different from the curve shown in Display 1. The curve resulting from the use of default values only, is shown in Display 18.

The numbers shown in Display 18 are cluster codes plotted at the positions of the events. The clusters are those displayed in the final dendrogram of the scaled optimum sequence. This option allows comparison of the spline curve to the succession of RASC zones rather than events. In this way hiatuses can also be better visualized or noticed. At the beginning of a CASC interactive session, the following question is asked: 'Do you want to set cluster limits for the data set'. If the response is positive, the user must enter the stratigraphically lowest event of each dendrogram cluster. Each cluster will be automatically numbered 1,2,... in the downward direction. The maximum number of dendrogram clusters that can be defined is 15. For example, for the present 5-2-3 run, the following 9 fossil numbers were entered: 17, 67, 20, 15, 259, 203, 41, 93, and 56. This resulted in

10 clusters approximately corresponding to the 10 clusters for the 7-2-4 run on 21 wells in Figure 15. The oldest cluster (No. 10) is labelled A in Display 18. It can be clearly seen in Display 18 that successive clusters generally show overlap in individual wells. The indirect method using defaults only was also applied to Hare Bay H-31 (Displays 19 to 21) using the same cluster codes. A small cluster of 5's (Oligocene) occur relatively low in Hare Bay H-31 in comparison with their average location which is based on all wells. Facts of this type can be brought out quickly by using the cluster code option. Display 22 shows the first derivative of spline-curve in Display 21. The rapid increase in sedimentation rate near the lowest points plotted for Hare Bay H-31 is artificial. It is an edge effect created by the relatively low position of one of the Early Eocene events represented by 9 in Display 21.

The remainder of this section (Displays 23 to 52) consists of various applications of the recently developed unconformity option. There are three methods by which an unconformity can be introduced into a given well. It can be set at a specific event in the scaled optimum sequence, between two successive events in the optimum sequence, or, by employing the cursor, in the final age-depth diagram. First, the unconformity is shown as a sine-curve at the position selected in the age-depth diagram. If either of the first two methods is used, it will intersect the spline-curve at the point where the age is equal to the estimated age of the event or equal to the mid-point between two successive events. Next, events observed above the theoretical depth corresponding to this age will be taken as a subgroup; and the indirect method is applied to the events belonging to this subgroup only. The events below the unconformity are taken as a second subgroup and will be analyzed separately.

In Adolphus D-50, the unconformity was set at event 201 representing the highest seismic marker. In the scaled optimum sequence, this event falls in cluster 4 (Early Miocene), some distance above the top of the Oligocene. In the 7-2-3 RASC-C run to prepare CASC input for the Gradstein-Thomas data base, all seismic events were treated as marker horizons. This implies that it is assumed that the location of these events is known with certainty in the wells for which they have been coded. This, in turn, means that the seismic events were given more weight during scaling than the biostratigraphic events. It is noted that the unconformity is plotted at the probable position of the event selected (or at the probable location of the point midway between two events), and not at its observed position in a well. The latter position generally will occur either slightly above or slightly below its probable position. It may also be absent from the well considered.

Using defaults only for the events above the unconformity in Adolphus D-50, the next three displays (no. 24 to 26) were obtained. Again using defaults only, the events below the unconformity gave Displays 27 to 29.

If the patterns of Display 26 and 29 are combined with one another, we see that the two spline-curves in these diagrams, together form a curve which is nearly identical to the spline-curve of Display 23 which was fitted to all events without an unconformity at event 201. It suggests that this seismic reflector does not coincide with a significant stratigraphic hiatus in Adolphus D-50.

The preceding experiment was repeated for Hare Bay H-31 (see Displays 30 to 36). Display 30 shows that the probable position of event 201 falls in a time period with a relatively low rate of sedimentation at this well site. This suggests

that an unconformity with an hiatus may indeed exist. However, if the age-depth curves for the events above the unconformity (see Display 33) and those below the unconformity (see Display 36) are combined with one another, the original pattern of Display 30 is reproduced almost exactly. The only difference is that during the time period between the points where the curves of Displays 33 and 36 reach the unconformity, the relatively low sedimentation rate in Display 30 has been replaced by zero sedimentation rate. The unconformity results for well 21 (Displays 26 and 29) and well 17 (Displays 33 and 36) are shown together in Display 37 for multiples of 10 Ma. The 20 Ma isochron in Hare Bay H-31 was not produced on the screen because it approximately coincides with the unconformity itself in this well. In Adolphus D-50, the 20 Ma isochron occurs slightly higher above the unconformity and is shown. On the other hand, the 10 Ma isochron is not shown for well 17 because the spline-curve in Display 26 does not extend to this age. When the indirect method is used (cf. Figure 7), discrete approximations of the level-depth and age-level spline-curves are combined with one another. To obtain the age-depth curve a narrow sampling interval of 50 m along the depth-scale is used in the process of discrete approximation. Because only points on the spline-curves were used without extrapolation, the final age-depth curve does not extend to the events with minimum and maximum depths in a well, respectively. Thus some information is lost at the end points of the age-depth curves. This loss of information becomes larger when the rate of sedimentation is relatively low.

A second example of application of the unconformity option is as follows. Agterberg and Gradstein (1983) have described results for 5 wells on the Labrador Shelf obtained during a pilot study performed when the development of CASC was starting in 1982. Figures 20 to 22 show locations of these 5 wells, multiwell comparison and interpretation in terms of an age-depth diagram by Gradstein and Srivastava (1980), respectively. Figure 21 displayed the conclusion in the latter publication that a broad shelf regression occurred at the site of Karlsefni H-31 in the Oligocene (37.5-23 Ma) probably accentuated by eustatic sea-level lowering.

Displays 38 to 52 result from using the new unconformity option, assuming the existence of an unconformity between events 259 and 82 at the sites of Karlsefni H-13 and Snorri J-90. Event 259 is the lowest event in the Oligocene cluster of the 5-2-3 run on 24 wells (cf. 7-2-4 dendrogram for 21 wells in Figure 15), and no. 82 the highest event in the Late Eocene cluster. Defaults were used in all runs for the experiment resulting in Displays 38 to 52. It is noted that in a number of displays obtained during the interactive CASC session for the 5-2-3 RASC-C run used as an example in this section, some events have zero age in the age-depth diagrams (e.g., see Display 38). The smallest fitted age value (see Display 8) amounts to 4.642 Ma corresponding to a RASC distance value of 0.7483. Events with RASC distance less than this smallest value will be assigned zero age by default in the CASC computer program. In the present application, this default provides satisfactory results, because the age – RASC distance curve selected (see Display 9) begins near the origin where age and RASC distance are both equal to zero.

Comparison of the combination of Displays 41 and 44 with Display 38 shows that the use of the unconformity option for Karlsefini H-13 is justified although the overall change in the age-depth curve remains minor. The corresponding change for Snorri J-90 is greater as can be seen by comparing Displays 48 and 51 with Display 45. In general, changes in pattern introduced by using the unconformity option are greater if other smoothing factors are selected for the spline-curves in the wells, which are greater than their default values.

The new multiwell comparison shown in Display 52 differs from the earlier result shown in Figure 21 in that the 10 Ma and 40 Ma isochrons in Karlsefni now occur at greater distances above and below the unconformity. The unconformity itself has approximately the same depth. Due to lack of information, it is not possible to obtain precise estimates of the rates of sedimentation in the immediate vicinity of the unconformity at the site of Karlsefni H-13. This uncertainty is brought out in the differences in locations of the 10 Ma and 40 Ma isochrons resulting from different experiments.

CASC INTERACTIVE COMPUTER PROGRAM

The purpose of this section is to provide an introduction to material contained in the Appendix (overview of options and documentation of subroutines) intended for CASC users and programmers, respectively.

A special version of RASC called RASC-C is listed on diskette and should be run on the data set to be studied so that selected output of RASC can be used as input to CASC. The Gradstein-Thomas data base for 24 wells which is listed on the same diskette can be processed with RASC-C. Part of the output will then be stored in file-form as input for CASC.

Additionally, a file with depths for the events retained in RASC output for all wells and a file with ages in Ma for a subgroup of events are required. These files are also contained on this diskette. In the course of an interactive CASC session, several options require additional input which is fed in during the session when required.

The RASC program consists of two parts – ranking and scaling. The end product of the ranking part is an optimum sequence. The scaling part yields a scaled optimum sequence with different intervals between successive events. Because of minor reordering, the scaled optimum sequence is generally different from the optimum sequence obtained by ranking. An option of revised RASC consists of construction of scatter plots of events in individual wells against the optimum sequence or the scaled optimum sequence. The starting point of CASC is either the optimum sequence or RASC distances plotted in the horizontal direction against the so-called event scale. Consequently, inspection of RASC scattergram output can be helpful in planning a CASC interactive session. For example, possibly anomalous events to be removed by using the cursor at the beginning of a CASC session may already be identified on RASC output. The optimum sequence option is considerably simpler than the distance option.

Spline-curve fitting is an important ingredient of CASC. The cubic spline-curves are fitted by using an algorithm originally developed by Reinsch (1967) and available as subroutine ICSSCU in IMSL (International Mathematical and Statistical Libraries, Inc., Computer Subroutines Libraries in Mathematics and Statistics, Houston, Texas, U.S.). A version of the algorithm in FORTRAN has been published by de Boor (1978, Subprogram SMOOTH, pp. 240-242).

The CASC program was developed on a CDC Cyber 730 and is coded in FORTRAN Extended Version 4. Two libraries are required to use CASC: The Tektronix Advanced Graphing Library is used in addition to the IMSL Library. Also, mass storage facilities are used.

CASC is divided into several segments in order to facilitate memory management. Only necessary parts of the program are successively loaded into memory. When the system is finished with one portion of the program, it is

returned and memory is completely cleared except for input or intermediate files, so that the next segment can be loaded. With regard to further program development, if a segment of the program needs to be expanded or enhanced, space restrictions can be readily met with relatively minor program restructuring.

A procedure for loading the segments and returning them is required. For our own usage at the Department of Energy, Mines and Resources (EMR), a procedure file was created which contains control language commands of the EMR computer system. It asks the user which option is wanted, and which files are to be loaded or returned. This method is machine-dependent and alternate procedures would have to be developed at other computer installations.

A quick option for running either the optimum sequence option or distance CASC is available to the user wishing to make use of predetermined defaults for the various options. It should be chosen if only a cursory glance of the plots and tables is required. This feature is particularly useful to reach the multiwell comparison faster.

In general, the sound of a bell (beep) generated by the program indicates that a space bar followed by a carriage return is expected from the user. This pause gives the user an opportunity to obtain hard copies of the tables, graphs, and other output as required.

PLOT-10 which is utilized in CASC is a software package consisting of FORTRAN subroutines developed by Tektronix. The standard package is called the Terminal Control System. Use is also made of an additional PLOT-10 software package called Advanced Graphing-II providing extended and more comprehensive capabilities for displaying graphs.

An Enhanced Graphics Module is available on 4014 and 4015 Tektronix terminals. This hardware feature offers the possibility of having a grid of 4096 by 3120 addressable screen points. The standard addressing grid on these terminals is 1024 by 780 points. Use of the Enhanced Graphics Module is optional, because CASC supports both the 4096 and the 1024 addressing modes.

To run CASC with its PLOT-10 calls, one must have a Tektronix terminal, and the installation must support Tektronix software with its "Advanced Graphing II" library. No matter where the Tektronix software is used, if the installation supports it, all calling sequences remain the same. Necessary subroutines are selected at load time. Release 3 of the Terminal Control System is used for CASC at the EMR Computer Science Centre in Ottawa.

'Mass Storage' which is also utilized in CASC is an alternate way of storing data. In a conventional sequential file, records are stored in the order in which they were written so that they can be read back in the same order. Constant awareness of the current file position and the position of the record required is necessary. A randomly accessible file capability is provided by the Mass Storage Input/Output (MSIO) subroutines to remove these limitations. In a random file, any record can be written or read without concern for the current position of the file.

When a record is first written for addition to the mass storage file, a unique and permanent key is selected by the programmer to identify that record. Later, this record can be retrieved or updated using the same key. Keys to the records are kept in an array for which the programmer must declare space. Mass Storage

is a machine-dependent feature. Other installations may provide alternative methods for random file manipulations. CASC uses mass storage subroutines compatible with CDC FORTRAN Extended Version 4. Random file manipulations keep interactive processing at a more easily manageable level. For our application, it would be inconvenient and slower to retrieve information in a sequential fashion because of the nature of the data.

The IMSL (International Mathematical and Statistical Libraries, see before) Library is a set of computational subroutines written in FORTRAN. The IMSL subroutine ICSSCU is called by CASC. It places a smooth cubic spline along the data provided. The user supplies the degree of smoothing desired. The output spline coefficients are used to draw a smooth curve. In general, the number of points used for plotting the spline curve is ten times the number of data points initially provided.

An important input parameter for fitting a spline-curve is the smoothing factor SF. It can be useful to establish a set of default values for SF by fitting spline-curves that do not decrease with depth. These default values will be applied automatically in all wells when the defaults only option is used. This procedure generally results in a good set of first approximations which can be refined later. When a new well is selected for study, one of the first questions asked is whether or not the user wants to use all defaults. If the answer is yes, the results are obtained quickly and shown only briefly on the screen. It is not possible to obtain hard copies when this option is used. If the answer is no, it becomes possible to change the value of SF from the default at each specific display and to obtain hard copies. After the spline-curve for a selected value of SF has been fitted, the user is given the opportunity to replace the fitted spline-curve by another one corresponding to a newly selected smoothing factor.

Appendix 1 contains an overview of the options successively available to the CASC user during an interactive session. Appendix 2 consists of sample copies of CASC results displayed on the screen of the Tektronix (see discussions in previous section). Finally, in Appendix 3, all individual subroutines of CASC are documented in more detail.

References

Agterberg, F.P., in press, Probabilistic method for automated stratigraphic correlation, in Quantitative Stratigraphy-Retrospective Evaluation and Future Development; Oleynikov, N.A., and Rubel, M., eds. Institute of Geology, Acad. Sci. Esturian S.S.R., Tallinn, U.S.S.R.

Agterberg, F.P. and Gradstein, F.M., 1983, Interactive system of computer programs for stratigraphic correlation: Current Research, Geol. Survey of Canada, Paper 83-1A, p. 83-87.

Agterberg, F.P. and Gradstein, F.M., in press, Recent developments in quantitative stratigraphy: Earth-Science Reviews.

Agterberg, F.P. and Nel, L.D., 1982a, Algorithms for the ranking of stratigraphic events: Computers and Geosciences, v. 8, no. 1, p. 69-90.

_____, 1982b, Algorithms for the scaling of stratigraphic events: Computers and Geosciences, v. 8, no. 2, p. 163-189.

Berggren, W.A., Kent, D.V. and Flynn, J., in press, Paleogene chronology and chronostratigraphy, Geol. Soc. London, Spec. Paper.

Blank, R.C., 1979, Applications of probabilistic biostratigraphy to chronostratigraphy, J. Geol., v. 87, p. 647-670.

De Boor, C., 1978, A Practical Guide to Splines, Springer Verlag, New York, 392 p.

Doeven, P.H., Gradstein, F.M., Jackson, A., Agterberg, F.P., and Nel, D., 1982, A quantitative nannofossil range chart: Micropaleontology, v. 28, no. 1, p. 85-92.

Drooger, C.W., 1974, The boundaries and limits of stratigraphy, Proc. Kon, Ned, Akad. Wet. Ser. 11B, v. 17, p. 159-176.

Edwards, L.E., 1984, Insights on why graphic correlation (Shaw's method) works, J. Geol., v. 92, p. 583-597.

Gradstein, F.M. and Agterberg, F.P., 1982, Models of Cenozoic foraminiferal stratigraphy – northwestern Atlantic margin, in 'Quantitative Stratigraphic Correlation', J.M. Cubitt and R.A. Reyment, eds., J. Wiley and Sons Ltd., p. 119-170.

Gradstein, F.M., Agterberg, F.P., Brower, J. and Schwarzacher, W., in press, Quantitative Stratigraphic Correlation, Unesco/Reidel publication.

Gradstein, F.M. and Berggren, W.A., 1981, Flysch-type agglutinated Foraminifera and the Maestrichtian to Paleogene history of the Labrador and North Seas: Marine Micropal. v. 6, p. 211-268.

Gradstein, F.M. and Srivastava, S.P., 1980, Aspects of Cenozoic stratigraphy and paleogeography of Labrador Sea and Baffin Bay: Palaeogeogr., Palaeoclimatol., Palaeoecol., v. 30, p. 261-295.

Harper, C.W., Jr., 1984, A Fortran IV program for comparing ranking algorithms in quantitative biostratigraphy: Computers and Geosciences, v. 10, no. 1, p. 3-29.

Hay, W.W., 1972, Probabilistic stratigraphy: Eclogae Geol. Helv., v. 65, no. 2, p. 255-266.

Heller, M., Gradstein, W.S., Gradstein, F.M., and Agterberg, F.P., 1983, RASC-Fortran IV computer program for ranking and scaling of biostratigraphic events: Geol. Survey of Canada, Open File 922, 54 p.

Jackson, A., Lew, S.N., and Agterberg, F.P., 1984, DISSPLA program for display of dendrograms from RASC output: Computers and Geosciences, v. 10, no. 1, p. 159-165.

Miller, F.X., 1977, The graphic correlation method in biostratigraphy, in 'Concepts and Methods of Biostratigraphy', E.G. Kauffman and J.E. Hazel, eds., Dowden, Hutchison and Ross, Inc., Stroudsburg, USA, p. 165-186.

Muller, C. and Willems, W., 1981, Nannoplankton en planktonische foraminiferen uit de Ieper-Formatie (Onder-Eoceen) in Vlaanderen (Belgie), Natuurw, Tijdschr., v. 62, p. 64-71.

Reinsch, C.H., 1967, Smoothing by spline functions: Num., Mathematik, v. 10, p. 177-183.

Rubel, M., 1978, Principles of construction and use of biostratigraphical scales for correlation: Computers & Geosciences, v. 4, no. 3, p. 243-246.

Shaw, A.B., 1964, Time in Stratigraphy, McGraw-Hill Book Co., New York, 365 pp.

Tjalsma, R.C. and Lohmann, G.P., 1983, Paleocene-Eocene bathyal and abyssal benthic foraminifera from the Atlantic Ocean, Micropal. Spec. Publ., no. 4, 76 pp.

Williamson, M.J., in press, Quantitative biozonation of the Late Jurassic and Early Cretaceous of the East Newfoundland Basin: Micropaleontology.

List of Illustrations

Figure 1. Example of ranking and scaling of ten biostratigraphic events in nine sections. (a) Original data after Hay (1972); explanation of symbols is given in text. Subjective ranking resulted in order of Column 1; original optimum sequence is shown in Column 2 on right side. (b) Dictionary for RASC computer program; LO = lowest occurrence; HO = highest occurrence. (c) Sequences of Figure 1a coded as RASC input; hyphens denote coeval events. (d) Optimum sequence (RASC output); range indicates undertainty of sequence position. (e) Optimum clustering (scaling output) of the ten events. Distances from each event to the next were also plotted horizontally and connected by vertical lines. Note that events 1 to 6 form a cluster because they tend to be coeval. For further explanation, see text.

Figure 2. Graphical illustration of correlation, using the computer program CASC (Correlation and SCaling in time); x_1 - observed sequence of events in Adolphus well; x_2 – observed sequence of events in Flying Foam well; y – optimum sequence of events in 21 wells (7-2-4 condition); z – depth scale. The most likely position of selected optimum sequence events in each well is found by projecting these events via the two best fit lines (line of correlation and line of observation) onto the (well) depth scale. The most likely position of event 29 (top of **Cyclammina amplectens**) in Flying Foam is at 4850' (observed 5300') and in Adolphus at 6050' (observed 5200').

Figure 3. Plot of the Cenozoic scaled optimum sequence (21 wells; 7-2-4 run) versus linear time in Ma. The interfossil distances are plotted cumulatively. For some selected events in the scaled optimum sequence the numerical age is known, which allows to scale the whole fossil sequence in linear time.

Figure 4. The RASC biochronology of Figure 3 is used to estimate rate of sedimentation (dashed line) in the Adolphus D-50 well. The solid line (subjective) shows approximately the same trend, using independent well history data.

Figure 5. Schematic illustration of method followed in CASC computer program to establish relation between RASC distance and age.

(a) Two (or more) RASC distances for the same age are averaged;

(b) Cubic spline curve is fitted using age as the dependent variable; smoothing factor (SF) representing standard deviation of differences between event ages and curve is chosen in advance, before curve fitting;

(c) Standard deviation (SD) for differences between original values and curve is computed after curve fitting; and

(d) Fitted curve is used to convert any RASC distance into corresponding age.

Figure 6. Schematic illustration of preliminary computing and optional editing procedure at beginning of CASC computer program;

(a) Events found to be anomalous with a probability of over 99 percent (asterisk) may be omitted from spline curve fitting and later plots; RASC distances of two (or more) coeval events are averaged;

(b) Cubic spline curve is fitted using RASC distance as the dependent variable; smoothing factor (SF) representing standard deviation of differences between RASC distances assigned to levels and curve is chosen in advance;

(c) Standard deviation (SD) is computed from differences between original values and curve after curve fitting; original values (e.g., those labelled R) can be deleted; and

(d) New curve with new standard deviation (SD) is obtained without use of deleted values.

Figure 7. Schematic illustration of calculation of an age-depth curve from RASC output for a well.

(a) RASC distances have been replaced by ages using relation illustrated in Figure 5d; new spline curve $f(\underline{x})$ is fitted; bar in $\underline{x}$ denotes use of regular sampling interval for x; smoothing factor (SF), which was selected before curve fitting using one age per level, is smaller than standard deviation (SD) for all original values;

(b) Spline curve g(x) is fitted to express depth as a function of level x; bar in $\underline{x}$ denotes use of regular sampling interval for x; bar in $\underline{x}$ denotes use of regular sampling interval for x; SM = SD is equal to some small value;

(c) $\hat{x}$ represents spline curve $g(\underline{x})$ in Figure 7b now coded as set of values for x at regular interval of z;

(d) $\hat{y}_{xz}$ denotes curve passing through set of values of y at regular interval of z obtained by combining spline curve of Figure 7a with that of Figure 7c;

(e) $\hat{y}$ is spline curve fitted to values y_{zx} of Figure 7d using new smoothing factor SF; and

(f) Standard deviation SD is computed after curve fitting, using one age per level.

Figure 8. Schematic illustration of estimation of local error bar and modified local error bar.

(a) Standard deviation SD was computed after curve fitting, using one age per level;

(b) Error bar of age value plus or minus SD along Y-axis is transformed into error bar along Z-axis using first derivative (ds/dy) of age-depth curve;

(c) Rate of sedimentation (=dx/dy) can be displayed on screen during CASC interactive session; and

(d) Modified local error bar is asymmetrical with respect to depth value for a given age.

Figure 9. Example of multiwell comparison with error bar. For locations of wells, see Figure 20. Methods used for constructing different types of error bars are illustrated in Figures 8 and 10. Local error bar (A) and global error bar (C) estimates can be displayed on screen during CASC interactive session. Modified local error bar (B) estimates were obtained from final age-depth curves for these five wells.

Figure 10. Schematic illustration of estimation of global error bar. Theoretical standard deviation σ (= 0.7071) along RASC distance scale is assumed to remain constant. It is transformed into variable SD along age scale (e.g., SD' and SD").

Figure 11. Example of CASC displays for Indian Harbour M-52 (based on 7-2-4 RASC results for 21 wells).

(a) Age-RASC distance relationship as derived from the 21 wells file, using method explained in Figure 5;

(b) Initial CASC plot for default smoothing factor;

(c) Age-level plot for default SF;

(d) First derivative of (c);

(e) Level-depth plot; and

(f) Age-depth plot for default SF; spline curve was fitted directly to the data, using irregularly spaced depths.

Figure 12. Example of CASC displays for Indian Harbour M-52 (continued from Figure 11).

(a) Spline curve for small (default) SF fitted to combination of Figures 11c and 11e; indirect method explained in Figure 7 was used;

(b) Sedimentation rate in 0.1 km/Ma (= first derivative of spline curve in Figure 12a multiplied by 10); local maximum and minimum are due to lack of smoothness of spline curve as explained in text;

(c) Age-level plot for SF = 4.0 instead of default, used in Figure 11c;

(d) First derivative for Figure 12c; magnitude of peak in Figure 11d had been reduced;

(e) Spline curve for small (default) SF fitted to combination of Figures 11e and 12c; and

(f) Sedimentation rate in 0.1 km/Ma corresponding to Figure 12e.

Figure 13. Example of CASC displays for Indian Harbour M-52 (continued from Figures 11 and 12).

(a) Unsmoothed combination of Figures 11e and 12c; note similarity with spline curve in Figure 12e for SF = 0.1;

(b) Curve of Figure 13a smoothed with SF = 1.0;

(c) Sedimentation rate in 0.1 km/Ma corresponding to Figure 13b;

(d) Level-depth plot for SF = 0.0

(e) Spline curve for small (default) SF fitted to combination of Figures 12c adn 13d; note similarity with spline curve in Figure 12e; and

(f) Sedimentation rate in 0.1 km/Ma corresponding to Figure 12e; local maxima and minima are due to lack of smoothness of spline-curve as explained in text.

Figure 14. Example of CASC displays for Adolphus D-50 (5-2-3 RASC results using 24 wells).

(a) Age-level plot for SF = 2.2;

(b) First derivative corresponding to Figure 14a; note small peak near level 14;

(c) Event-depth plot; note relatively steep slopes at depths near 0.7 km and 2.2 km, respectively;

(d) Spline curve with small (default) SF fitted to combination of Figures 14a and 14c;

(e) Sedimentation rate in 0.1 km/Ma corresponding to Figure 14d; two relatively high peaks correspond to steeper slopes in Figure 14c; intermediate small peak corresponds to highest first derivative in Figure 14b; and

(f) Age-depth spline curve fitted directly to the data using irregularly spaced depths; note similarity with spline curve of Figure 14d; direct method yields poorer results than indirect method when one or more intervals between successive ages are much larger than average due to high sedimentation rate or relative lack of microfossils.

Figure 15. Cenozoic optimum sequence and scaled optimum sequence based on last occurrences of foraminifera in 21 wells, Labrador – Grand Banks (7-2-4 run). This is the same zonation as presented in Gradstein et al. (in press).

Figure 16. Tracing of ten foraminiferal events through six wells, using the CASC (optimum sequence) method to calculate the most likely depth. Black bars show the deviation of this depth to the observed one. The chronostratigraphic segmentation is based on observed depths only.

Figure 17. Correlation of the RASC zones of **Spiroplectammina carinata** (taxa no.'s 28, 71, 21 and 20), Miocene, and of **Turborotalia pomeroli – Cyclammina amplectens** (taxa no.'s 260, 261, 263, 32 and 29), Eocene in six wells. CASC depths for the oldest and youngest of the used zone fossils, are shown in meters. Limits over which the zones would extend using the subjective, observed events depths are shown hatched. A – is the most likely depth of **Ammodiscus latus**, at the base of the RASC zone of **Turrilina alsatica,** Oligocene.

Figure 18. Correlation of 8 Cenozoic isochrons, according to their most likely depths in 10 wells, Grand Banks – Labrador Shelf. The depths were computed by means of the RASC-CASC method explained in the text. Subjective estimates for the depths of these isochrons are shown with x.

Figure 19. Correlation of the subjective and RASC-CASC derived, most likely depth for Early Cretaceous isochrons (=RASC zonal boundaries) in northern Grand Banks wells, (after Williamson, in press).

Figure 20. Locations of five wells on Labrador Shelf used for example in Figures 21 and 22 (and Displays 38 to 52).

Figure 21. Correlation of 5 wells shown in Figure 20. Results obtained by means of early version of CASC (from Agterberg and Gradstein, 1983).

Figure 22. Cumulative sediment accumulation (SA) is plotted relative to paleoseafloor through time, as derived from paleowaterdepth (PWD) interpretations to illustrate subsidence and depositional history. WEll site is Karlsefni H-13 (from Gradstein and Srivastava, 1980, p. 274). Note similarity with results for Karlsefni H-13 shown in Figure 21 and Display 52.

LIST OF TABLES

a

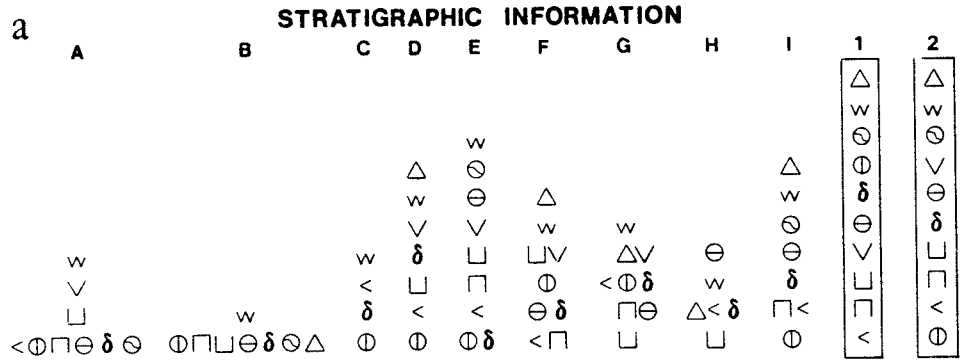

b

1 LO DISCOASTER DISTINCTUS
2 LO COCCOLITHUS CRIBELLUM
3 LO DISCOASTER GERMANICUS
4 LO COCCOLITHUS SOLITUS
5 LO COCCOLITHUS GAMMATION
6 LO RHABOOSPHAERA SCABROSA
7 LO DISCOASTER MINIMUS
8 LO DISCOASTER CRUCIFORMIS
9 HO DISCOASTER TRIBRACHIATUS
10 LO DISCOLITHUS DISTINCTUS

c

Section	Observed events
A	1 -2 -3 -4 -5 -6 7 8 9
B	2 -3 -7 -4 -5 -6 -10 9
C	2 5 1 9
D	2 1 7 5 8 9 10
E	2 -5 1 3 7 8 4 6 9
F	1 -3 4 -5 2 7 -8 9 10
G	7 3 -4 1 -2 -5 10 -8 9
H	7 10 -1 -5 9 4
I	2 3 -1 5 4 6 9 10

d OPTIMUM FOSSIL SEQUENCE

SEQUENCE POSITION	FOSSIL NUMBER	RANGE	FOSSIL NAME
1	9	0 — 3	HO DISCOASTER TRIBRACHIATUS
2	10	0 — 3	LO DISCOLITHUS DISTINCTUS
3	8	2 — 5	LO DISCOASTER CRUCIFORHIS
4	6	1 — 5	LO RHABOOSPHAERA SCABROSA
5	4	4 — 6	LO COCCOLITHUS SOLITUS
6	7	5 — 8	LO DISCOASTER MINIMUS
7	5	5 — 8	LO COCCOLITHUS GAMMATION
8	1	7 — 10	LO DISCOASTER DISTINCTUS
9	3	7 — 11	LO DISCOASTER GERMANICUS
10	2	8 — 11	LO COCCOLITHUS CRIBELLUM

e

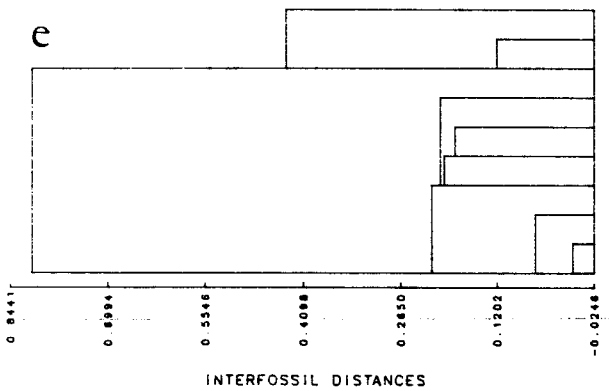

9	0.4354	HO DISCOASTER TRIBRACHIATUS
10	0.1205	LO DISCOLITHUS DISTINCTUS
8	0.8120	LO DISCOASTER CRUCIFORHIS
6	0.2060	LO RHABOOSPHAERA SCABROSA
4	0.1835	LO COCCOLITHUS SOLITUS
7	0.2002	LO DISCOASTER MINIMUS
5	0.2189	LO COCCOLITHUS GAMMATION
1	0.0635	LO DISCOASTER DISTINCTUS
3	0.0076	LO DISCOASTER GERMANICUS
2		LO COCCOLITHUS CRIBELLUM

Fig. 1

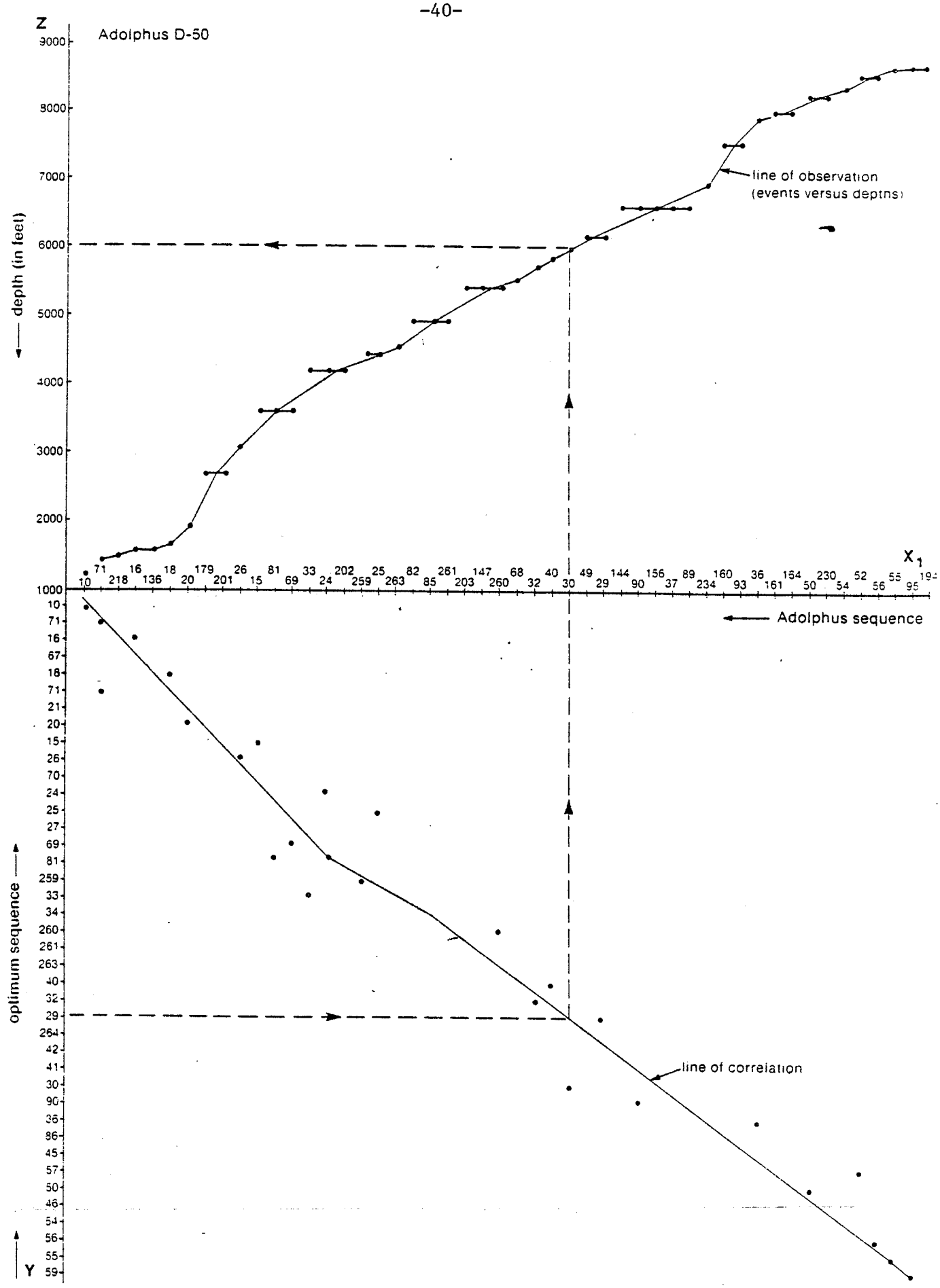

Fig. 2 (left side)

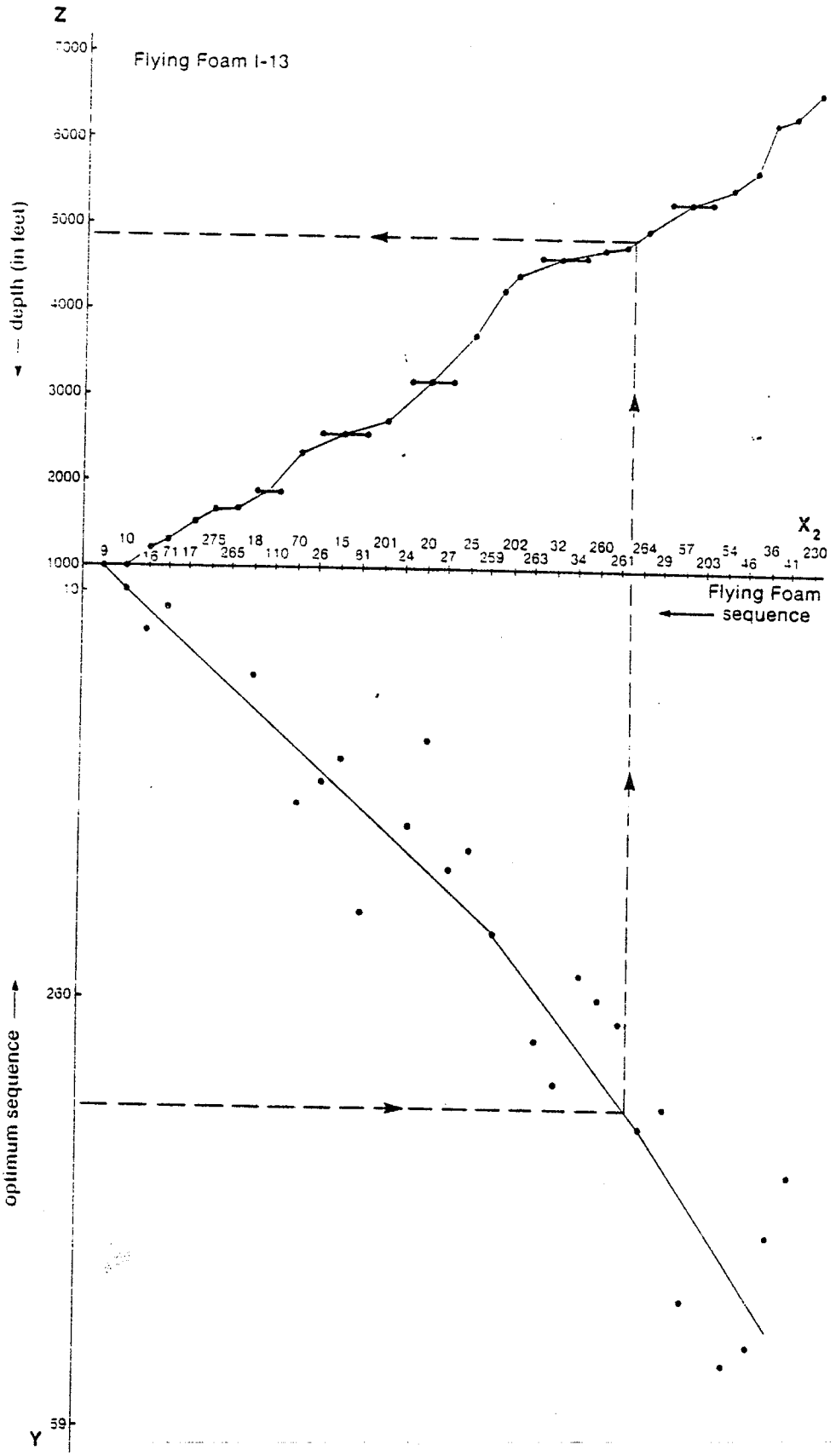
Z
Flying Foam I-13
7000
6000
5000
4000
3000
2000
1000
depth (in feet)
X_2
9 10 15 71 17 275 265 18 110 70 26 15 81 201 24 20 27 25 259 202 263 32 34 260 261 264 29 57 203 54 46 36 41 230
Flying Foam sequence
optimum sequence
260
Y
59

Fig. 2

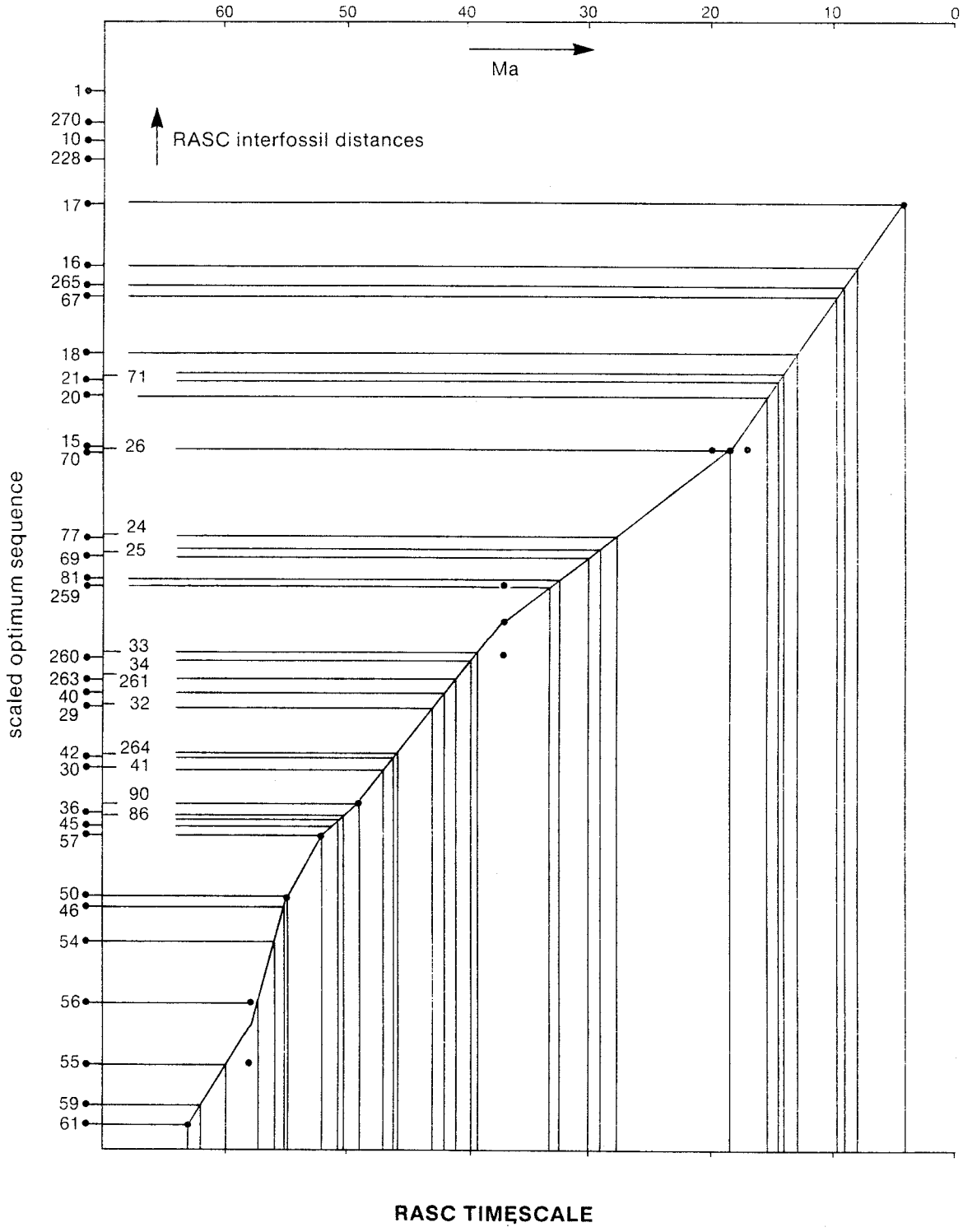
60
50
40
30
20
10
0
Ma
RASC interfossil distances
scaled optimum sequence
1
270
10
228
17
16
265
67
18
21
71
20
15
26
70
77
24
69
25
81
259
260
33
34
263
261
40
32
29
42
264
30
41
36
90
45
86
57
50
46
54
56
55
59
61
RASC TIMESCALE

Fig. 3

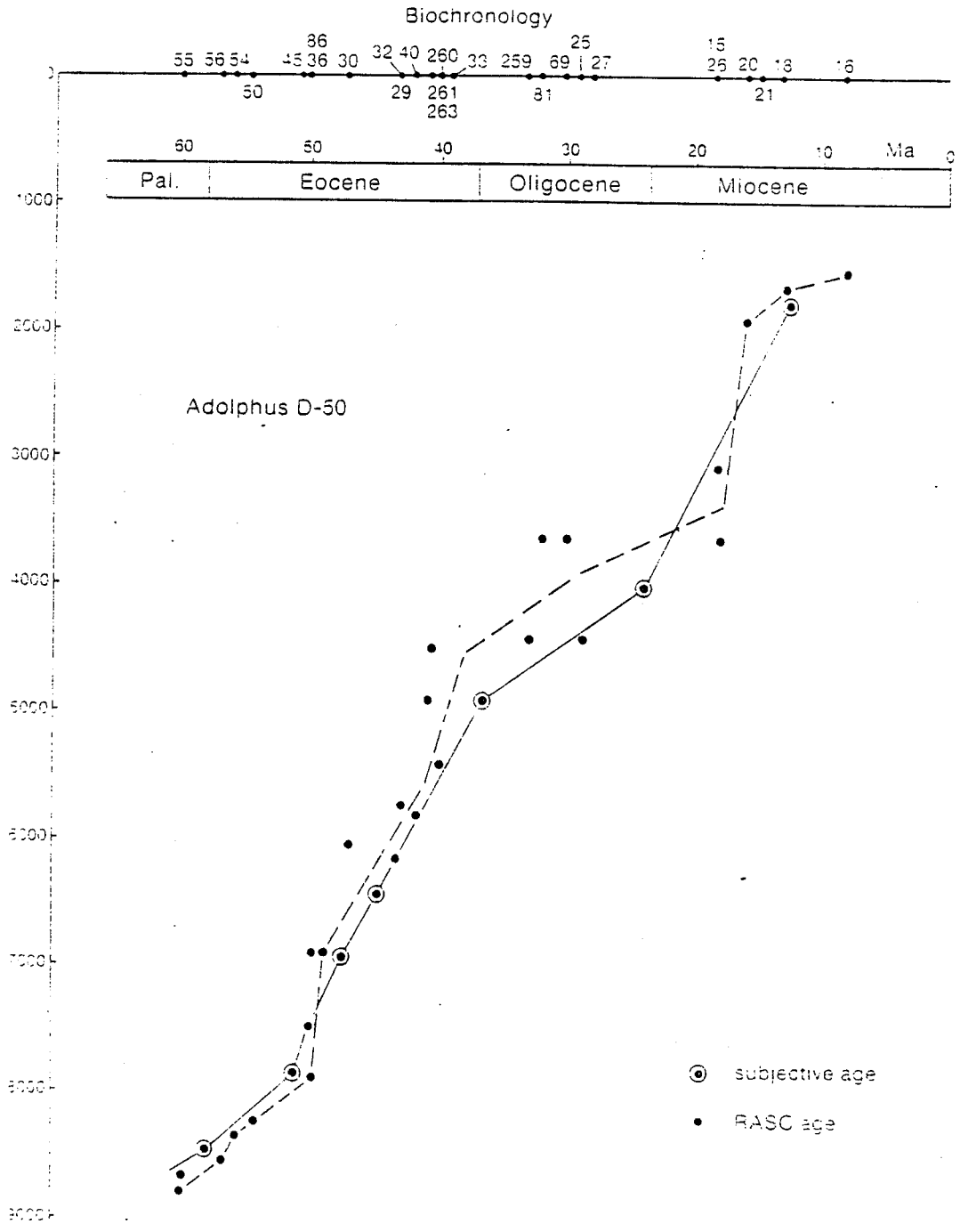
Biochronology
55 56 54 86 45 36 30 32 40 260 33 259 69 25 27 15 26 20 18 16
50 29 261 263 81 21
60 50 40 30 20 10 Ma 0
Pal. Eocene Oligocene Miocene
1000
2000
3000
4000
5000
6000
7000
8000
9000
Adolphus D-50
subjective age
RASC age
SEDIMENT ACCUMULATION

Fig. 4

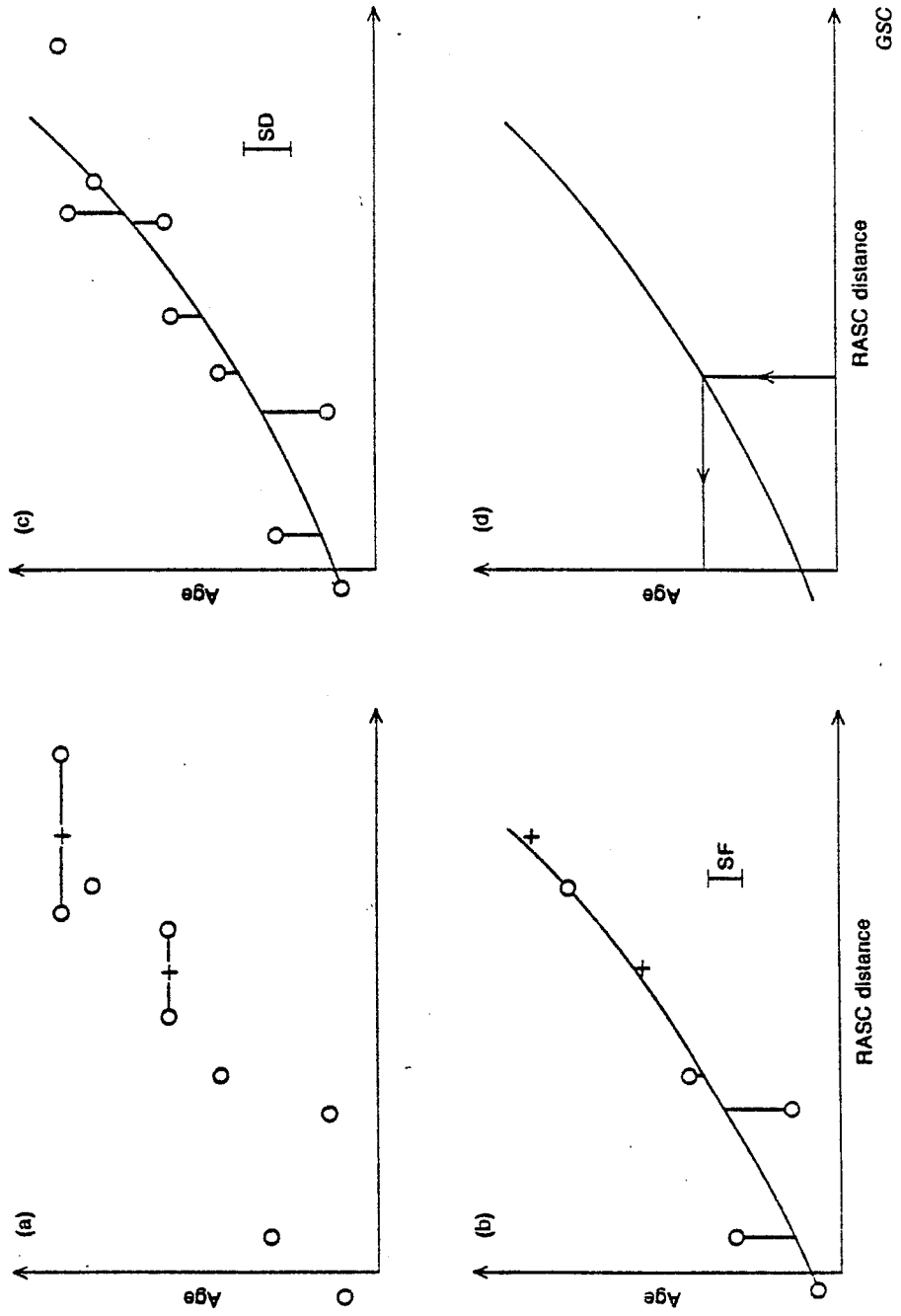

Fig. 5

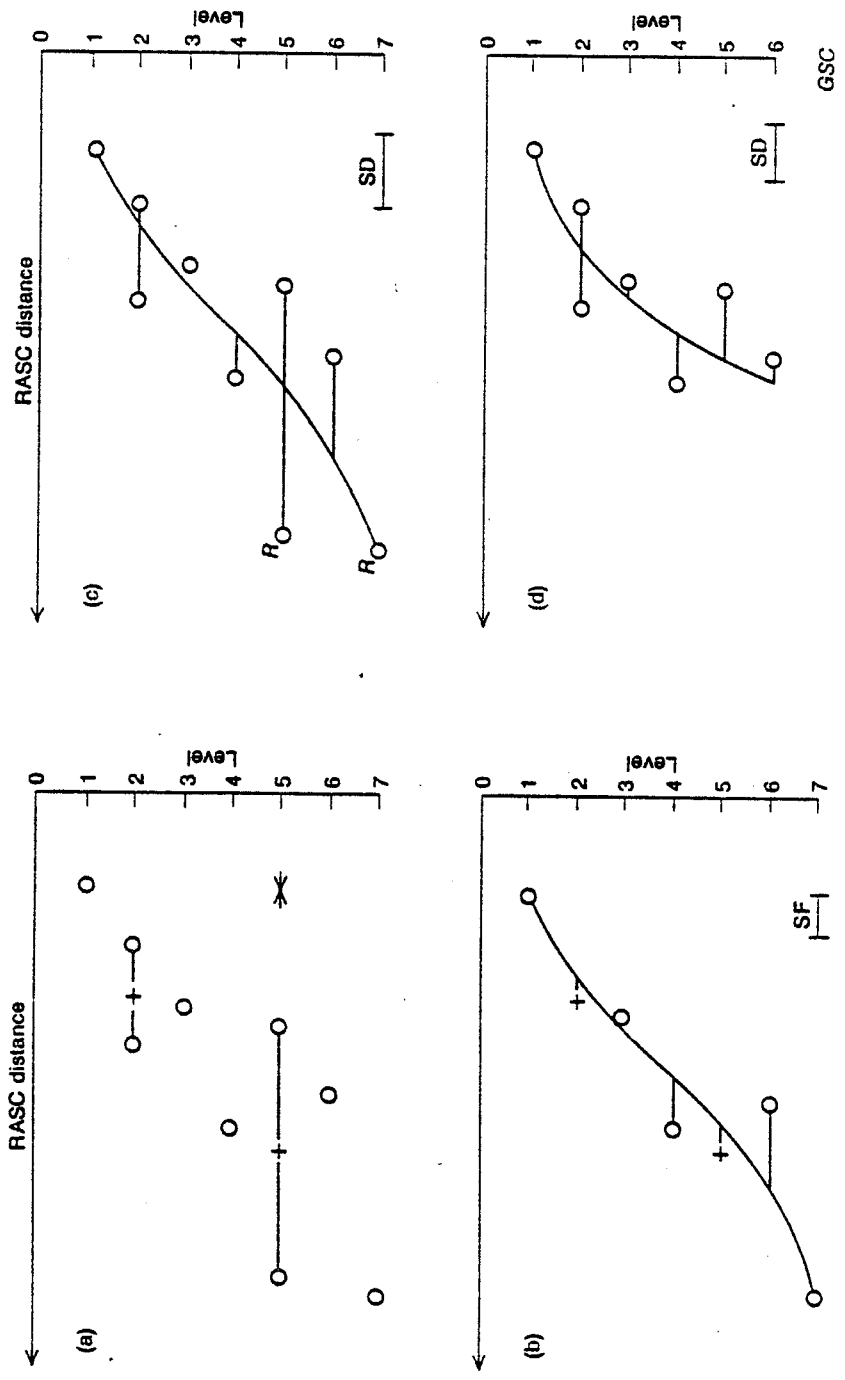

Fig. 6

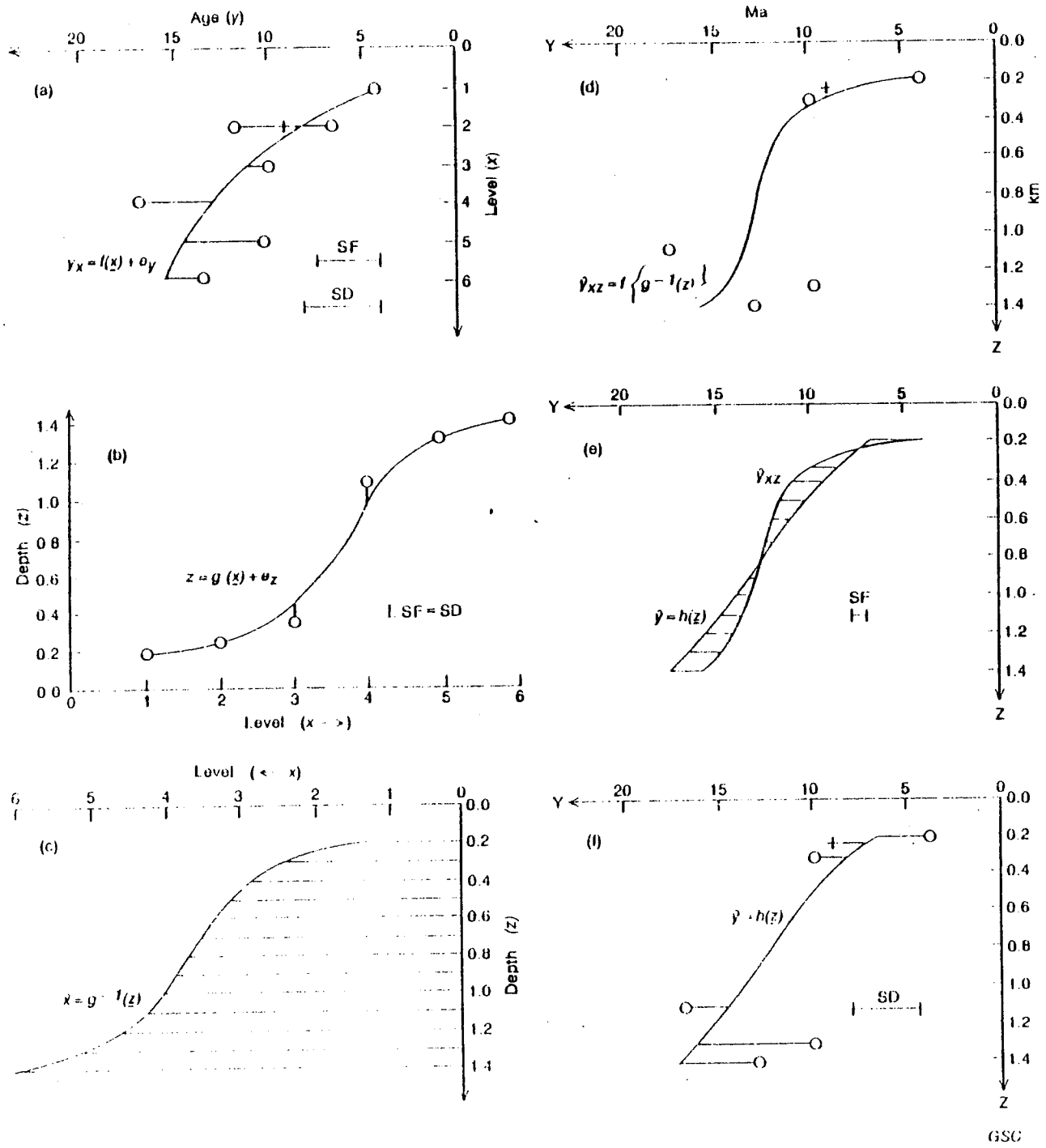
Age (y)
20
15
10
5
0
(a)
Level (x)
SF
SD
Ma
(d)
km
Z
(b)
Depth (z)
Level (x →)
I. SF = SD
(e)
SF
(c)
Level (← x)
Depth (z)
(f)
SD
GSC

Fig 7

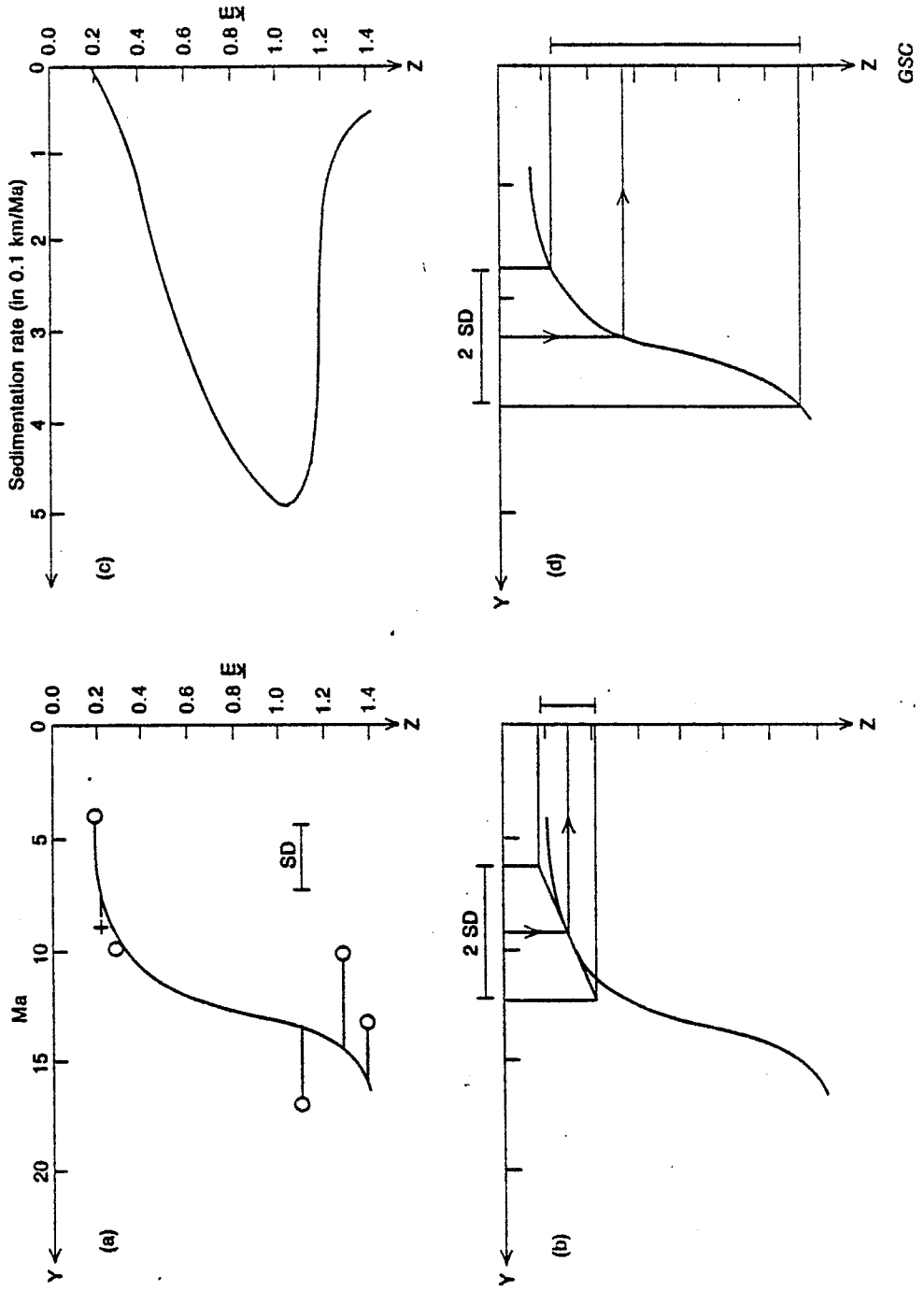
Sedimentation rate (in 0.1 km/Ma)
0
1
2
3
4
5
0.0
0.2
0.4
0.6
0.8
1.0
1.2
1.4
Ξ
Z
(c)
Ma
0
5
10
15
20
SD
Y
(a)
2 SD
(d)
GSC
(b)

Fig. 8

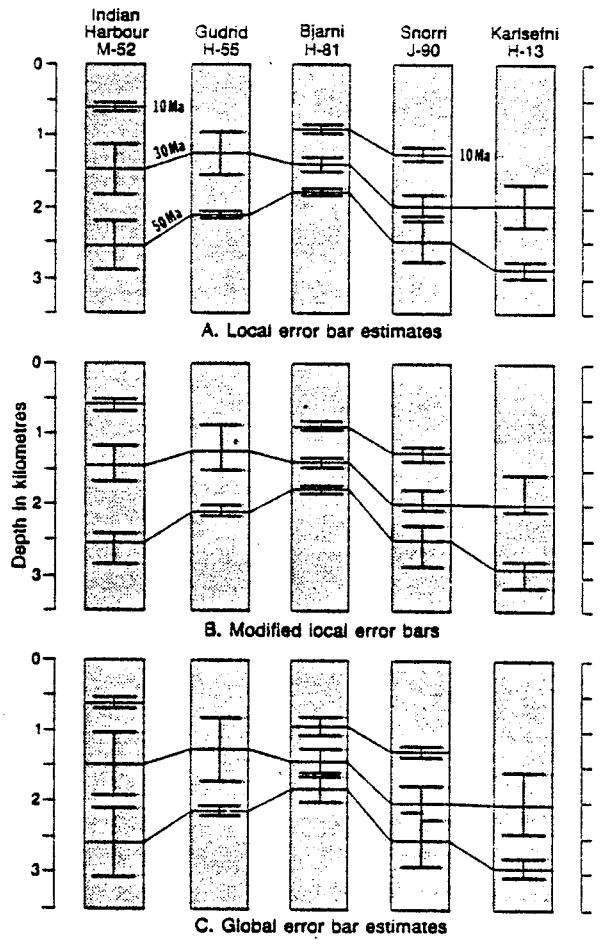
Indian Harbour M-52
Gudrid H-55
Bjarni H-81
Snorri J-90
Karlsefni H-13
10 Ma
30 Ma
50 Ma
10 Ma
0
1
2
3
A. Local error bar estimates
Depth in kilometres
B. Modified local error bars
C. Global error bar estimates

Fig. 9

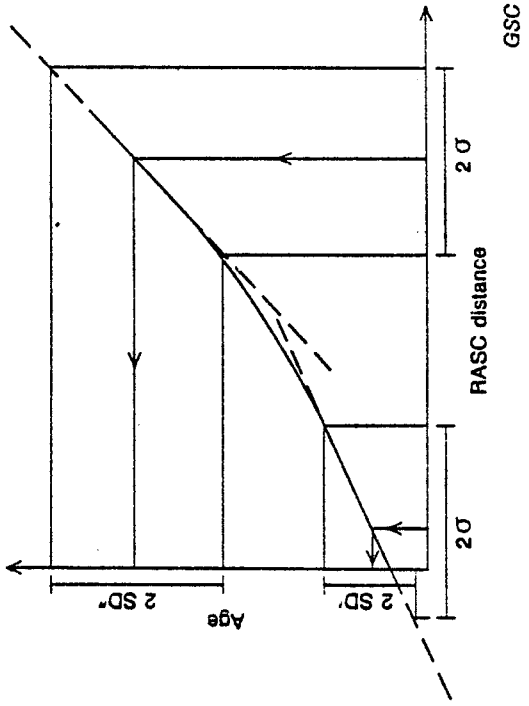

Fig. 10

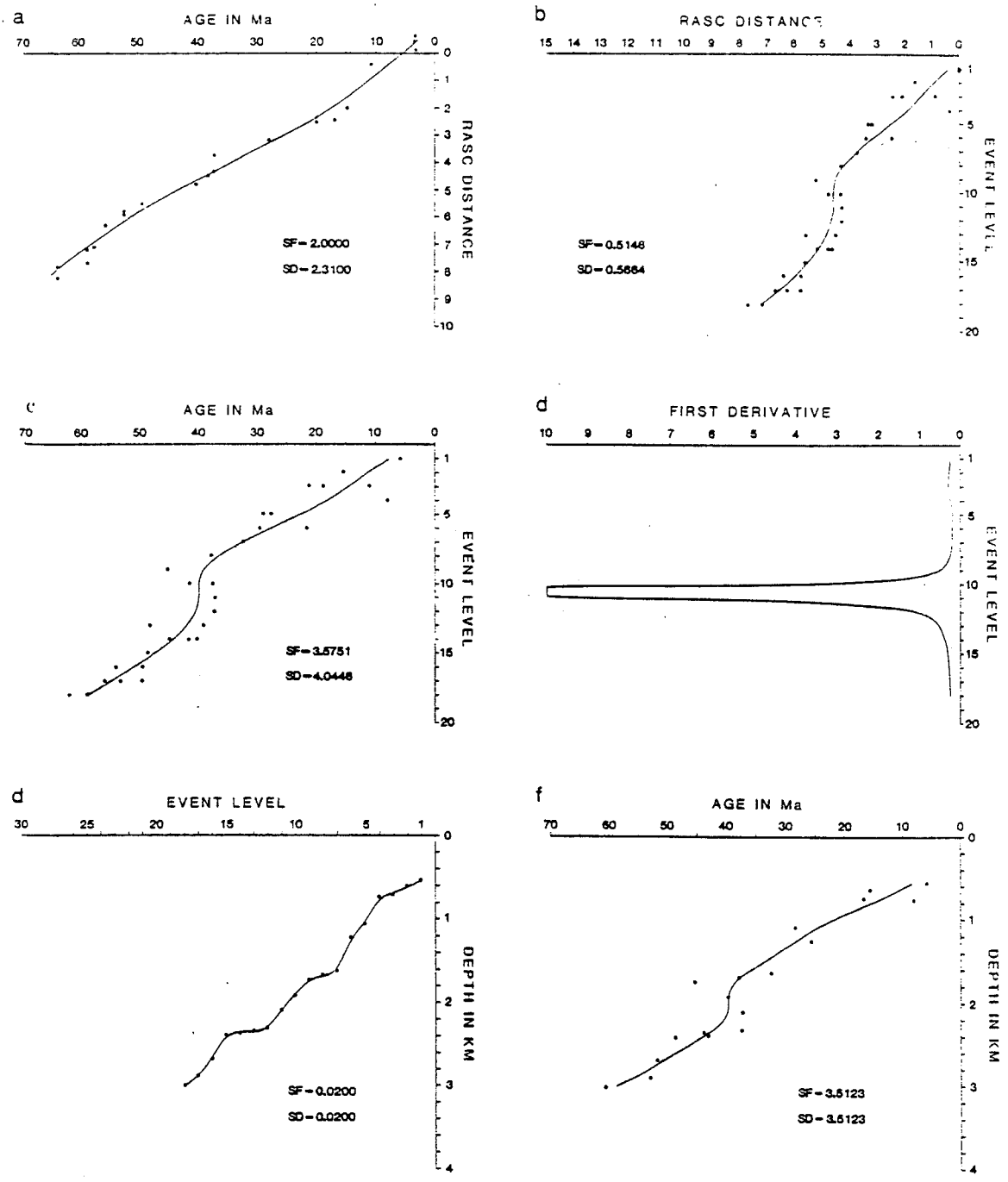
a
AGE IN Ma
70 60 50 40 30 20 10 0
RASC DISTANCE
0 1 2 3 4 5 6 7 8 9 10
SF = 2.0000
SD = 2.3100
b
RASC DISTANCE
15 14 13 12 11 10 9 8 7 6 5 4 3 2 1 0
EVENT LEVEL
1 5 10 15 20
SF = 0.5146
SD = 0.5664
c
AGE IN Ma
70 60 50 40 30 20 10 0
EVENT LEVEL
1 5 10 15 20
SF = 3.5751
SD = 4.0446
d
FIRST DERIVATIVE
10 9 8 7 6 5 4 3 2 1 0
EVENT LEVEL
1 5 10 15 20
d
EVENT LEVEL
30 25 20 15 10 5 1
DEPTH IN KM
0 1 2 3 4
SF = 0.0200
SD = 0.0200
f
AGE IN Ma
70 60 50 40 30 20 10 0
DEPTH IN KM
0 1 2 3 4
SF = 3.5123
SD = 3.5123

Fig. 11

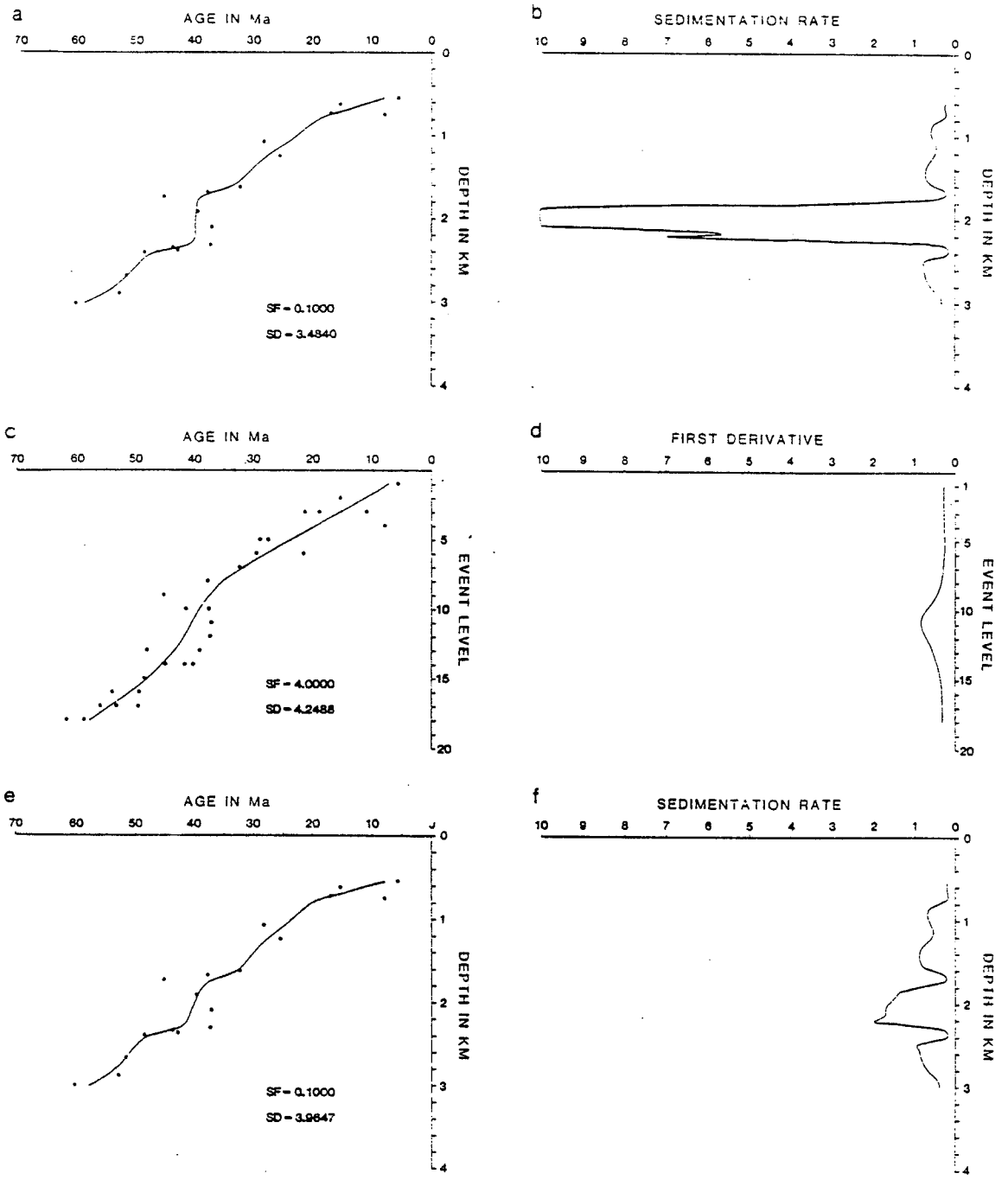
a
AGE IN Ma
70 60 50 40 30 20 10 0
DEPTH IN KM
SF = 0.1000
SD = 3.4840
b
SEDIMENTATION RATE
10 9 8 7 6 5 4 3 2 1 0
DEPTH IN KM
c
AGE IN Ma
70 60 50 40 30 20 10 0
EVENT LEVEL
SF = 4.0000
SD = 4.2488
d
FIRST DERIVATIVE
10 9 8 7 6 5 4 3 2 1 0
EVENT LEVEL
e
AGE IN Ma
70 60 50 40 30 20 10 0
DEPTH IN KM
SF = 0.1000
SD = 3.9647
f
SEDIMENTATION RATE
10 9 8 7 6 5 4 3 2 1 0
DEPTH IN KM

Fig. 12

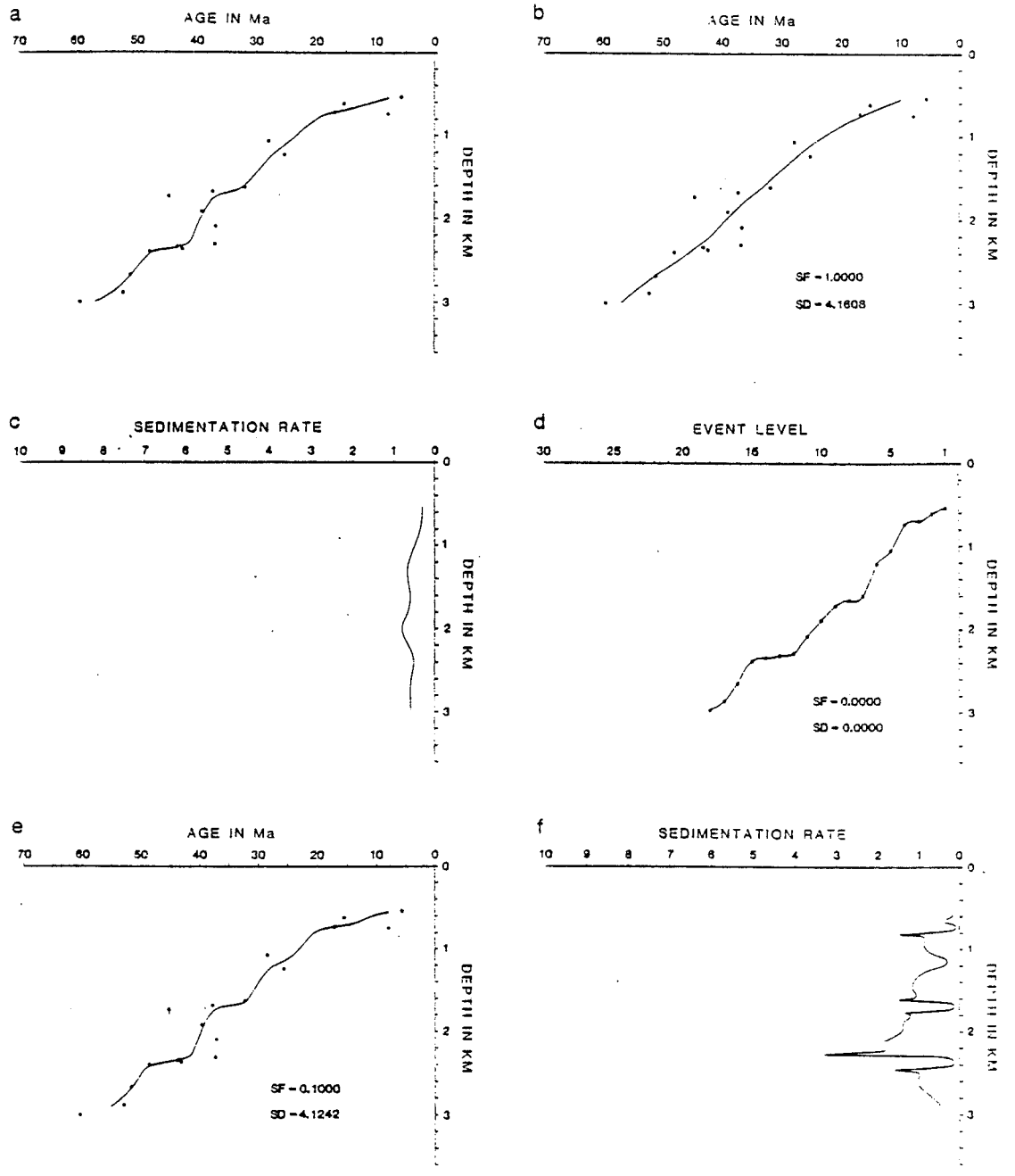
a
AGE IN Ma
70 60 50 40 30 20 10 0
DEPTH IN KM
b
AGE IN Ma
70 60 50 40 30 20 10 0
SF = 1.0000
SD = 4.1608
DEPTH IN KM
c
SEDIMENTATION RATE
10 9 8 7 6 5 4 3 2 1 0
DEPTH IN KM
d
EVENT LEVEL
30 25 20 15 10 5 1
SF = 0.0000
SD = 0.0000
DEPTH IN KM
e
AGE IN Ma
70 60 50 40 30 20 10 0
SF = 0.1000
SD = 4.1242
DEPTH IN KM
f
SEDIMENTATION RATE
10 9 8 7 6 5 4 3 2 1 0
DEPTH IN KM

Fig. 13

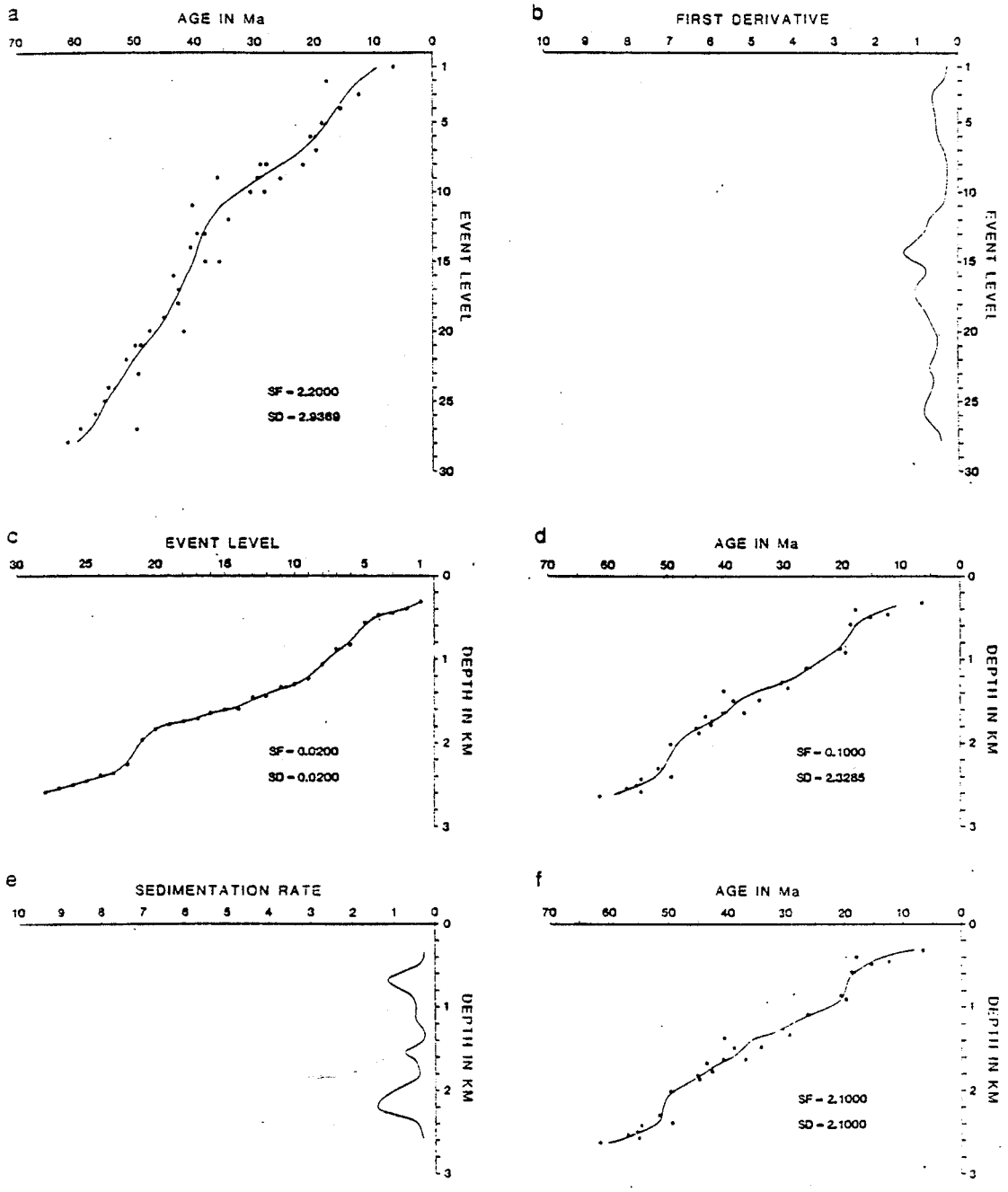
a
AGE IN Ma
70 60 50 40 30 20 10 0
EVENT LEVEL
SF = 2.2000
SD = 2.9369
b
FIRST DERIVATIVE
10 9 8 7 6 5 4 3 2 1 0
EVENT LEVEL
c
EVENT LEVEL
30 25 20 15 10 5 1
DEPTH IN KM
SF = 0.0200
SD = 0.0200
d
AGE IN Ma
70 60 50 40 30 20 10 0
DEPTH IN KM
SF = 0.1000
SD = 2.3285
e
SEDIMENTATION RATE
10 9 8 7 6 5 4 3 2 1 0
DEPTH IN KM
f
AGE IN Ma
70 60 50 40 30 20 10 0
DEPTH IN KM
SF = 2.1000
SD = 2.1000

Fig. 14

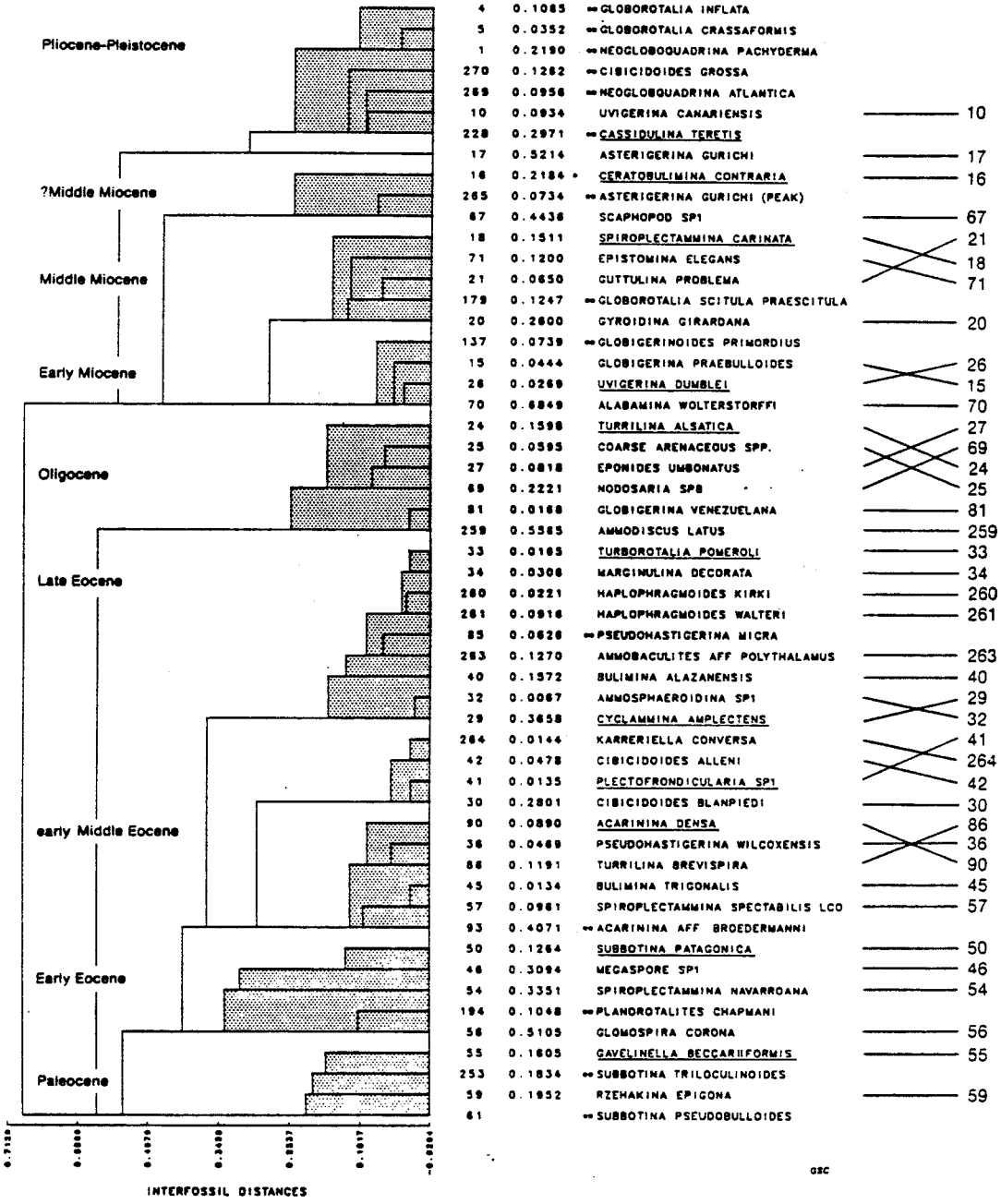

CENOZOIC ZONATION GRAND BANKS/LABRADOR

Fig. 15

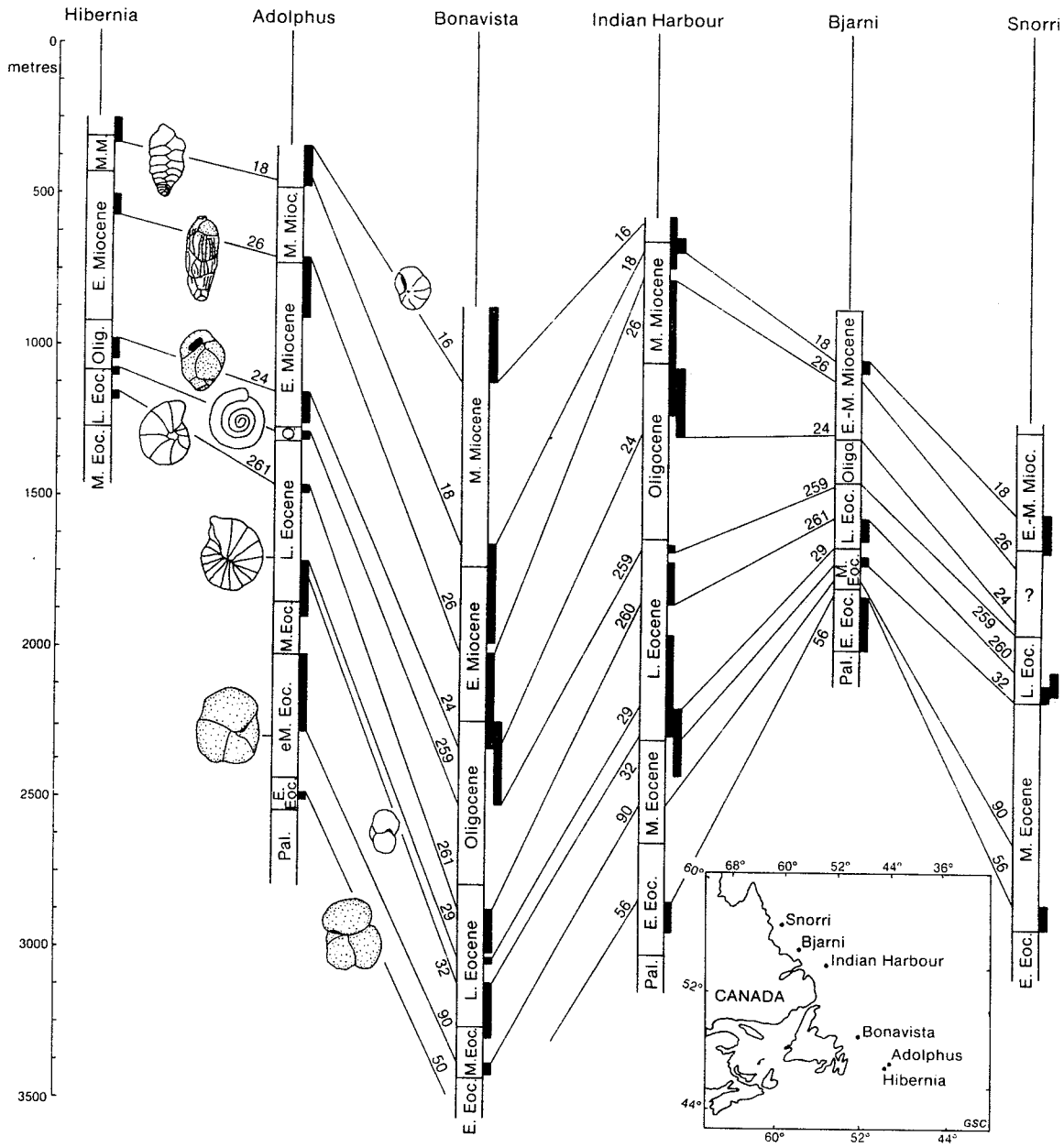

EVENT CORRELATION

Fig. 16

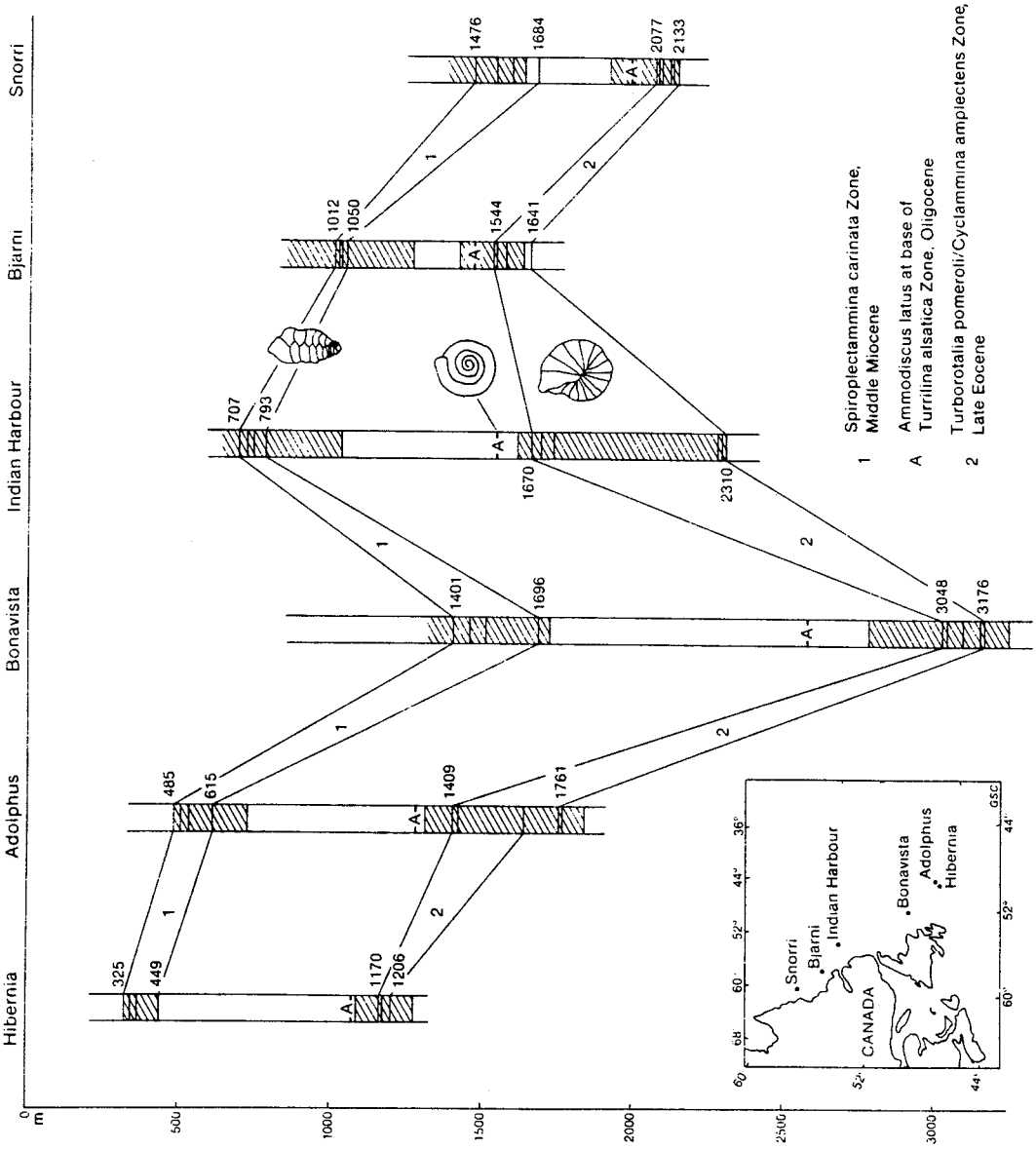

ZONAL CORRELATION

Fig. 17

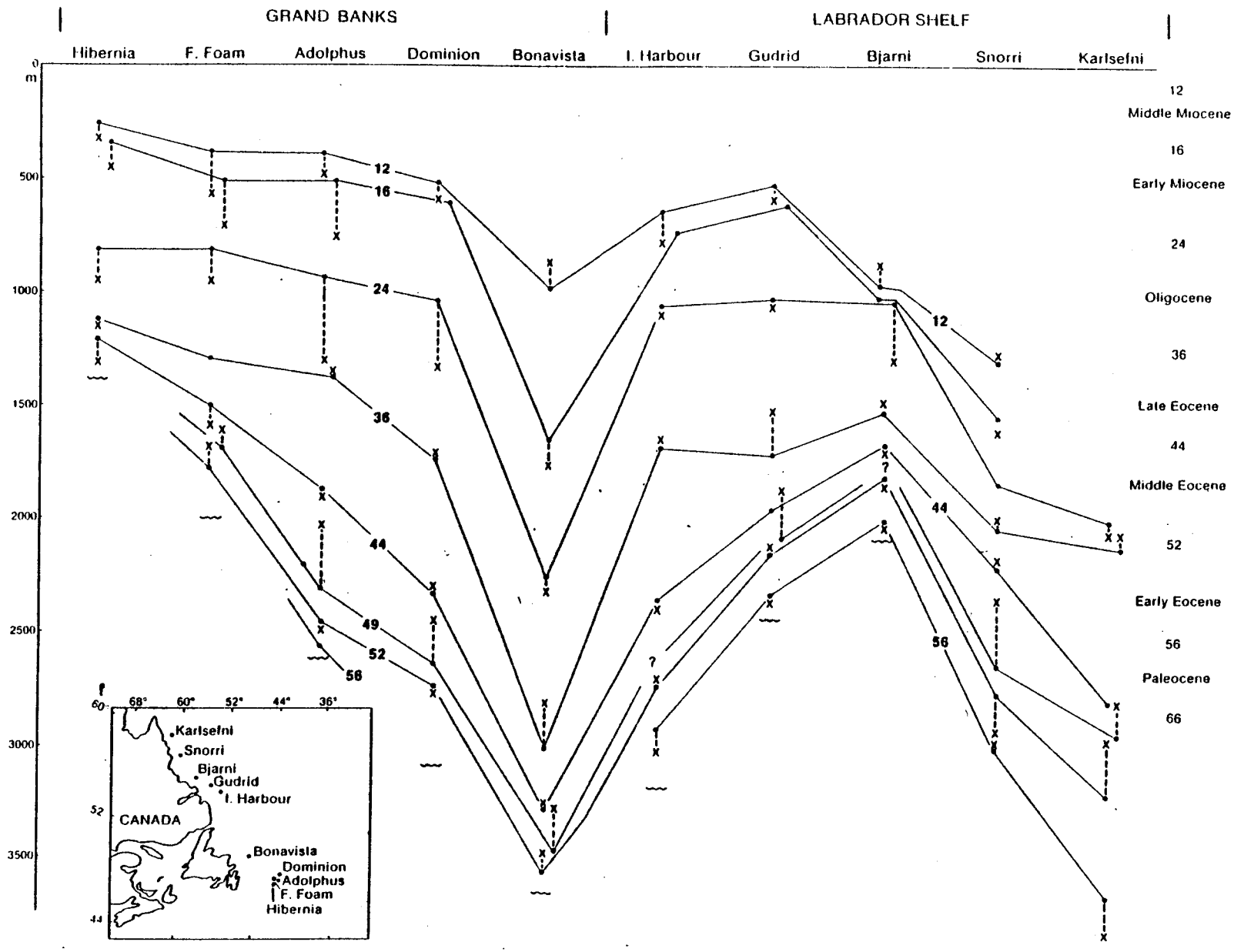

CORRELATIONS OF WELLS

Fig. 18

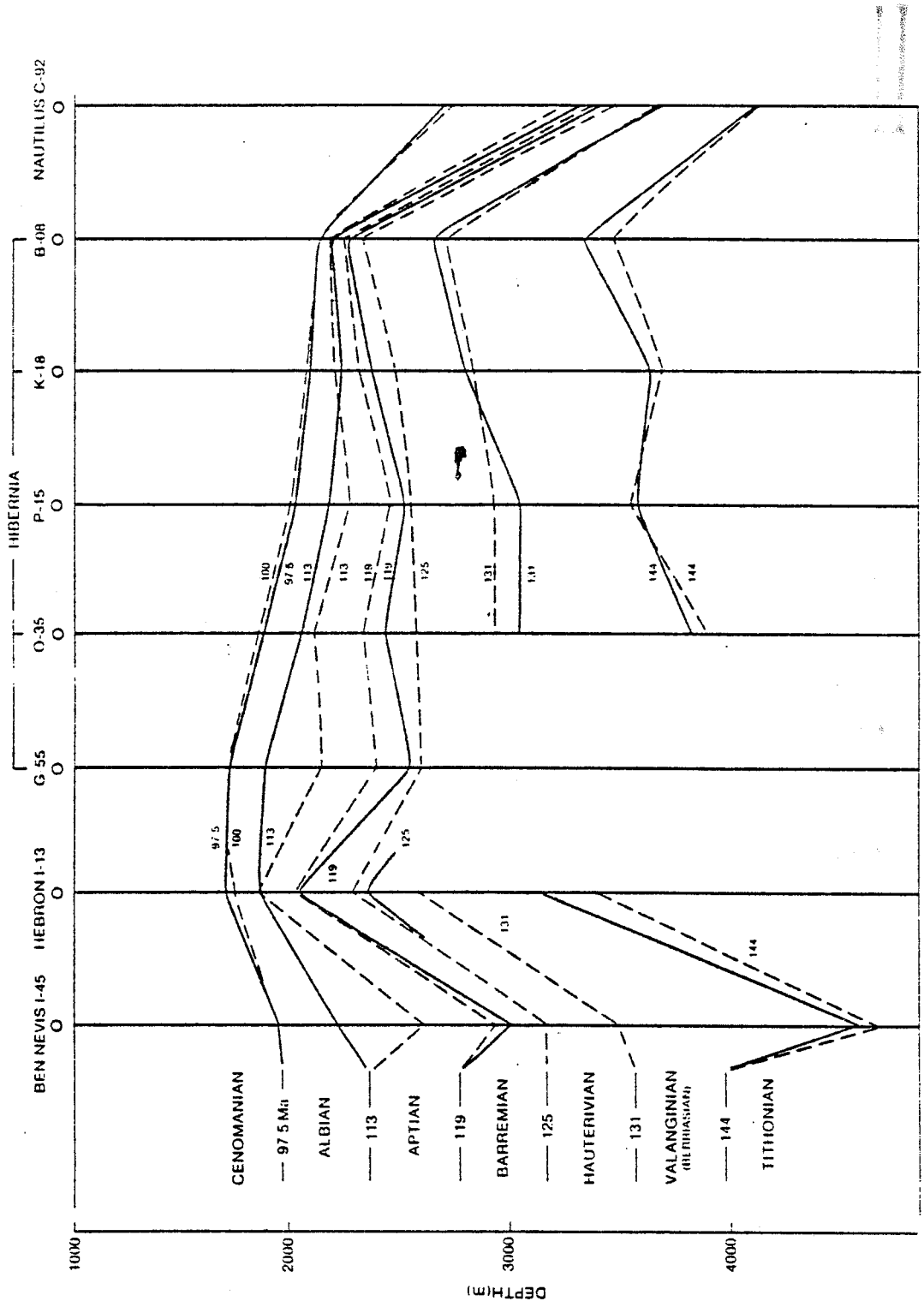
BEN NEVIS I-45
HEBRON I-13
G-55
O-35
HIBERNIA
P-15
K-18
B-08
NAUTILUS C-92
CENOMANIAN
97.5 Ma
ALBIAN
113
APTIAN
119
BARREMIAN
125
HAUTERIVIAN
131
VALANGINIAN
144
TITHONIAN
DEPTH(m)
1000
2000
3000
4000

Fig. 19

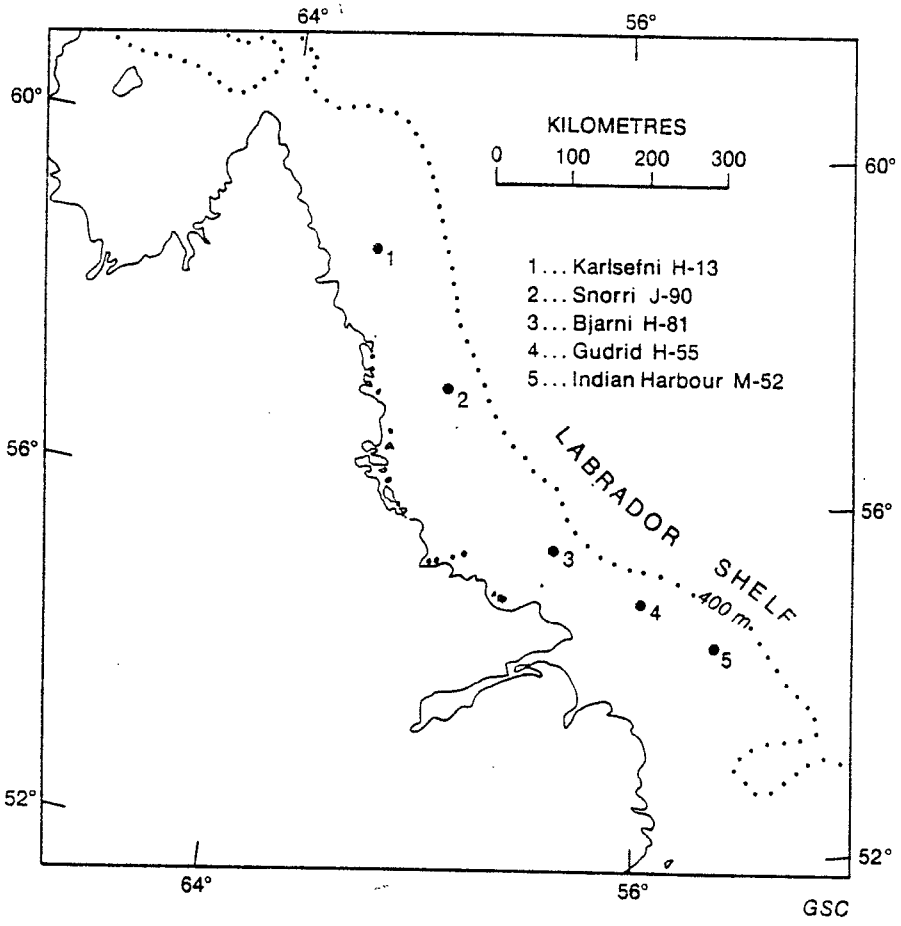
64°
56°
60°
KILOMETRES
0 100 200 300
1... Karlsefni H-13
2... Snorri J-90
3... Bjarni H-81
4... Gudrid H-55
5... Indian Harbour M-52
LABRADOR SHELF
400 m.
56°
52°
64°
56°
GSC

Fig. 20

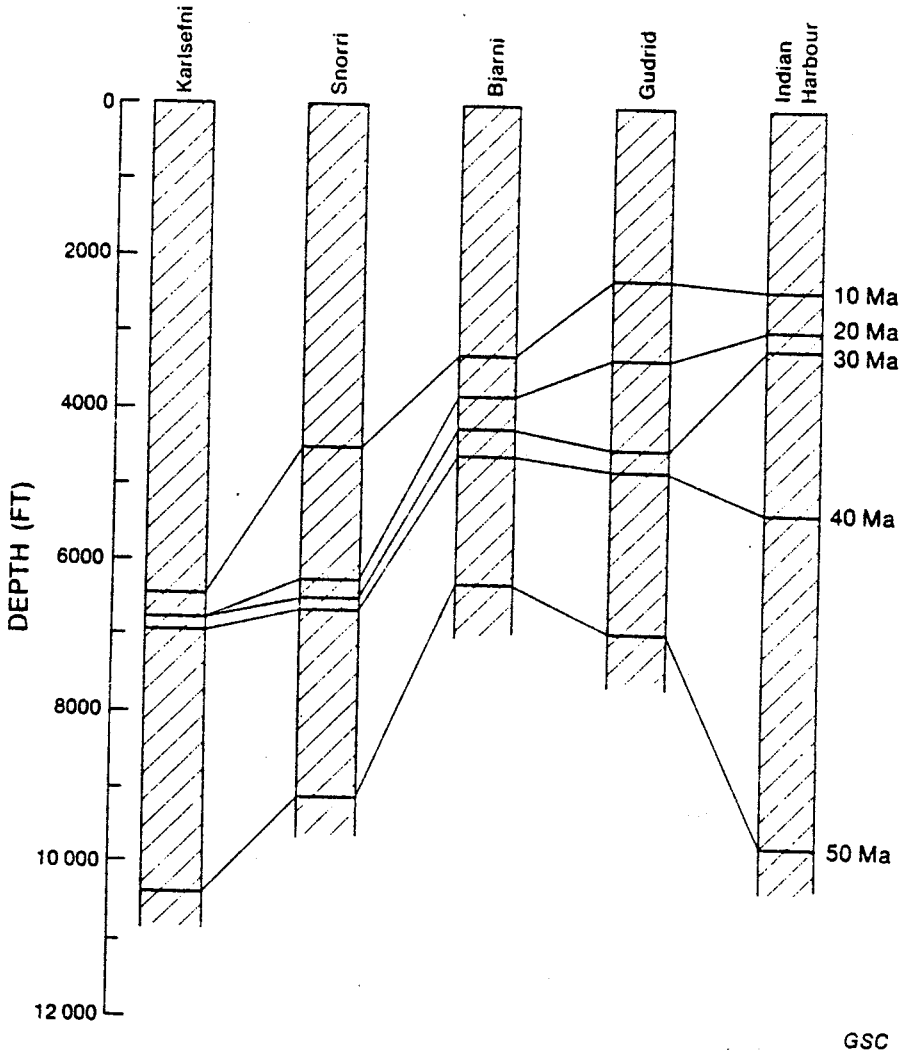
Karlsefni
Snorri
Bjarni
Gudrid
Indian Harbour
0
2000
4000
6000
8000
10 000
12 000
DEPTH (FT)
10 Ma
20 Ma
30 Ma
40 Ma
50 Ma
GSC

Fig. 21

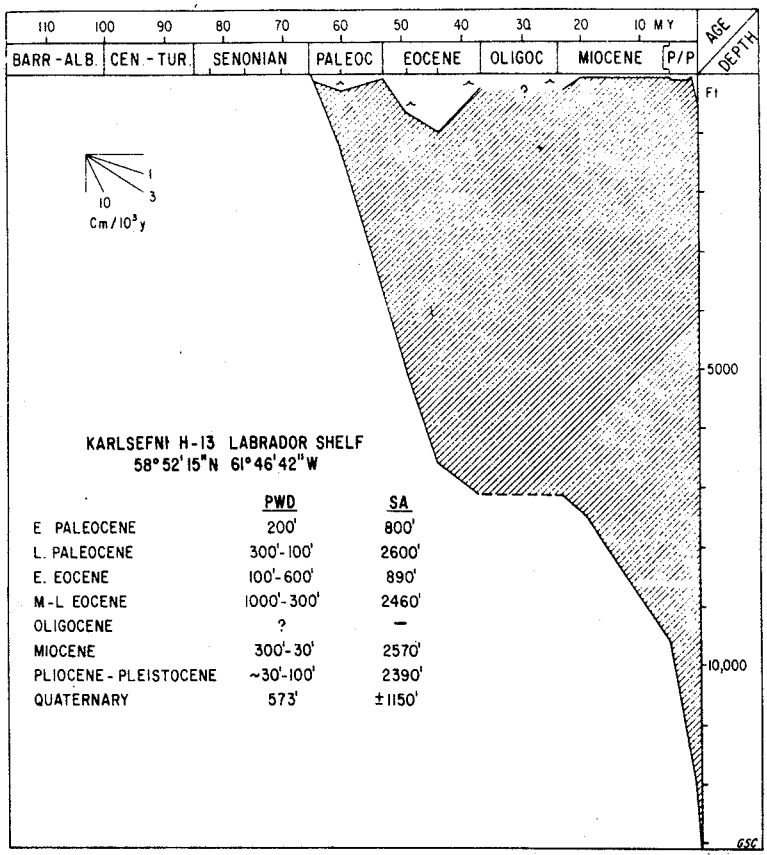

	PWD	SA
E PALEOCENE	200'	800'
L. PALEOCENE	300'-100'	2600'
E. EOCENE	100'-600'	890'
M-L EOCENE	1000'-300'	2460'
OLIGOCENE	?	—
MIOCENE	300'-30'	2570'
PLIOCENE-PLEISTOCENE	~30'-100'	2390'
QUATERNARY	573'	±1150'

Fig. 22

Table 1

A	B	C	RASC Distance	A	B	C	RASC Distance
1	10	10	0.000	21	261	261	4.364
2	17	17	0.391	22	263	263	4.518
3	16	16	0.912	23	40	40	4.645
4	67	67	1.204	24	29	32	4.802
5	21	18	1.647	25	32	29	4.809
6	18	71	1.799	26	41	264	5.175
7	71	21	1.919	27	264	42	5.189
8	20	20	2.108	28	42	41	5.237
9	26	15	2.442	29	30	30	5.251
10	15	26	2.486	30	86	90	5.531
11	70	70	2.513	31	36	36	5.620
12	27	29	3.198	32	90	86	5.667
13	69	25	3.358	33	45	45	5.786
14	24	27	3.418	34	57	57	5.799
15	25	69	3.499	35	50	50	6.302
16	81	81	3.722	36	46	46	6.429
17	259	259	3.738	37	54	54	6.738
18	33	33	4.295	38	56	56	7.178
19	34	34	4.311	39	55	55	7.689
20	260	260	4.342	40	59	59	8.033

Table 2

Event No.	Age (Ma)	RASC Distance	Average Distance	Event No.	Age (Ma)	RASC Distance	Average Distance
4	3.5	-0.585	-0.385	85	38	4.456	4.456
5	3.5	-0.476		29	40	4.809	4.809
				90	49	5.531	5.531
269	3.5	-0.096		57	52	5.799	5.247
17	11	0.391	0.391	93	52	5.895	
179	15	1.984	1.984	50	55	6.302	6.302
15	17	2.442	2.442	194	57	7.073	7.073
26	20	2.486	2.427	55	58	7.689	7.434
137	20	2.368		56	58	7.178	
24	28	3.198	3.198	61	63	8.228	8.039
33	37	4.295	4.017	253	63	7.849	
259	37	3.738					

Table 3

Event No.	Age (Ma)	RASC Distance	Age (Ma)	Event No.	Age (Ma)	RASC Distance	Age (Ma)
10	1	0.000	5.6	34	12	4.311	37.0
18	2	1.647	15.2	263	13	4.518	38.9
15	3	2.442	21.0	-36	13	5.620	47.9
-20	3	2.108	18.6	29	14	4.809	41.4
-16	3	0.912	10.9	-40	14	4.645	39.9
17	4	0.391	7.9	-41	14	5.237	44.2
24	5	3.198	27.3	-42	14	5.189	44.4
-25	5	3.358	28.7	86	15	5.667	48.2
26	6	2.486	21.4	45	16	5.786	49.1
-27	6	3.418	29.2	-46	16	6.429	53.7
259	7	3.738	32.0	57	17	5.779	49.2
261	8	4.364	37.5	-54	17	6.738	55.6
30	9	5.251	44.9	-50	17	6.302	52.9
260	10	4.342	37.3	55	18	7.689	61.5
-32	10	4.302	41.2	-56	18	7.178	58.4
33	11	4.295	36.9	(59)			

Table 4

Event Level	Depth (m)	Average Distance	Average Age	Event Level	Depth (m)	Average Distance	Average Age
1	546	0.000	5.6	10	1912	4.572	39.3
2	619	1.647	15.2	11	2045	4.295	36.9
3	720	1.821	16.8	12	2305	4.311	37.0
4	747	0.391	7.9	13	2335	5.069	43.4
5	1067	3.278	28.0	14	2366	4.970	42.6
6	1232	2.952	25.3	15	2396	5.667	48.2
7	1616	3.738	32.0	16	2671	6.107	51.4
8	1674	4.364	37.5	17	2884	6.280	52.6
9	1732	5.251	44.9	18	3000	7.434	59.9

Table 5.

	Hibernia P-15	Adolphus D-50	Bonavista C-99	I. Harbour M-52	Bjarni H-81	Snorri J-90
Ceratobulimina contraria - 16	310	485	887	750	872	1262
		350 ± 85	1130 ±381	571 ±132		
Spiroplectammina carinata - 18	275	512	2030	649	1085	1701
	334 ± 65	481 ± 78	1681 ±363	673 ±126	1025 ± 18	1533 ±167
Uvigerina dumblei - 26(15)	550	933	2377	1261		
	619 ±330	726 ±228	2059 ±162	786 ±155*	1094 ± 14	1756 ± 42
Turrilina alsatica - 24	1075	1280	2377	2097	1298	
	1000 ± 75	1164 ±115	2372 ±13	1344 ±532	1307 ± 31	1910 ± 29
Ammodiscus latus - 259	1125	1153	2316	1646		
	1083 ± 45	1291 ± 71	2571 ±135	1655 ±147	1490 ± 27	1983 ± 26
Haplophragmoides walteri - 261(260)	1185	1509	3078	1704	1634	213
	1176 ± 40	1471 ±171	2889 ±215	1864 ±404*	1577 ± 16	2067 ± 22*
Cyclammina amplectens - 29	1195	1890	3109	2396	1634	
		1721 ± 95	3099 ± 17	2212 ±489	1635 ± 14	
Ammosphaeroidina sp. 1 - 32	1125	1761	3386	1935	1695	2112
		1767 ± 62	3144 ± 99	2275 ±266	1653 ± 15	2155 ± 27
Acarinina densa - 90		2062	3478			
		2293 ±249	3423 ± 96	2528 ±497	1763 ± 8	2651 ± 59
Subbotina patagonica - 50(56)		2517		2914	2009	2932
		2501 ± 66		2861 ±327*	1812 ± 15	2798 ± 51*

Table 6.

		Hibernia P-15	Adolphus D-50	Bonavista C-99	I. Harbour M-52	Bjarni C-99	Snorri J-90
Spiroplectammina carinata Zone–Middle Miocene							
Spiroplectammmina carinata	– 18	325 ± 64*	485 ± 57*	1401 ±264	707 ± 73	1012 ± 15	1476 ±141
Epistomina elegans	– 71	347 ± 76*	512 ± 63*	1467 ±278	726 ± 76	1022 ± 14	1550 ±149
Globigerina praebulloides	– 21	371 ± 91*	535 ± 72	1522 ±296	742 ± 82	1029 ± 14	1603 ±116
Gyroidina girardana	– 20	449 ±154*	615 ±118	1696 ±475*	793 ±130	1050 ± 18	1684 ± 62
Turborotalia pomeroli – Cyclammina amplectens Zone – Late Eocene							
Ammodiscus latus	– 259	1075 ± 53	1276 ± 61	2579 ±197	1536 ±214	1476 ± 15	2000 ± 30
Haplophragmoides kirki	– 260	1170 ± 51	1409 ±111	3048 ±141	1670 ± 85	1544 ± 23	2077 ± 23
Haplophragmoides walteri	– 261	1174 ± 53	1424 ±175*	3055 ±136	1702 ± 90	1547 ± 25	2089 ± 23
Ammobaculites aff. polythalamus	– 263	1206 ± 83	1645 ±154	3106 ±144	1749 ±189	1584 ± 48	2097 ± 23
Ammosphaeroidina sp. 1	– 32		1757 ± 63	3172 ±107	2307 ± 87	1638 ± 25	2131 ± 26
Cyclammina amplectens	– 29		1761 ± 62	3176 ±107	2310 ± 83	1641 ± 25	2133 ± 26

Table 7.

		Hibernia P-15	Fl. Foam I-13	Adolphus D-50	Bonavista C-99	Dominion O-23	I. Harbour M-52	Gudrid H-55	Bjarni H-81	Snorri J-90	Karlsefni H-13
12 Ma	Middle Miocene	330	576	485	585	859	676	613	871	1261	
		262 ± 42	382 ± 92	385 ± 44	521 ± 45	986 ± 46	638 ± 82	528 ± 65	952 ± 53	1288 ± 88	
16 Ma	Early Miocene	460	713	762		1767				1618	
		344 ± 77	502 ±114	508 ± 56	584 ± 84	1636 ± 56	723 ± 68	619 ±117	1019 ± 15	1546 ±159	
24 Ma	Oligocene	960	960	1310	1335	2320	1097	1066	1298		2060
		813 ± 71	809 ±147	935 ± 94	1041 ±306	2254 ± 78	1072 ±164	1025 ±241	1041 ± 20	1826 ± 43	1977 ± 40
36 Ma	Late Eocene	1125	1289	1353	1719	2804	1645	1505	1481	1975	2060
		1128 ± 41	2398 ± 98	1364 ± 46	1732 ±223	3027 ±113	1668 ± 65	1719 ±231	1524 ± 18	2041 ± 27	2137 ±118
44 Ma	Middle Eocene	1315	1585	1890	2307	2161	2377		1695	2164	
		1216	1501 ±133	2324 ±298	3274 ±184	2359 ± 50	1961 ±138	1670 ± 32	2189 ± 68	2784 ± 49	
49 Ma	Early Middle Eocene		1615	2026	2438	3265		1862		2316	2791
			1687	2311 ±133	2643 ±173	3426 ±208	2509 ±250	2091 ± 44	1779 ±178	2636 ±100	2949 ±179
52 Ma	Early Eocene		1763	2469	2764	3478	2700	2118	1847	2926	2944
			1796	2467 ± 71	2730	3564 ±20	2726 ±225	2149 ±127	1824 ± 24	2770 ± 73	3220
56 Ma	Paleocene			2569			3030	2395	2029	2993	3828
				2561 ± 29			2919 ±118	2324 ±179	2000	2995	3663 ±251
	Cretaceous	1400	2002	2667	3118	3660	3194	2400			

APPENDIX 1

CASC – Main Menu and Overview of Options
(Sample Session)

CASC

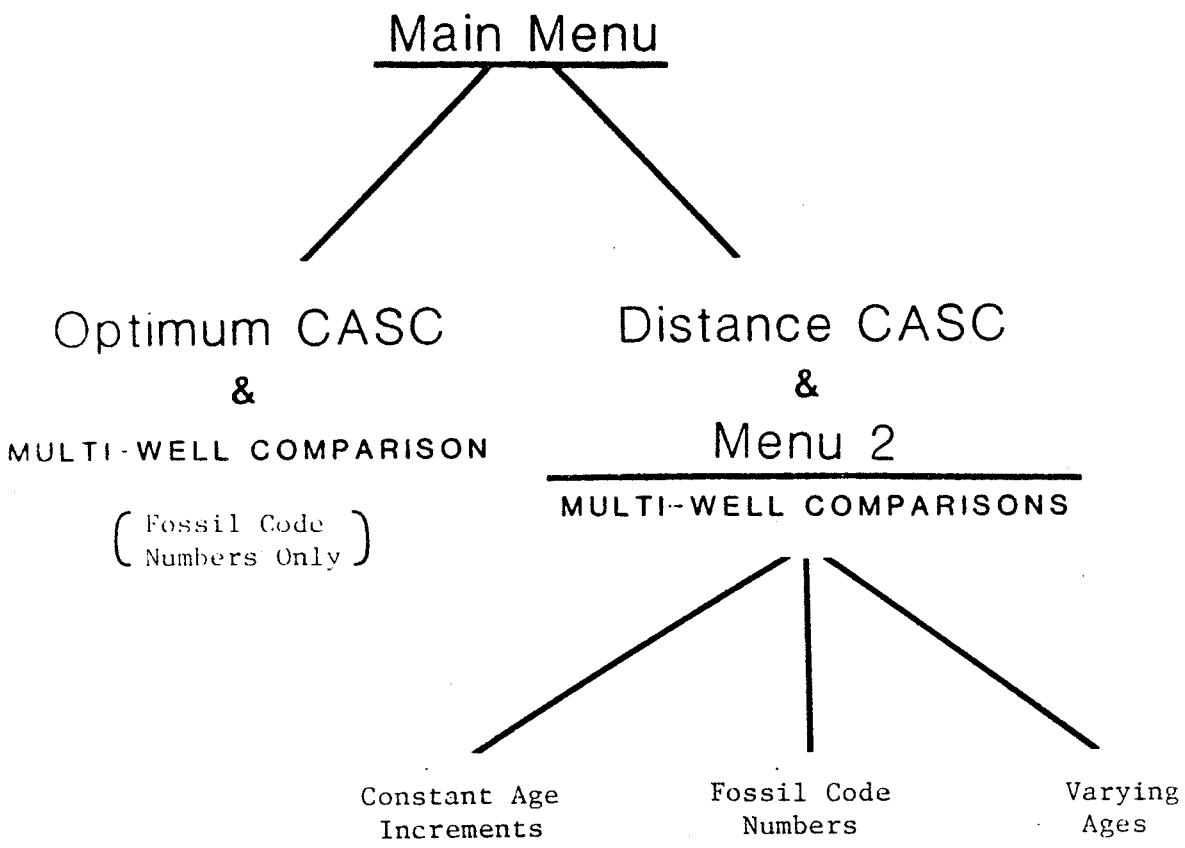
Main Menu
Optimum CASC
&
MULTI-WELL COMPARISON
(Fossil Code Numbers Only)
Distance CASC
&
Menu 2
MULTI-WELL COMPARISONS
Constant Age Increments
Fossil Code Numbers
Varying Ages

Main Menu

WELCOME TO THE CASC PROGRAMMES

-1- OPTIMUM SEQUENCE OPTION
-2- DISTANCE OPTION
-0- QUIT CASC PROGRAMMES

PLEASE CHOOSE (0 - 2) ... [1] for example

Start of O.S. Option

WHAT IS YOUR LINE SPEED (BAUD RATE) ?
(EXAMPLES: 300, 1200, 2400, 9600) --->

You may have to check your terminal settings or ask someone who knows.

PLEASE IDENTIFY YOUR TERMINAL AS
1. MODEL 4006, 4010, 4012, OR 4013
2. MODEL 4014 OR 4015
3. MODEL 4014 OR 4015 WITH ENHANCED GRAPHICS MODULE

TYPE 1, 2, OR 3 ... [2] for example

DO YOU WANT TO SET CLUSTER LIMITS FOR THE DATASET ? [N]

Table is displayed

Start of Main Loop

WELL NO.	WELL NAME
1	XX XXXXXXXXXX
2	YYYYYYY YYY
3	FLYING GOLDFISH 007
:	

TYPE IN THE NUMBER OF THE WELL TO BE ANALYSED.
IF NO MORE WELLS ARE TO BE SEEN, TYPE IN 0 [5]

DO YOU WANT ALL DEFAULTS FOR THIS WELL ? [N]

Answering 'Y' gives you the "speedy version".
'N' is the more typical response.

INDIAN HARBOUR M-52 CONTAINS 36 EVENTS

OPTIMUM SEQUENCE VS. EVENT SCALE

RECODED FOSSIL NUMBERS

Table

10	1.0
13	2.0
15	3.0
-20	3.0
-16	3.0
:	

SEE THE VALUES TO BE USED FOR THE SPLINE ? [N]

KEEP THE DEFAULT SMOOTHING FACTOR ? [Y]
(DEFAULT = 4.3304)

DO YOU WANT SPLINE APPROXIMATIONS DISPLAYED ? [N]

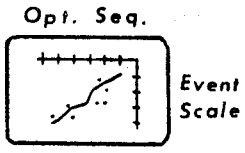

Beep means you must press [SPACE-BAR] Return

'SF OKAY?' lets you change SF if you answer 'N'

Cross-hairs will appear:

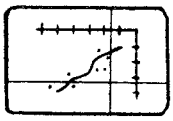

PRESS 'D' ON POINT TO DELETE
PRESS 'E' IF NO POINTS TO BE DELETED
PRESS 'S' WHEN YOU'VE FINISHED DELETING

SEE THE VALUES TO BE USED FOR THE SPLINE ? [N]

KEEP S.F. ? [Y]

SPLINE APPROX. ? [N]

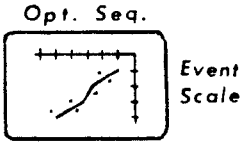

DEPTH IN KM VS. EVENT SCALE

KEEP S.F. ? [Y]

SPLINE APPROX. ? [N]

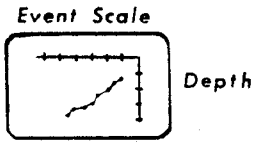

SF OKAY ?

DO YOU WANT TO USE

-1- OBSERVED DEPTHS ("the shortcut")
-2- DEPTHS FROM SPLINE CURVE

PICK 1 OR 2 [2]

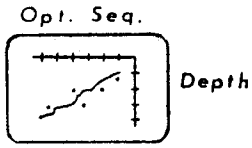

OPTIMUM SEQUENCE VS. DEPTH IN KM

KEEP S.F. ? [Y]

SPLINE APPROX. ? [N]

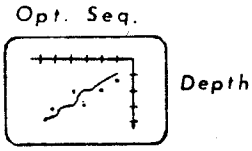

DO YOU WANT TO SPECIFY AN UNCONFORMITY ? [N]

('N' takes you directly to top of next page) →

[Y]

HOW DO YOU WANT TO SPECIFY IT ?

A. MAKE AN EVENT THE UNCONFORMITY
B. ENTER FOSSIL OCCURRING IMMED'LY ABOVE THE UNC.
C. USE CURSOR TO POINT AT THE DEPTH OF THE UNC.

After the unconformity is drawn, we redraw all graphs (starting with 'O.S. vs E.S.') using only the points <u>above</u> the unconformity, and then again for only the points <u>below</u> the unconformity. Then we continue with the next page.

IF YOU HAVE SEEN AT LEAST TWO WELLS AND WANT A MULTI-WELL COMPARISON, TYPE 'READY', ELSE ENTER 'NO'

'NO' takes you back to 'Start of Main Loop'
("Type in number of well to be analysed ....")

'READY' ... continues below

MULTI-WELL COMPARISON

WHICH WELLS DO YOU WANT TO COMPARE ?

CHOOSE NUMBERS 1 THROUGH 21
CHOOSE A MAXIMUM OF 5 WELLS.
ENTER ZERO IF NO MORE ARE TO BE ENTERED.

ENTER WELL 1 [6]

ENTER WELL 2 [5]

ENTER WELL 3 [9]

ENTER WELL 4 [0]

CHOOSE THE FOSSILS (Maximum 10; '0' to end)

ENTER DICTIONARY NUMBER OF FOSSIL 1 [1][6]

ENTER DICTIONARY NUMBER OF FOSSIL 2 [2][0]

⋮ (and so on ...)

SHOULD THE ERROR ANALYSIS BE PERFORMED ? [N]

Depth 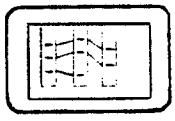

PLEASE TYPE TITLE/REMARKS REGARDING THIS DISPLAY
(80 CHARS. MAX.)

Back to Start of Main Loop

TYPE IN THE NUMBER OF THE WELL TO BE ANALYSED.
IF NO MORE WELLS ARE TO BE SEEN, TYPE IN 0

Takes you back to Main Menu

Main Menu

-1- OPTIMUM SEQUENCE OPTION
-2- DISTANCE OPTION
-0- QUIT CASC PROGRAMMES

2

Start of Distance Option

(Give line speed and terminal type)

AGE IN MA VS. RASC DISTANCE

SEE THE VALUES TO BE USED FOR THE SPLINE ? N

KEEP S.F. ? (DEFAULT = 2.000) Y

DISPLAY SPLINE APPROXIMATIONS ? N

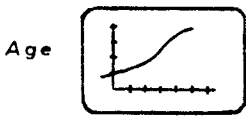

≥Beep≤ means Press SPACE-BAR Return

'SF OKAY ?' lets you change SF if you wish.

DO YOU WANT TO SET CLUSTER LIMITS FOR THE DATASET ? N

Start of Main Loop

(Table of wells is displayed)

TYPE IN THE NUMBER OF THE WELL TO BE ANALYSED.
IF NO MORE WELLS ARE TO BE SEEN, TYPE IN 0

5

DO YOU WANT ALL DEFAULTS FOR THIS WELL ?
("Speedy version" ?) N

INDIAN HARBOUR M-52 CONTAINS 36 EVENTS

RASC DISTANCE VS. EVENT SCALE

RECODED FOSSIL NUMBERS

Table

10	1.0
18	2.0
15	3.0
:	

DO YOU WANT TO CONSIDER ANOMALOUS EVENTS ? N

SEE VALUES TO BE USED FOR SPLINE ? N

KEEP S.F. ? Y

DISPLAY SPLINE APPROXIMATIONS ? [N]

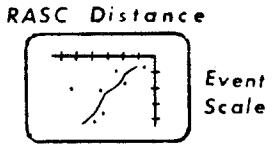

SF OKAY ?

Cross-hairs:

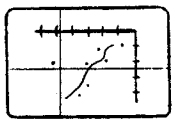

If you press 'D', the target point will be outlined, and you'll be asked

DELETE THIS POINT ? (Y OR N)

Redrawn:

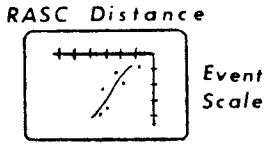

DEPTH IN KM VS. EVENT SCALE

KEEP S.F. ? [Y]

SPLINE APPROX. ? [N]

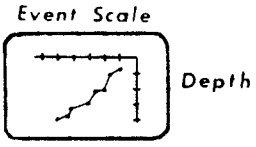

DO YOU WANT TO USE

-1- OBSERVED DEPTHS
-2- DEPTHS FROM SPLINE CURVE

PICK 1 OR 2 [2]

AGE IN MA VS. EVENT SCALE

RASC DISTANCE CONVERTED INTO AGE FOR INDIAN HARBOUR

Table

RASC DISTANCE	AGE (MA)
1.0842	6.6
2.6801	15.3
3.3652	21.5
3.0154	18.6
:	

SEE VALUES TO BE USED FOR SPLINE ? [N]

KEEP S.F. ? [Y]

SPLINE APPROX. ? [N]

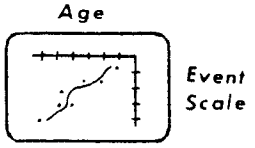

SEE THE FIRST DERIVATIVE GRAPH ? [Y]

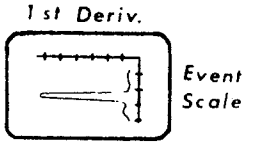

Press [SPACE-BAR] Return

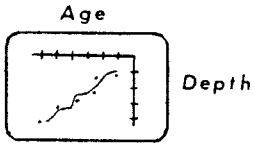

AGE IN MA VS. DEPTH IN KM

KEEP S.F. ? [Y]

SPLINE APPROX. ? [N]

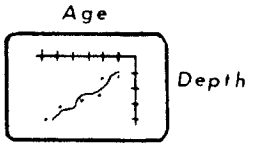

DO YOU WISH TO SEE CLUSTERS ?
(Asked only if cluster limits were set earlier)

DO YOU WANT TO SPECIFY AN UNCONFORMITY ? [N]

GRAPH FOR SEDIMENTATION RATE ? [Y]

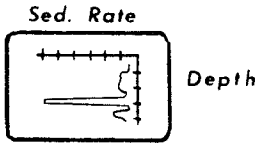

Back to Start of Main Loop

(Table of wells is displayed)

TYPE IN THE NUMBER OF THE WELL TO BE ANALYSED.
IF NO MORE WELLS ARE TO BE SEEN, TYPE IN 0

Takes you to the multi-well comparisons

MULTI-WELL COMPARISONS

Menu 2

-1- CONSTANT AGE INTERVAL (Ex. by '10's of MA)
-2- FOSSIL CODE NUMBERS (Ex. 16, 258, 201, 33,...)
-3- VARIABLE AGE INPUT (Ex. 12MA, 24MA, 25MA,...)
-0- RETURN TO MAIN (Return to 'Main Menu')

[1]

MULTI-WELL COMPARISONS

WHICH WELLS DO YOU WANT TO COMPARE ?

CHOOSE 1 - 21 (Maximum 5; '0' to end choosing)

ENTER WELL 1

⋮

ENTER AN AGE INTERVAL (1 - 30)

AVAILABLE ARE TWO CHOICES

A) PLOT FOR AGE INTERVALS OF 1 MA OR MORE
B) TABLE OF THE AGES AND INTERPOLATED DEPTHS

CHOOSE AN OPTION: A OR B

[A]

WHICH TYPE OF ERROR ANALYSIS SHOULD BE APPLIED ?

1) LOCAL ESTIMATION
2) LOCAL AND GLOBAL (on two separate plots)
3) NONE

[1]

Depth 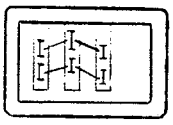

≥ Beep ≤ We return to Menu 2 above

MULTI-WELL COMPARISONS

Menu 2

-1- CONSTANT AGE INTERVAL
-2- FOSSIL CODE NUMBERS
-3- VARIABLE AGE INPUT
-0- RETURN TO MAIN

2

:

WHICH WELLS DO YOU WANT TO COMPARE ?

ENTER WELL 1 (Maximum of 5 wells)

:

ENTER DICTIONARY NUMBER OF FOSSIL 1 (Maximum of 10)

:

WHICH TYPE OF ERROR ANALYSIS SHOULD BE APPLIED ?

1) LOCAL ESTIMATION
2) LOCAL AND GLOBAL
3) NONE

1

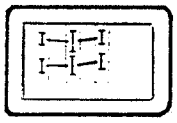

3

PLEASE TYPE TITLE/REMARKS REGARDING THIS DISPLAY

We go back to Menu 2

ENTER WELL 1

:

CHOOSE THE CHRONOSTRATIGRAPHIC UNITS FOR COMPARISON
(NOTE: THEY MUST BE IN CHRONOLOGICAL ORDER)

ENTER UNIT BOUNDARY (IN MA) 1:

:

WHICH TYPE OF COMPARISON IS WANTED ?

1) ERROR ANALYSIS WITH LOCAL ESTIMATION
2) WITH LOCAL AND GLOBAL ESTIMATION
3) SIMPLE PLOT
4) PATTERN SCHEME

4

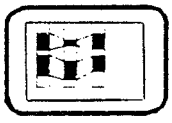

We return to Menu 2 above

Example of setting cluster limits:

DO YOU WANT TO SET CLUSTER LIMITS FOR THE DATASET ? [Y]

DEFINE CLUSTERS BY ENTERING THE LAST FOSSIL
A MAXIMUM OF 15 CLUSTERS IS PERMITTED.
ENTER ZERO TO TERMINATE SELECTION.

ENTER LIMIT OF CLUSTER 1
17

ENTER LIMIT OF CLUSTER 2
67

ENTER LIMIT OF CLUSTER 3
20

ENTER LIMIT OF CLUSTER 4
15

ENTER LIMIT OF CLUSTER 5
259

⋮

(Then, later on you will be asked ...)

DO YOU WISH TO SEE CLUSTERS ? [Y]

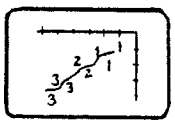

APPENDIX 2

Displays 1 to 52

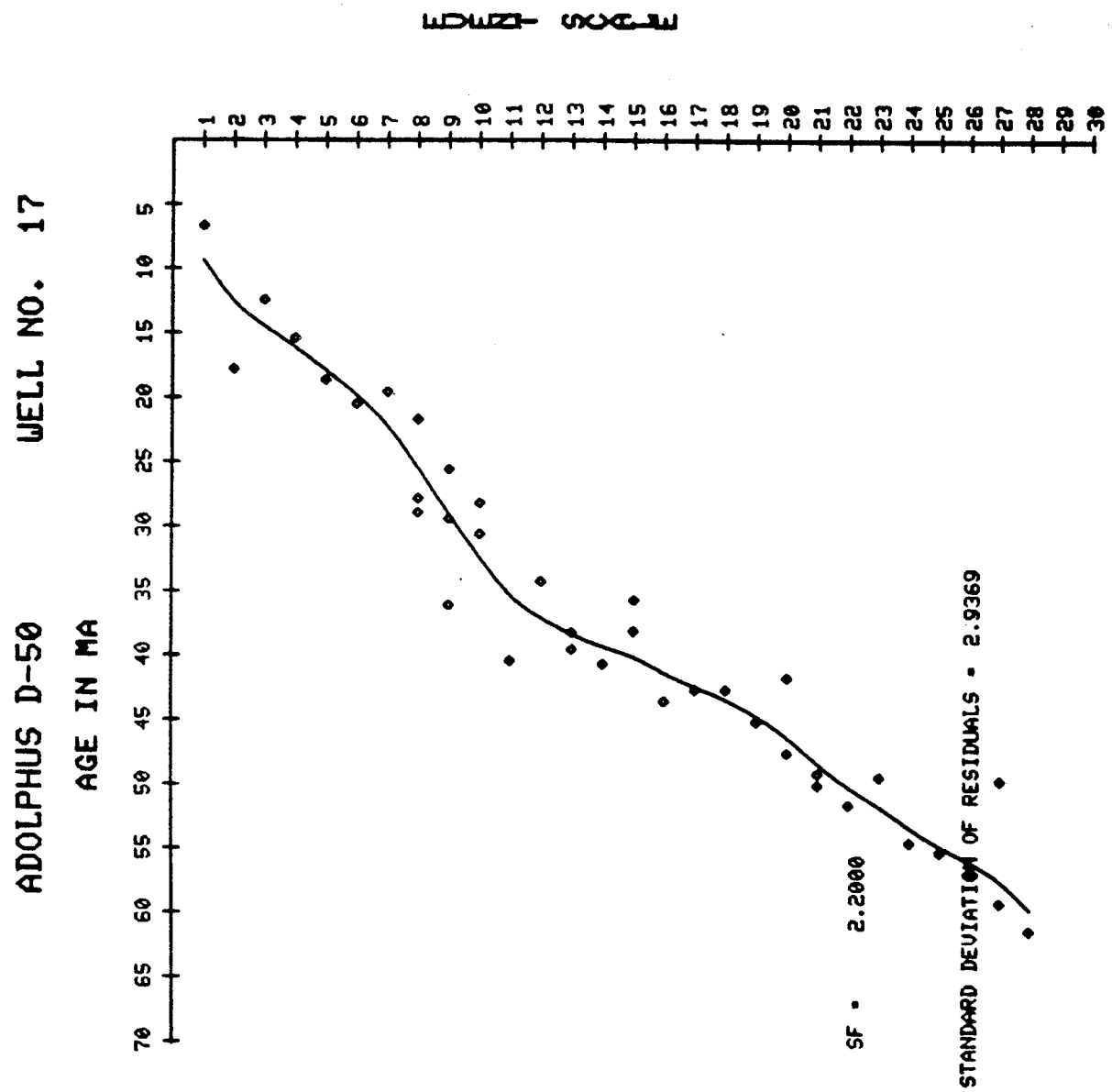
ADOLPHUS D-50
WELL NO. 17
AGE IN MA
EDWR SCALE
SF = 2.2000
STANDARD DEVIATION OF RESIDUALS = 2.9369

Display 1

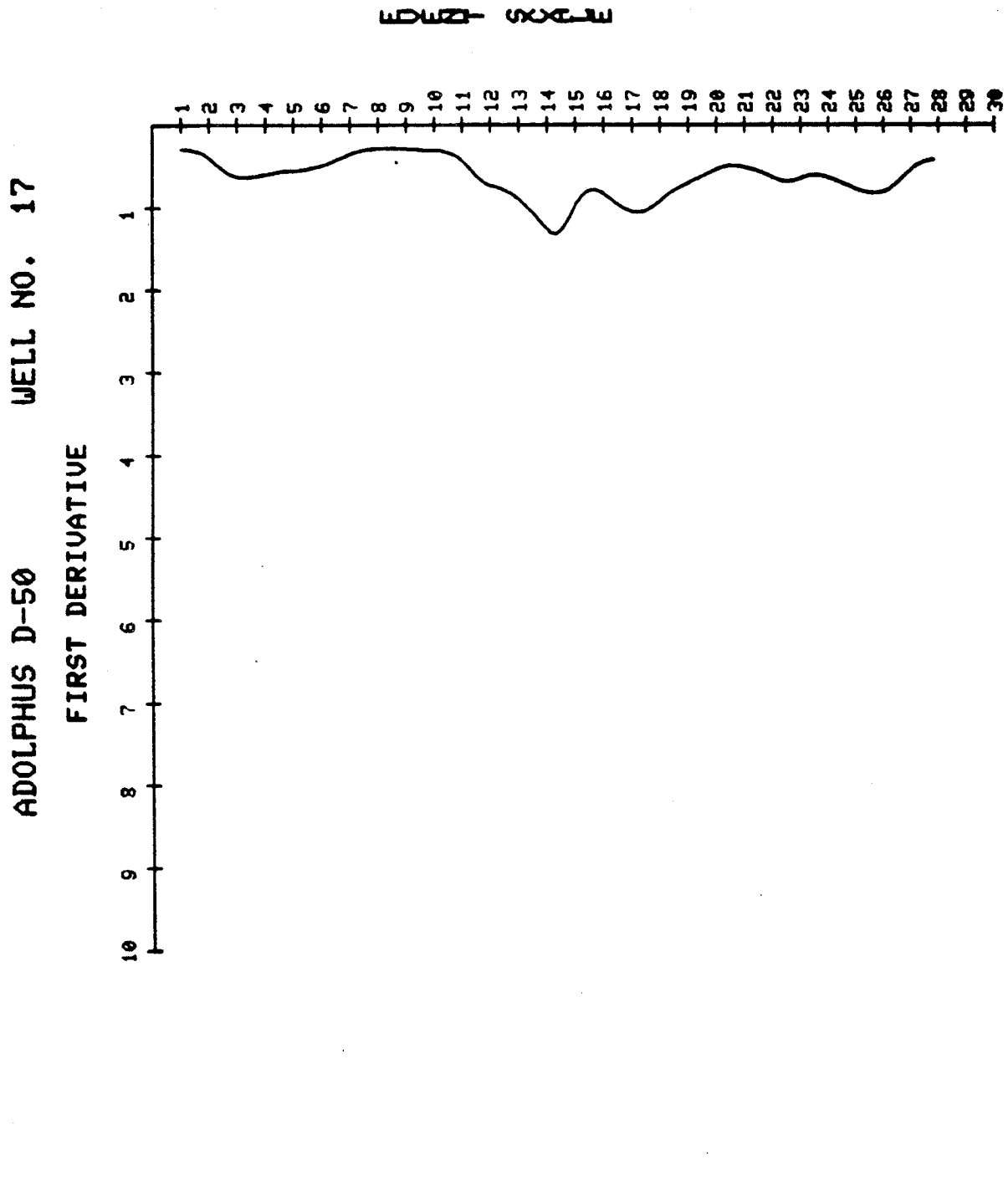
ADOLPHUS D-50
WELL NO. 17
FIRST DERIVATIVE
DEPTH SCALE
1
2
3
4
5
6
7
8
9
10
1 2 3 4 5 6 7 8 9 10 11 12 13 14 15 16 17 18 19 20 21 22 23 24 25 26 27 28 29 30

Display 2

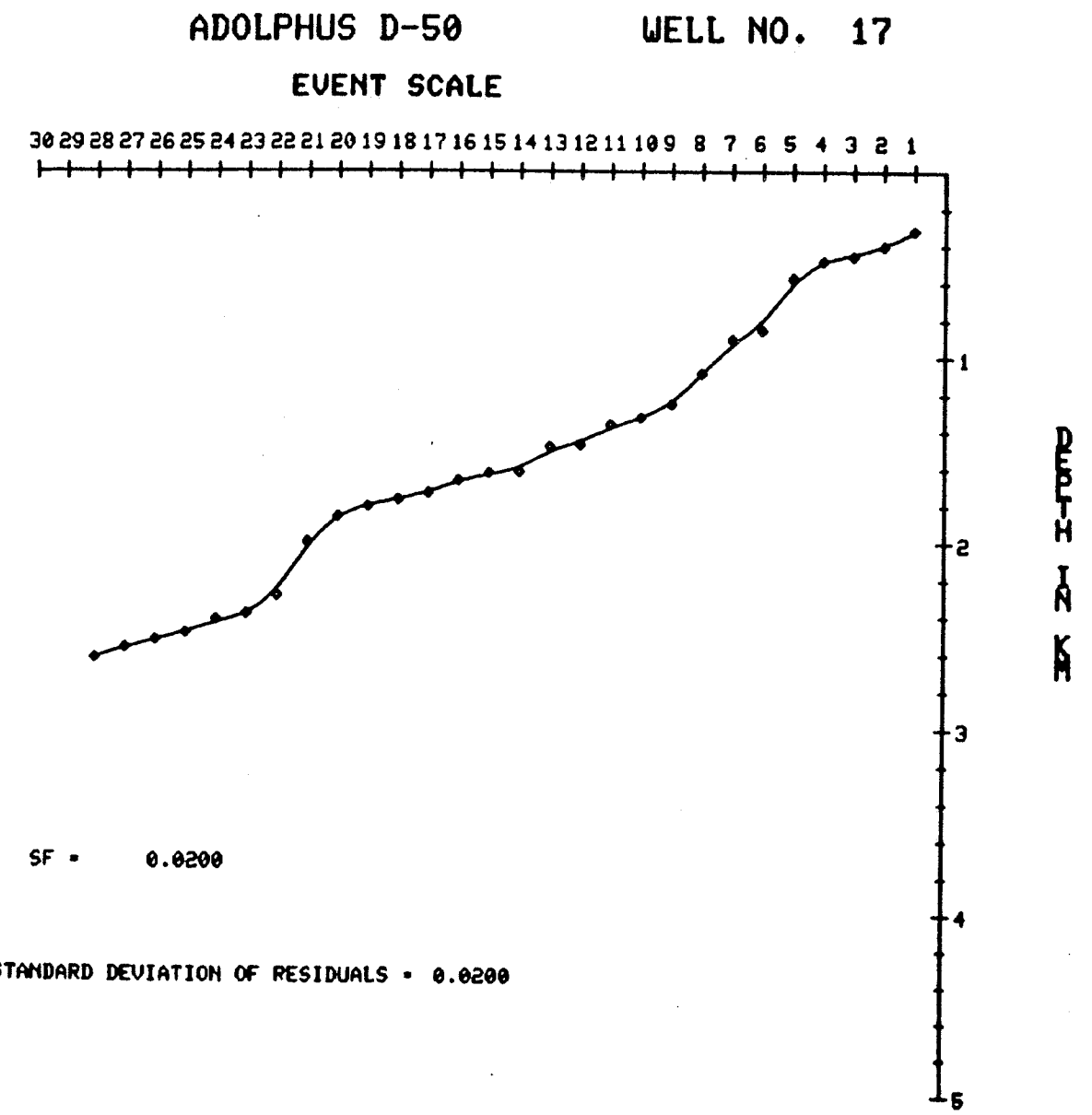
ADOLPHUS D-50
WELL NO. 17
EVENT SCALE
30 29 28 27 26 25 24 23 22 21 20 19 18 17 16 15 14 13 12 11 10 9 8 7 6 5 4 3 2 1
1
2
3
4
5
DEPTH IN KM
SF = 0.0200
STANDARD DEVIATION OF RESIDUALS = 0.0200

Display 3

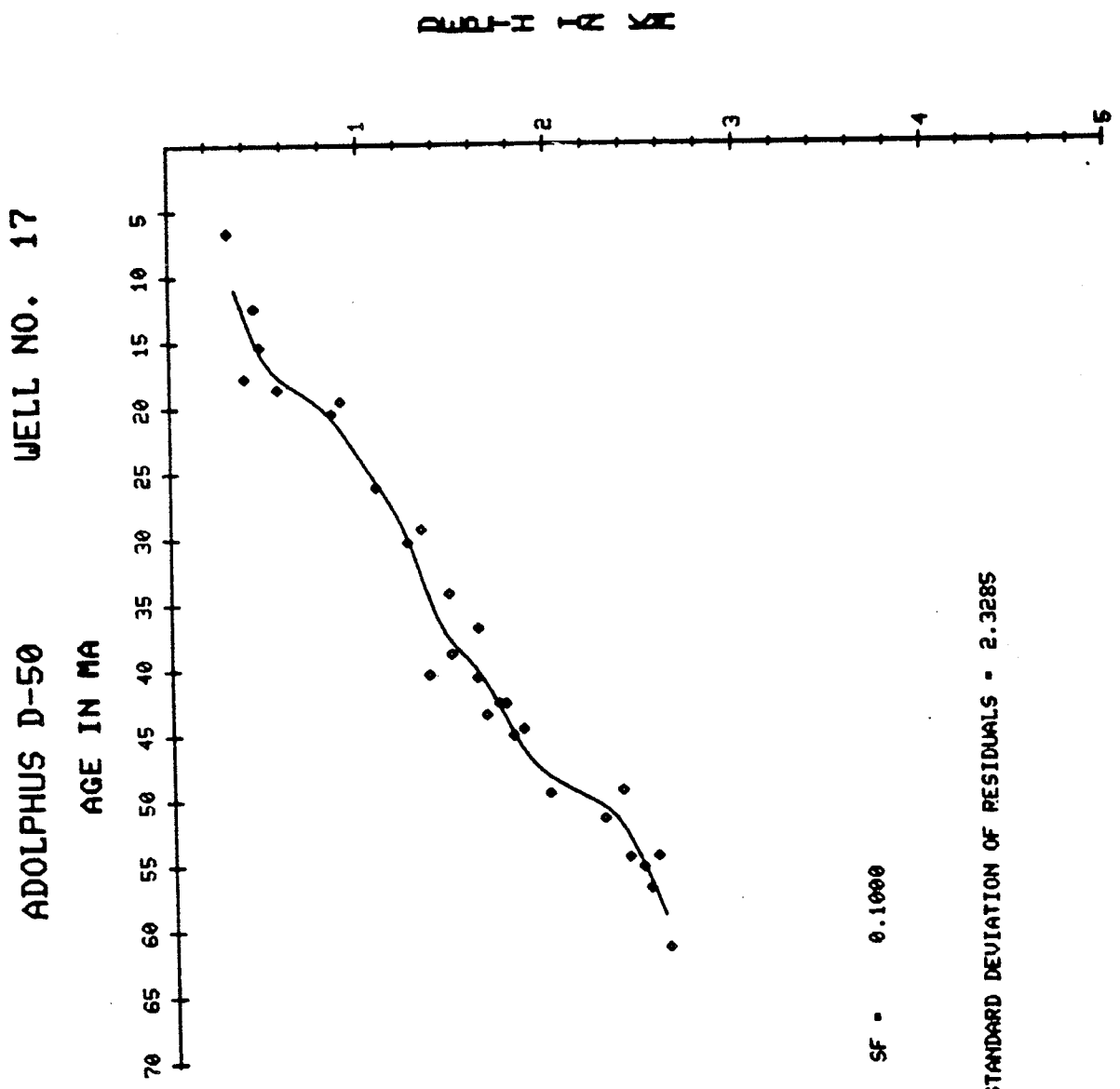
ADOLPHUS D-50
WELL NO. 17
AGE IN MA
5
10
15
20
25
30
35
40
45
50
55
60
65
70
DEPTH IN KM
1
2
3
4
5
SF = 0.1000
STANDARD DEVIATION OF RESIDUALS = 2.3285

Display 4

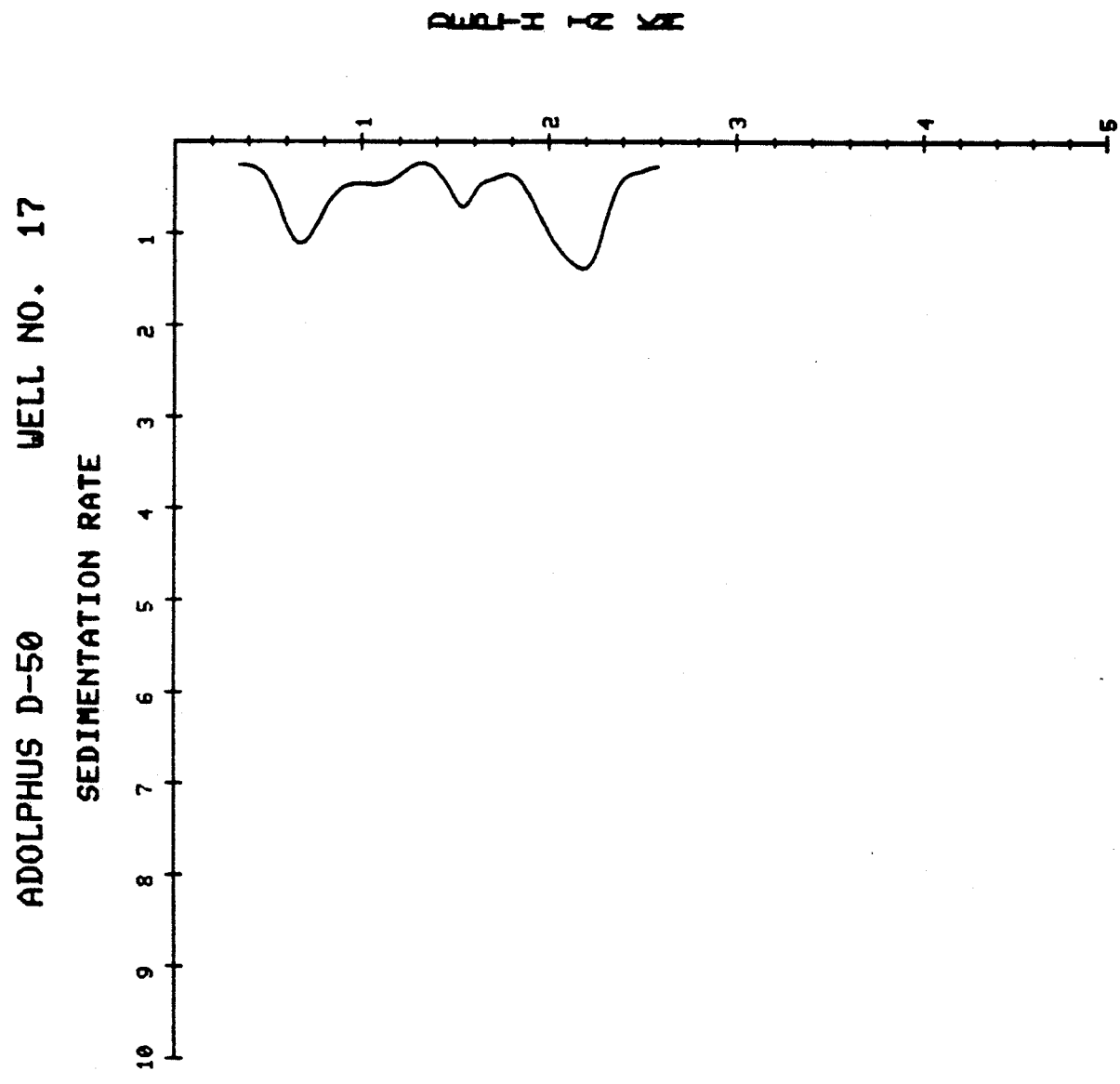
ADOLPHUS D-50
WELL NO. 17
SEDIMENTATION RATE
DEPTH IN KM
1
2
3
4
5
1
2
3
4
5
6
7
8
9
10

Display 5

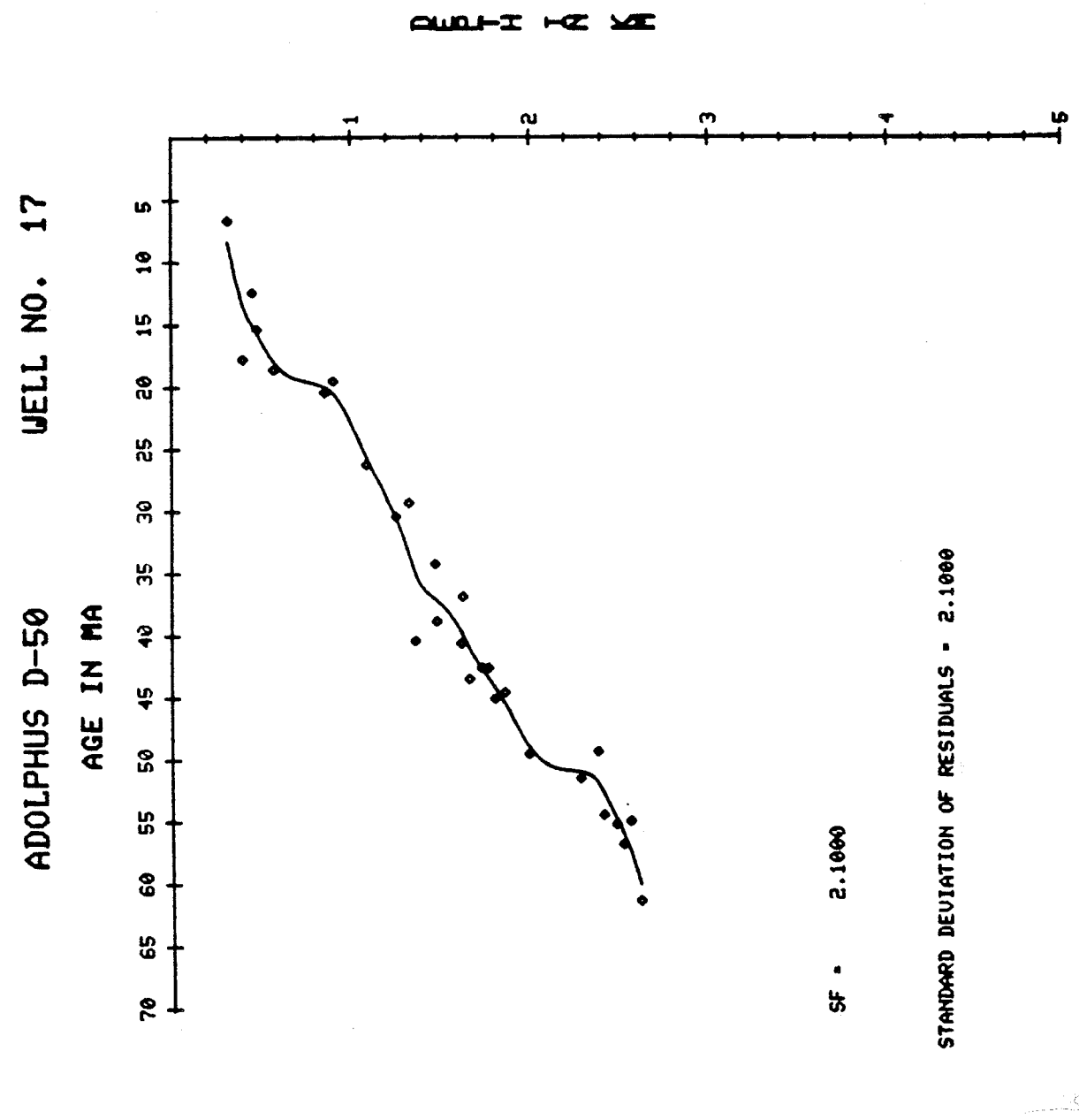
DEPTH IN KM
1
2
3
4
5
ADOLPHUS D-50
WELL NO. 17
AGE IN MA
5
10
15
20
25
30
35
40
45
50
55
60
65
70
SF = 2.1000
STANDARD DEVIATION OF RESIDUALS = 2.1000

Display 6

***** CORRELATION AND SUBSIDENCE CURVES *****

AGE IN MA VERSUS RASC DISTANCE
****

DO YOU WANT TO SEE THE VALUES TO BE USED FOR THE SPLINE?
Y

AVERAGED VALUES FOR SPLINE

RASC DISTANCE	AGE IN MA
.7483	3.5
1.3541	11.0
2.3326	15.0
3.3652	17.0
3.0389	20.0
3.7076	23.0
4.4934	37.0
5.2371	38.0
5.5339	40.0
6.4673	49.0
6.7065	52.0
7.5269	55.0
7.9653	57.0
8.7103	58.0
9.0659	63.0

DO YOU WANT TO KEEP THE DEFAULT SMOOTHING FACTOR?
DEFAULT - 2.0000
Y

Display 7

INDEPENDENT	FITTED VALUE
.7483	4.642
1.3541	8.641
2.8326	16.697
3.0889	18.824
3.3652	21.542
3.7076	25.444
4.4934	33.808
5.2371	39.358
5.5339	41.523
6.4673	48.912
6.7065	50.602
7.5269	55.003
7.9653	56.819
8.7103	59.943
9.0659	61.743

Display 8

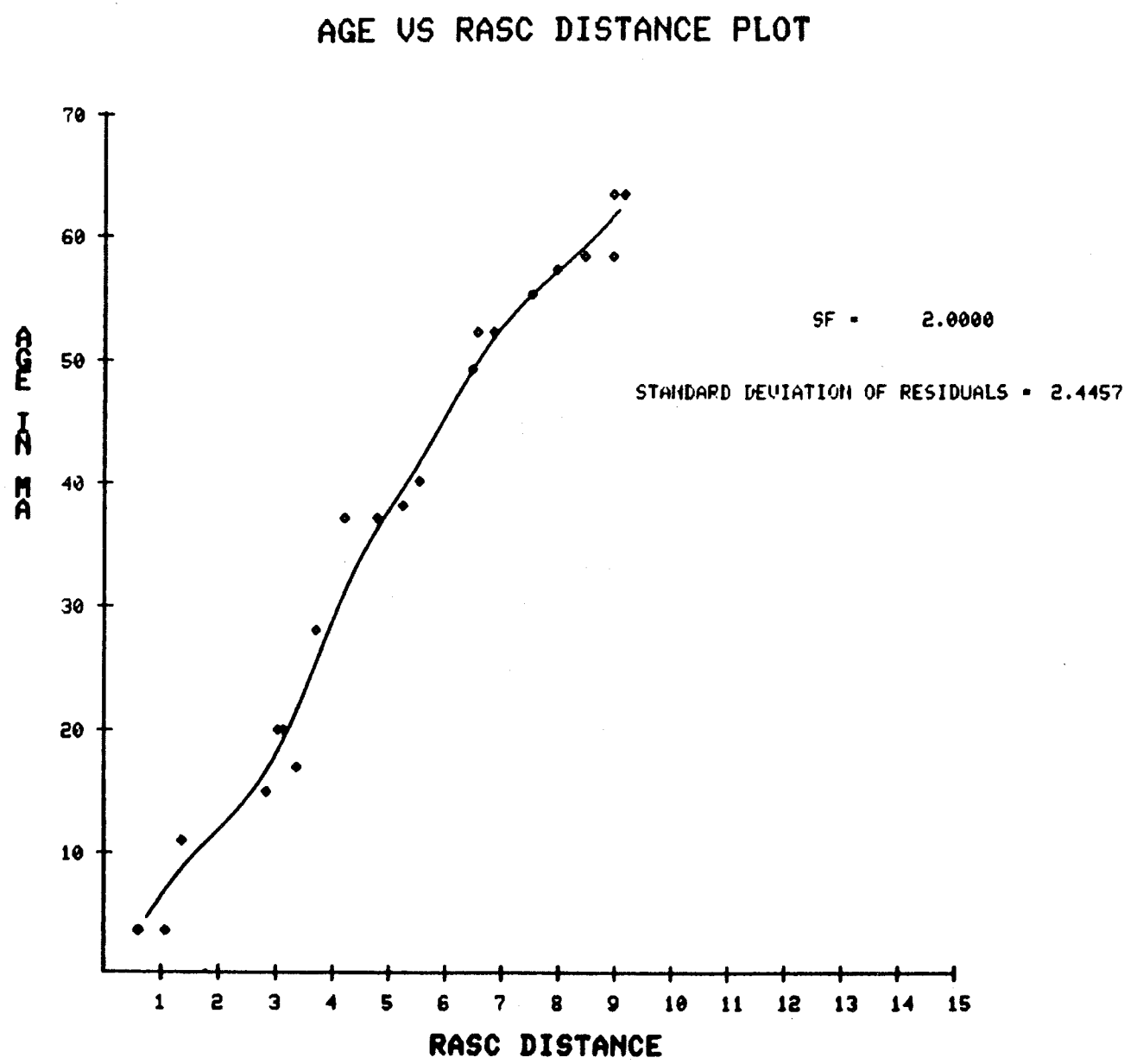
AGE VS RASC DISTANCE PLOT
AGE IN MA
70
60
50
40
30
20
10
1
2
3
4
5
6
7
8
9
10
11
12
13
14
15
RASC DISTANCE
SF = 2.0000
STANDARD DEVIATION OF RESIDUALS = 2.4457

Display 9

WELL NO.	NAME
1	BJARNI H-81
2	CARTIER D-70
3	FREYDIS B-87
4	GUDRID H-55
5	INDIAN HARBOUR M-52
6	KARLSEFNI H-13
7	LEIF M-48
8	LEIF E-38
9	SNORRI J-90
10	HERJOLF M-32
11	BONAVISTA C-99
12	DOMINION O-23
13	EGRET K-36
14	OSPREY H-84
15	CUMBERLAND B-55
16	EGRET N-46
17	ADOLPHUS D-50
18	HIBERNIA O-35
19	FLYING FOAM I-13
20	BLUE H-28
21	HARE BAY H-31
22	HIBERNIA K-18
23	HIBERNIA B-08
24	HIBERNIA P-15

TYPE IN THE NUMBER OF THE WELL TO BE ANALYSED.
IF NO MORE WELLS ARE TO BE SEEN, TYPE IN 0.

Display 10

DO YOU WANT ALL THE DEFAULTS TO BE SET
FOR THIS WELL?

n

ADOLPHUS D-50 CONTAINS 39 EVENTS

RASC DISTANCE VERSUS EVENT SCALE
****

RECODED FOSSIL NUMBERS

FOSSIL	EVENT
10	1.0
71	2.0
16	3.0
18	4.0
20	5.0
201	6.0
26	7.0
15	8.0
-31	8.0
-69	8.0
24	9.0
-33	9.0
-202	9.0
259	10.0
-25	10.0
263	11.0
82	12.0
85	13.0
-261	13.0
203	14.0
147	15.0
-260	15.0
68	16.0
32	17.0
40	18.0
30	19.0
49	20.0
-29	20.0
90	21.0
-37	21.0
93	22.0
36	23.0
164	24.0
50	25.0
-230	25.0
54	26.0
57	27.0
-58	27.0
55	28.0

DO YOU WANT TO CONSIDER ANOMALOUS EVENTS ?

Display 11

AGE IN MA VERSUS EVENT SCALE
****

RASC DISTANCE CONVERTED INTO AGE FOR ADOLPHUS D-50

RASC DISTANCE	AGE(MA)
1.0842	6.6
2.9307	17.7
2.0922	12.4
2.6301	15.3
3.0154	18.6
3.2153	20.4
3.1405	19.5
3.3652	21.5
4.0328	28.8
3.9291	27.7
3.7076	25.4
4.7835	36.0
4.0864	29.3
4.2032	30.5
3.9620	28.0
5.3465	40.3
4.5347	34.1
5.2371	39.4
5.0652	38.1
5.3729	40.5
4.7293	35.6
5.0497	37.9
5.7662	43.4
5.6524	42.5
5.6550	42.5
5.9646	44.9
6.2722	47.3
5.5339	41.5
6.4673	48.9
6.6322	49.8
6.8475	51.3
6.5200	49.2
7.4170	54.3
7.5269	55.0
7.5375	55.0
7.9288	56.6
6.5655	49.4
8.4595	59.0
8.9610	61.2

AVERAGED VALUES FOR SPLINE

AVERAGED VALUES	RANK
6.6342	1.0
17.6951	2.0
12.3539	3.0
15.3115	4.0
18.5571	5.0
20.3934	6.0
19.4647	7.0
26.0052	8.0
30.2267	9.0
29.2336	10.0
40.2631	11.0
34.1151	12.0
38.7076	13.0
40.4814	14.0
36.7514	15.0
43.3533	16.0
42.4569	17.0
42.4774	18.0
44.9162	19.0
44.4313	20.0
49.3449	21.0
51.3306	22.0
49.1885	23.0
54.2740	24.0
55.0247	25.0
56.6404	26.0
54.2182	27.0
61.1578	28.0

DO YOU WANT TO KEEP THE DEFAULT SMOOTHING FACTOR?
DEFAULT = 1.8164

Display 12

DO YOU WANT TO SEE THE VALUES TO BE USED FOR THE SPLINE?

```
AGE IN MA VERSUS DEPTH IN KM
****************************
```

RASC DISTANCE CONVERTED INTO AGE FOR ADOLPHUS D-50

RASC DISTANCE	AGE(MA)
1.0842	6.6
2.9307	17.7
2.0922	12.4
2.6801	15.3
3.0154	18.6
3.2153	20.4
3.1405	19.5
3.7777	26.2
4.1925	30.3
4.0826	29.2
5.3465	40.3
4.5347	34.1
5.1512	38.7
5.3729	40.5
4.8895	36.8
5.7662	43.4
5.6524	42.5
5.6550	42.5
5.9646	44.9
5.9031	44.4
6.5498	49.3
6.8475	51.3
6.5200	49.2
7.4170	54.3
7.5322	55.0
7.9288	56.6
7.5125	54.8
8.9610	61.2

```
DO YOU WANT TO KEEP THE DEFAULT SMOOTHING FACTOR?
DEFAULT =   2.0488
n

ENTER SMOOTHING FACTOR
2.1
```

Display 13

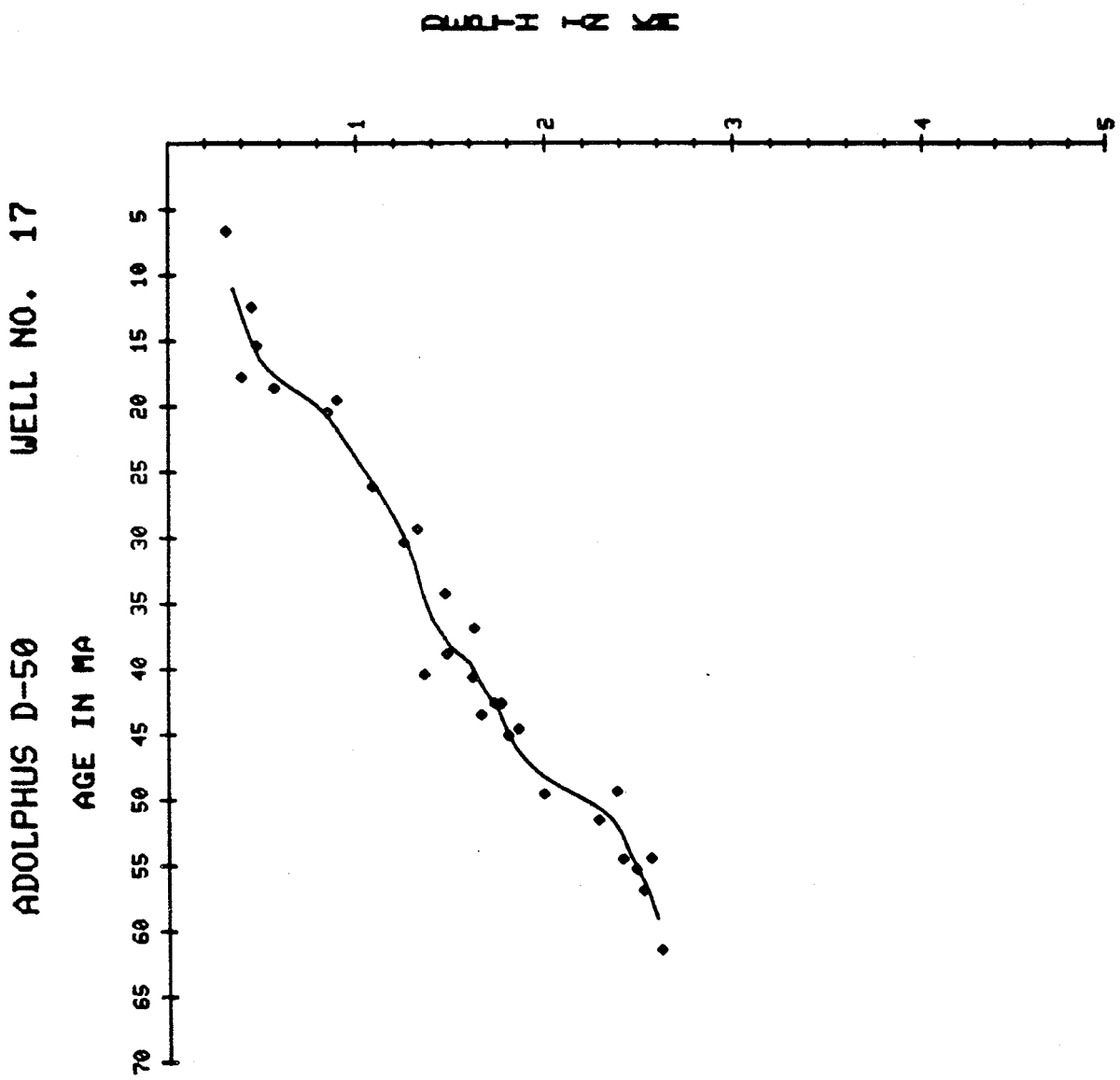
ADOLPHUS D-50
WELL NO. 17
AGE IN MA
DEPTH IN KM
5
10
15
20
25
30
35
40
45
50
55
60
65
70
1
2
3
4
5

Display 14

AGE IN MA VERSUS DEPTH IN KM
****

DO YOU WANT TO KEEP THE DEFAULT SMOOTHING FACTOR?
DEFAULT = .1000

SHOULD THE SPLINE APPROXIMATIONS BE DISPLAYED?

INDEPENDENT	FITTED VALUE
.3500	10.382
.4000	12.975
.4500	14.303
.5000	16.266
.5500	17.265
.6000	17.925
.6500	18.423
.7000	18.878
.7500	19.367
.8000	19.957
.8500	20.712
.9000	21.649
.9500	22.707
1.0000	23.805
1.0500	24.898
1.1000	25.985
1.1500	27.108
1.2000	28.362
1.2500	29.903
1.3000	31.836
1.3500	33.977
1.4000	35.825
1.4500	37.153
1.5000	38.092
1.5500	38.819
1.6000	39.605
1.6500	40.647
1.7000	41.839
1.7500	43.141
1.8000	44.558
1.8500	45.840
1.9000	46.821
1.9500	47.542
2.0000	48.099
2.0500	48.563
2.1000	48.975
2.1500	49.356
2.2000	49.719
2.2500	50.098
2.3000	50.567
2.3500	51.258
2.4000	52.303
2.4500	53.669
2.5000	55.181
2.5500	56.854
2.6000	58.705

Display 15

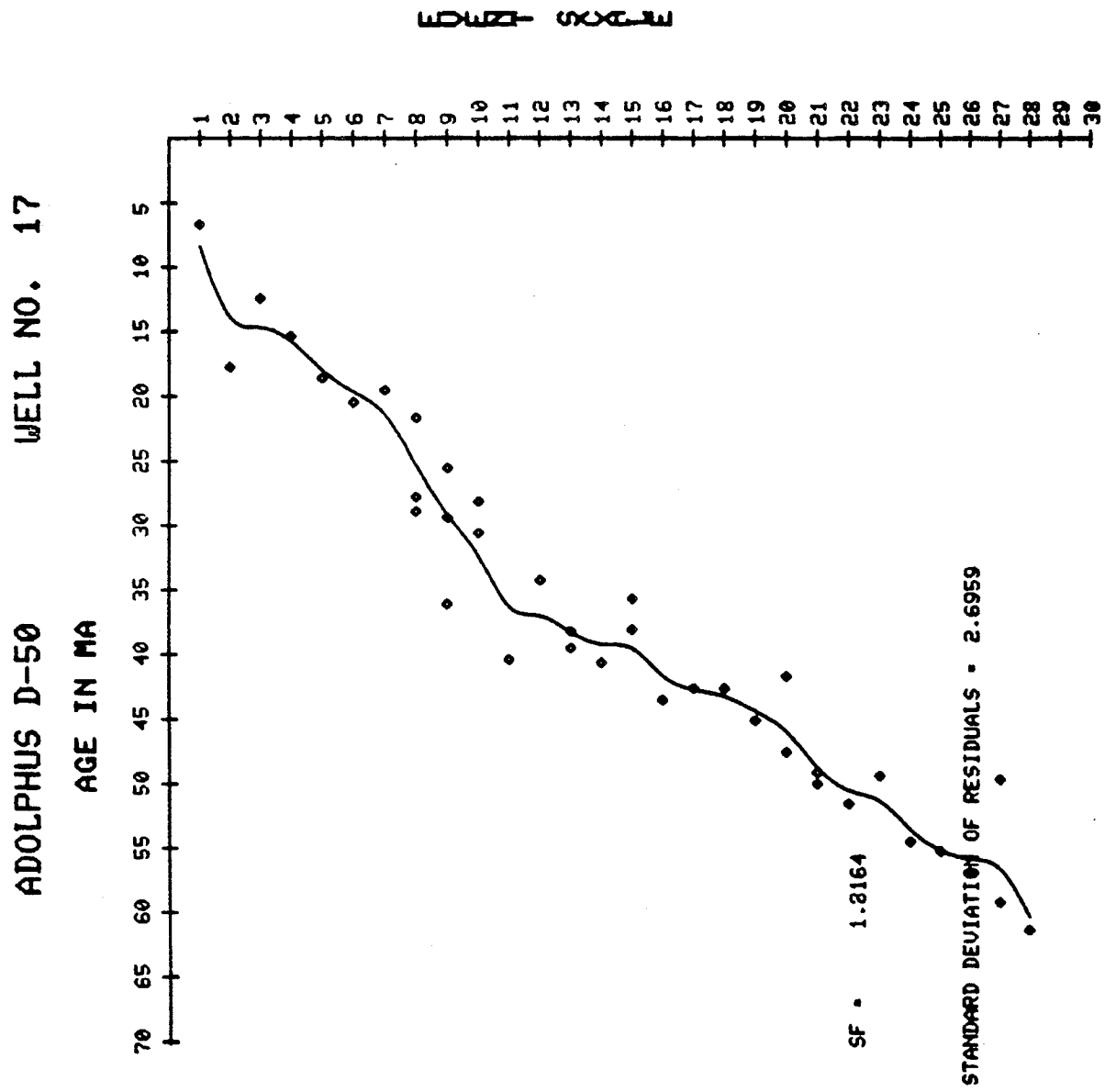
ADOLPHUS D-50
WELL NO. 17
AGE IN MA
70 65 60 55 50 45 40 35 30 25 20 15 10 5
1 2 3 4 5 6 7 8 9 10 11 12 13 14 15 16 17 18 19 20 21 22 23 24 25 26 27 28 29 30
SF = 1.3164
STANDARD DEVIATION OF RESIDUALS = 2.6959
EDEN SCALE

Display 16

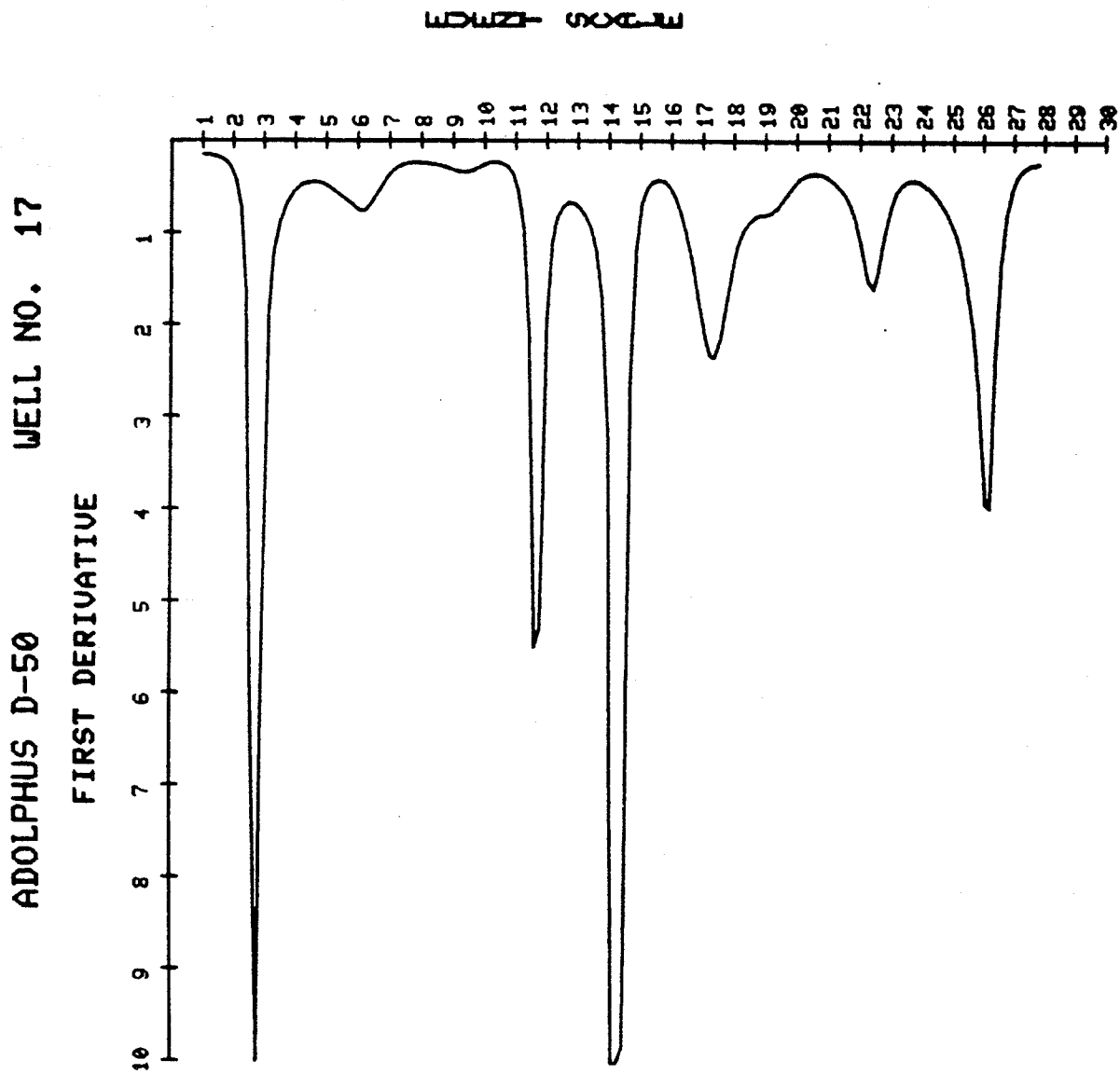
ADOLPHUS D-50
WELL NO. 17
FIRST DERIVATIVE
1
2
3
4
5
6
7
8
9
10
1
2
3
4
5
6
7
8
9
10
11
12
13
14
15
16
17
18
19
20
21
22
23
24
25
26
27
28
29
30

Display 17

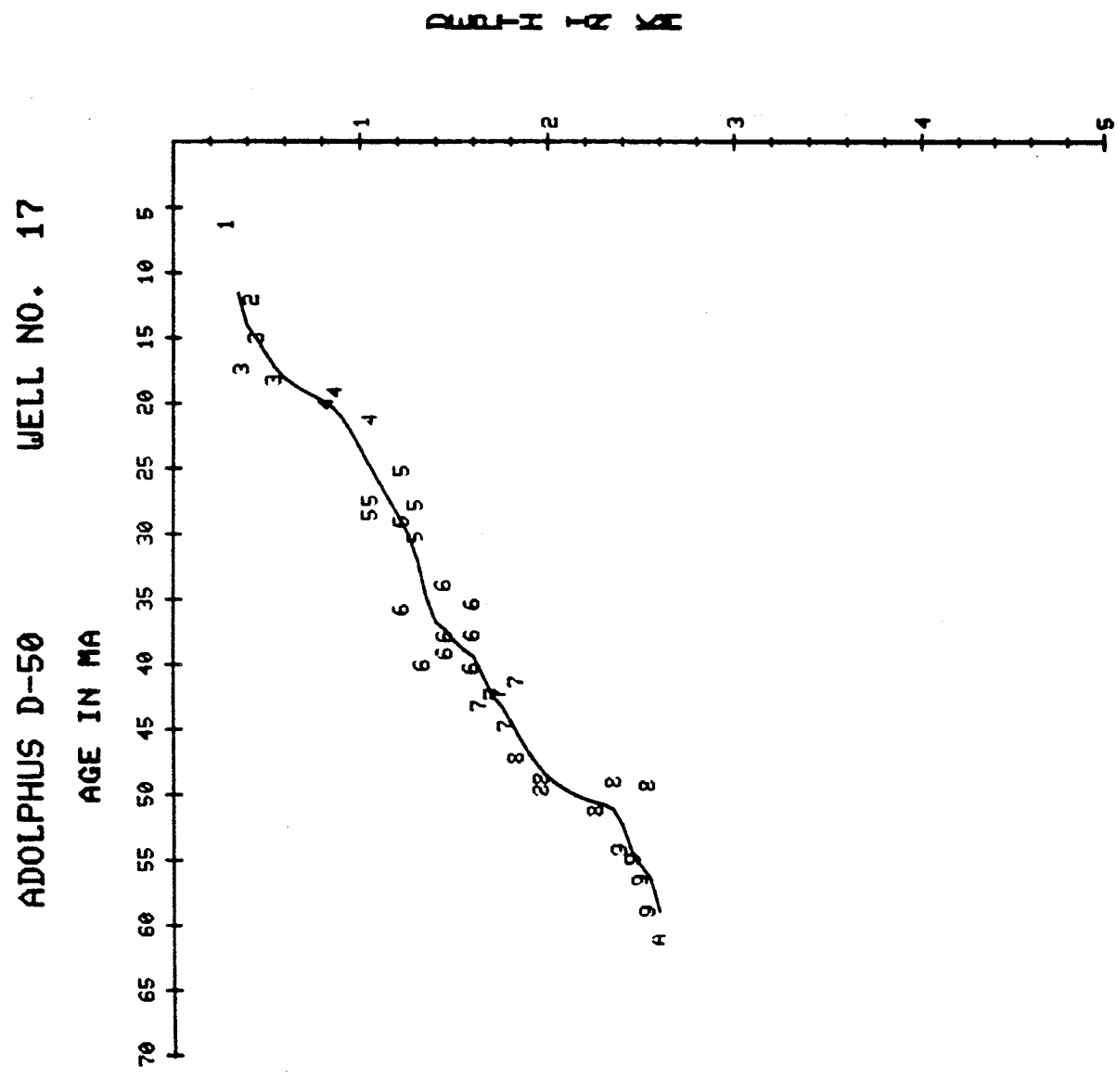
ADOLPHUS D-50
WELL NO. 17
AGE IN MA
DEPTH IN KM
1
2
3
4
5
5
10
15
20
25
30
35
40
45
50
55
60
65
70

Display 18

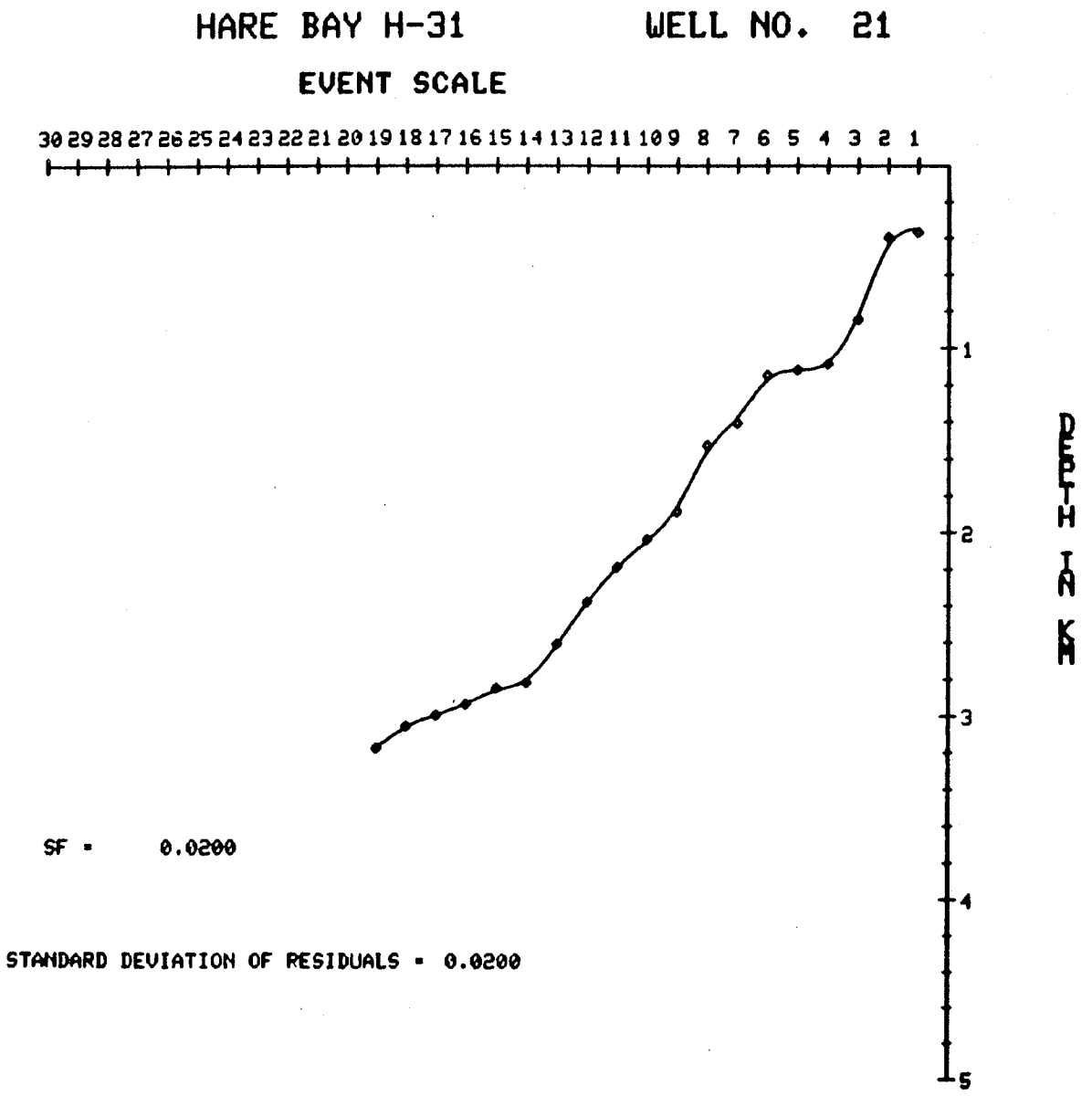
HARE BAY H-31 WELL NO. 21
EVENT SCALE
30 29 28 27 26 25 24 23 22 21 20 19 18 17 16 15 14 13 12 11 10 9 8 7 6 5 4 3 2 1
1
2
3
4
5
DEPTH IN KM
SF = 0.0200
STANDARD DEVIATION OF RESIDUALS = 0.0200

Display 19

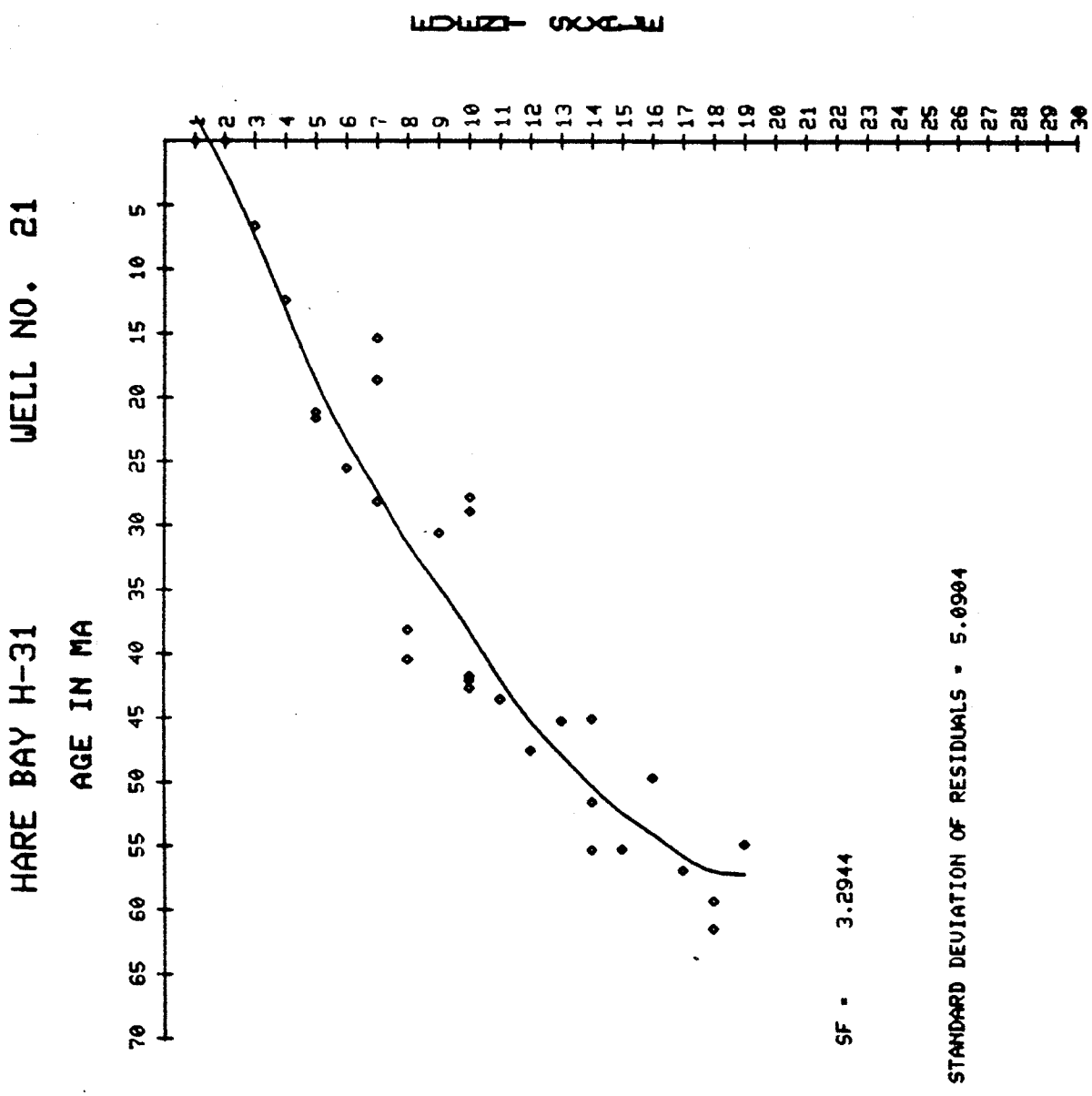
HARE BAY H-31
WELL NO. 21
AGE IN MA
70 65 60 55 50 45 40 35 30 25 20 15 10 5
1 2 3 4 5 6 7 8 9 10 11 12 13 14 15 16 17 18 19 20 21 22 23 24 25 26 27 28 29 30
EDEN SCALE
SF = 3.2944
STANDARD DEVIATION OF RESIDUALS = 5.0904

Display 20

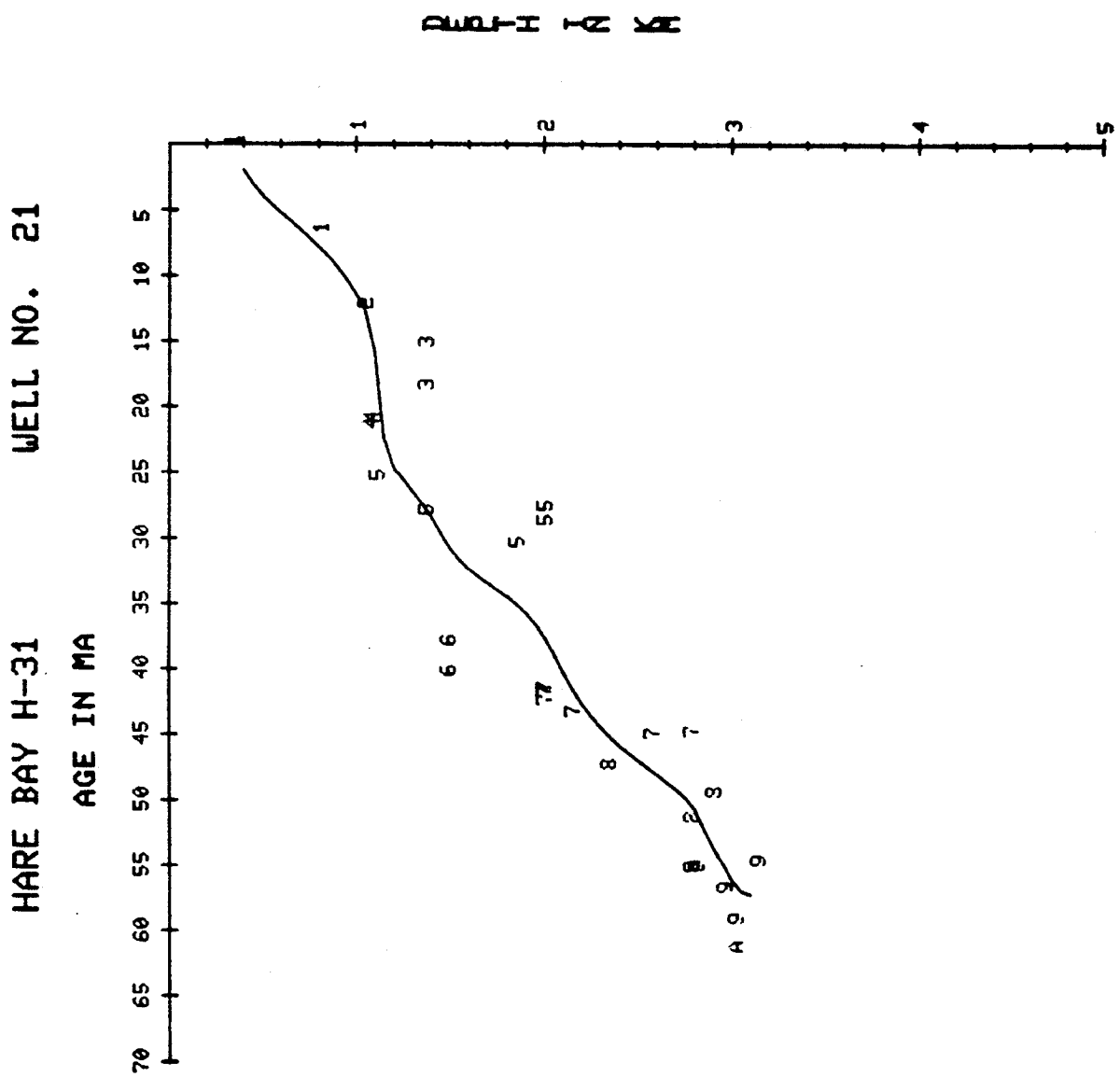
HARE BAY H-31
WELL NO. 21
AGE IN MA
DEPTH IN KM
1
2
3
4
5
10
15
20
25
30
35
40
45
50
55
60
65
70

Display 21

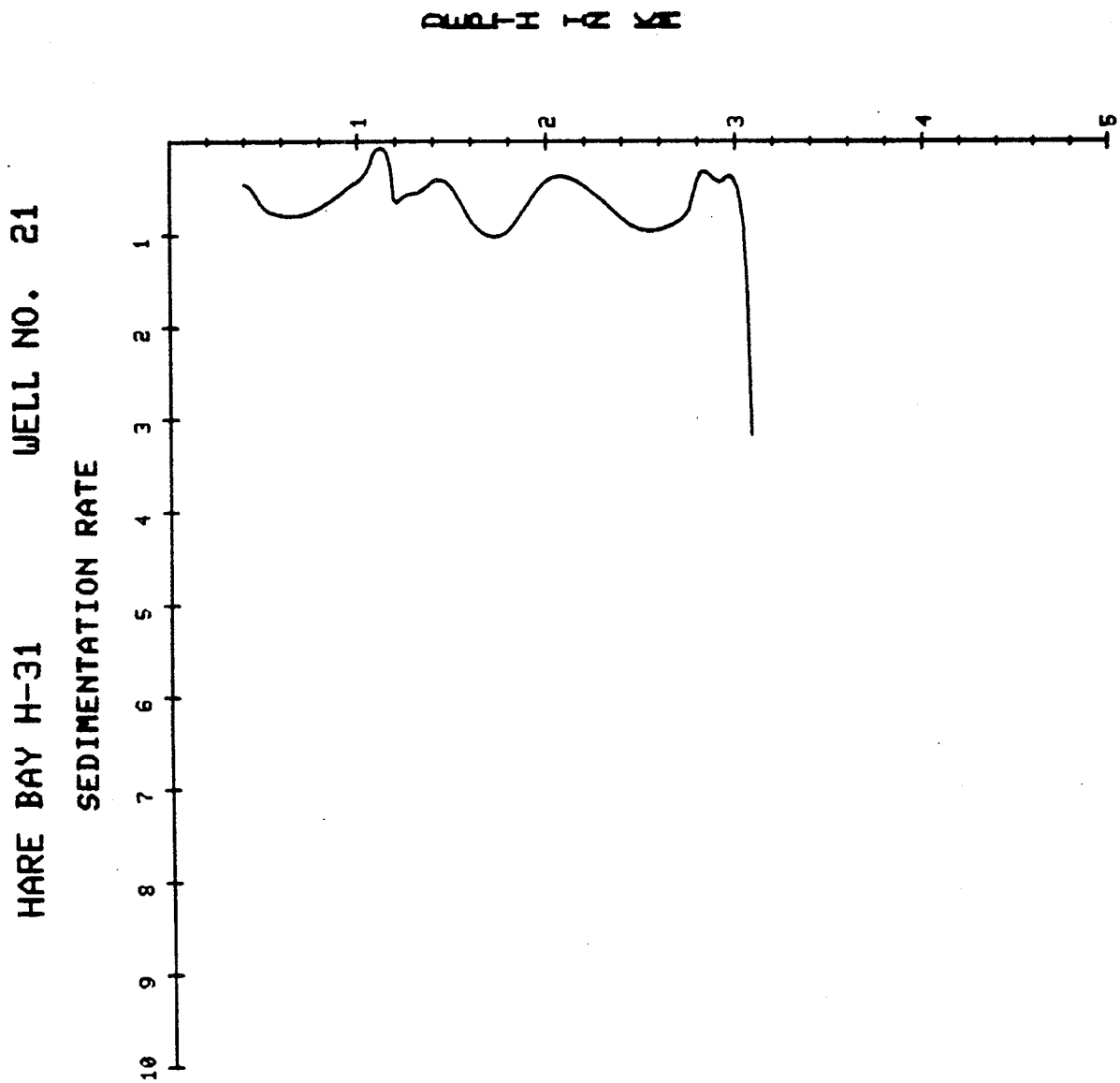
HARE BAY H-31
WELL NO. 21
SEDIMENTATION RATE
DEPTH IN KM
1
2
3
4
5
1
2
3
4
5
6
7
8
9
10

Display 22

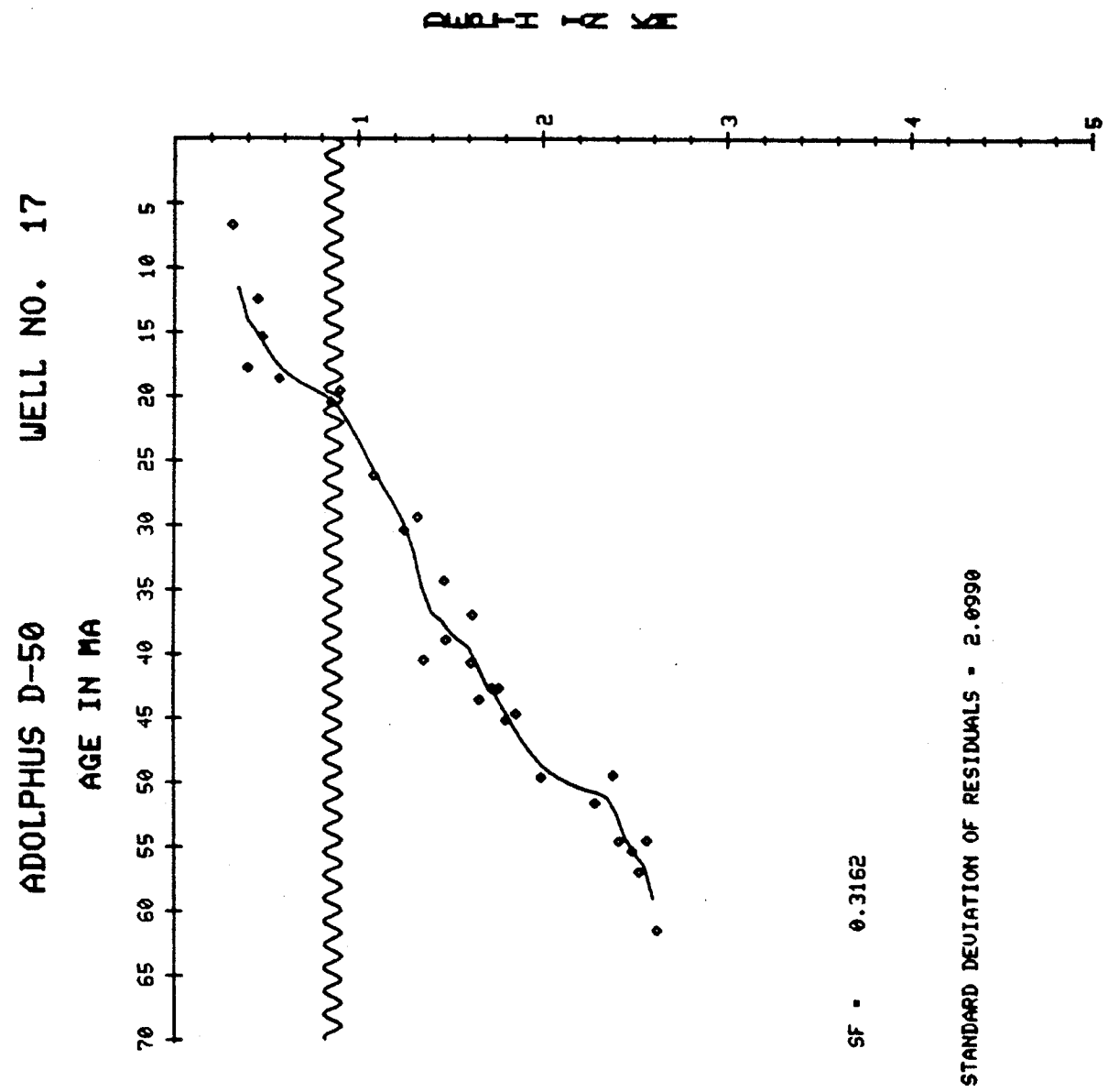
ADOLPHUS D-50
WELL NO. 17
AGE IN MA
5
10
15
20
25
30
35
40
45
50
55
60
65
70
DEPTH KM
1
2
3
4
5
SF = 0.3162
STANDARD DEVIATION OF RESIDUALS = 2.0990

Display 23

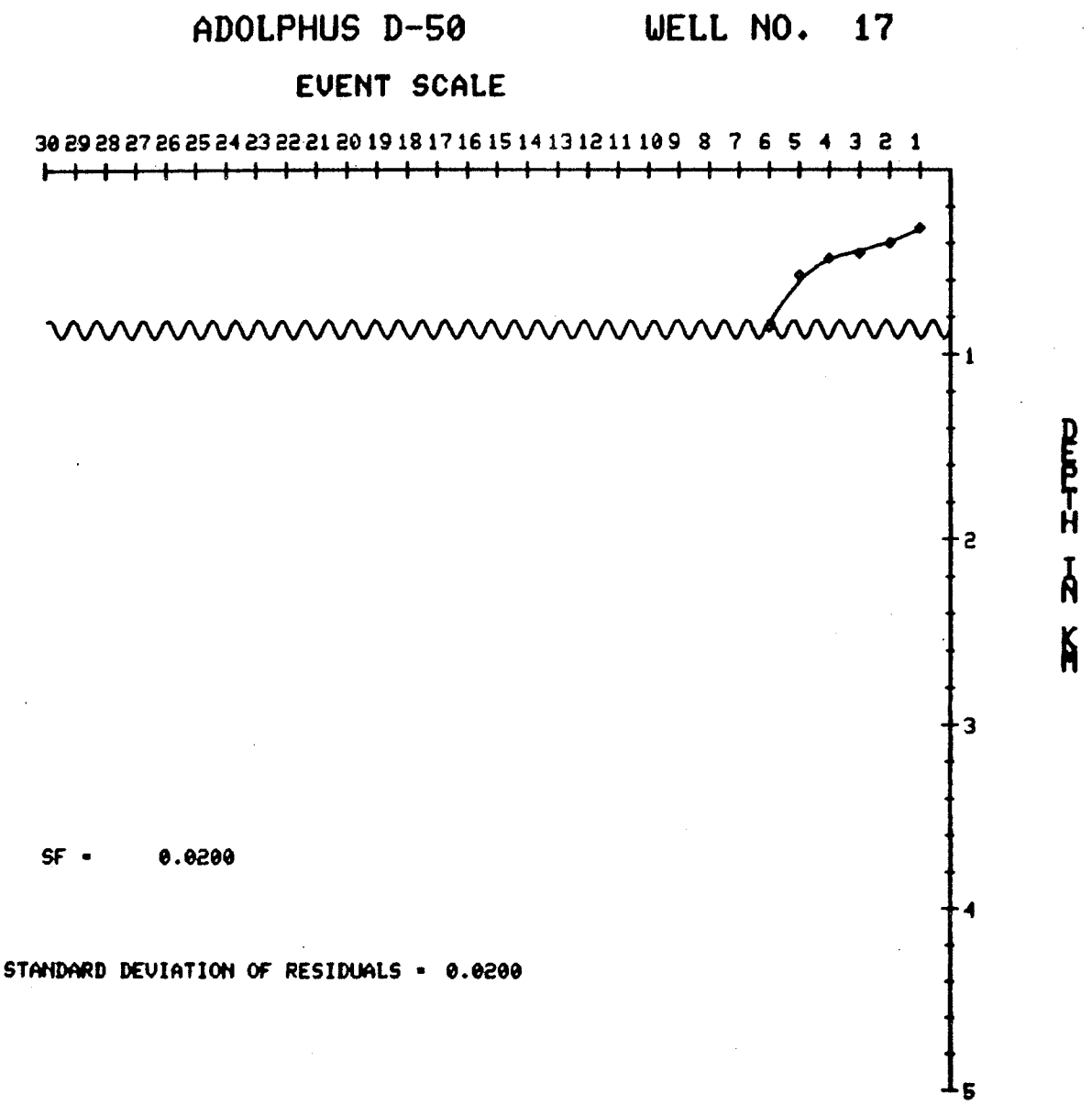
ADOLPHUS D-50
WELL NO. 17
EVENT SCALE
30 29 28 27 26 25 24 23 22 21 20 19 18 17 16 15 14 13 12 11 10 9 8 7 6 5 4 3 2 1
1
2
3
4
5
DEPTH IN KM
SF = 0.0200
STANDARD DEVIATION OF RESIDUALS = 0.0200

Display 24

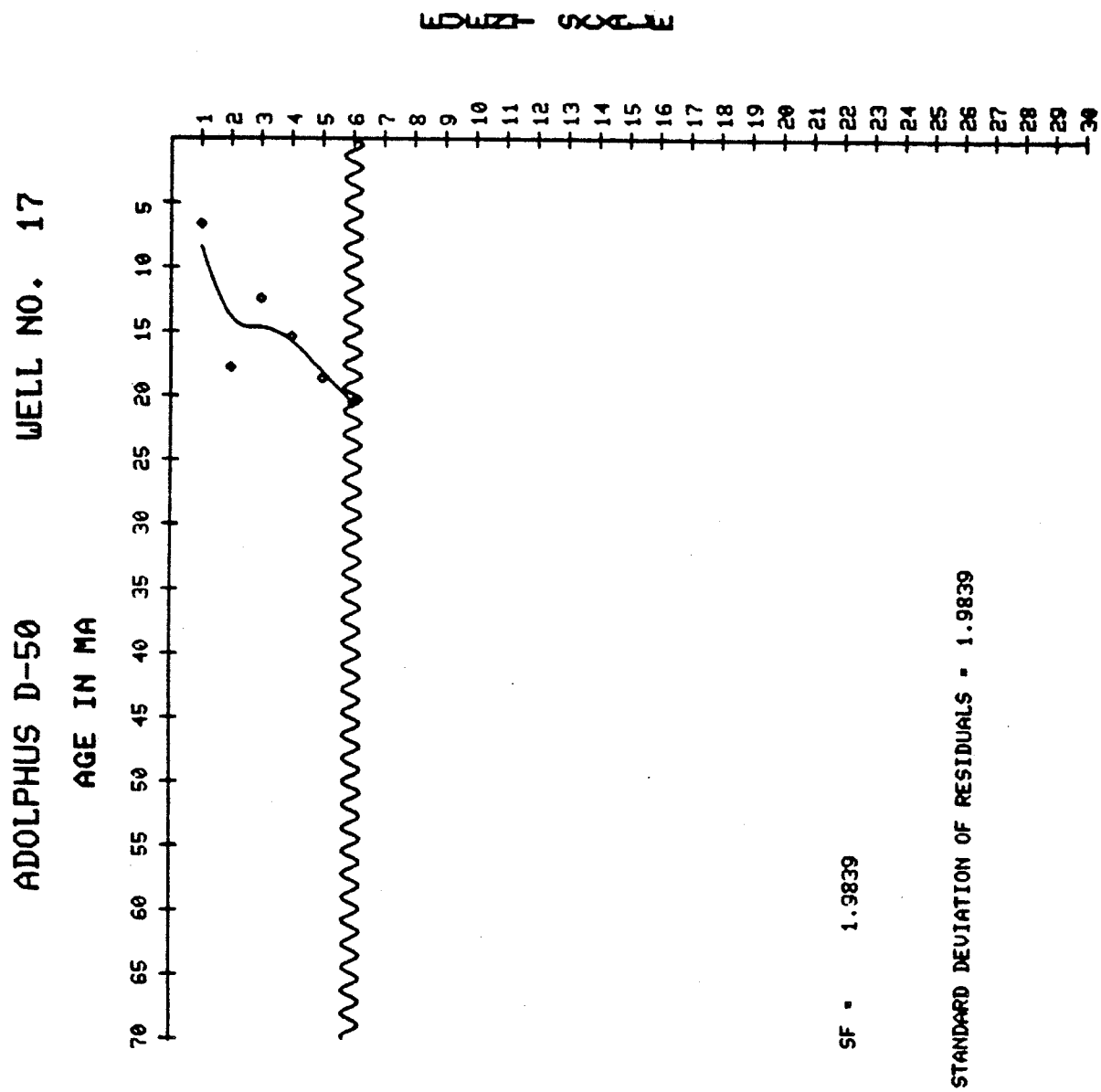
ADOLPHUS D-50
WELL NO. 17
AGE IN MA
70 65 60 55 50 45 40 35 30 25 20 15 10 5
1 2 3 4 5 6 7 8 9 10 11 12 13 14 15 16 17 18 19 20 21 22 23 24 25 26 27 28 29 30
DEPTH SCALE
SF = 1.9839
STANDARD DEVIATION OF RESIDUALS = 1.9839

Display 25

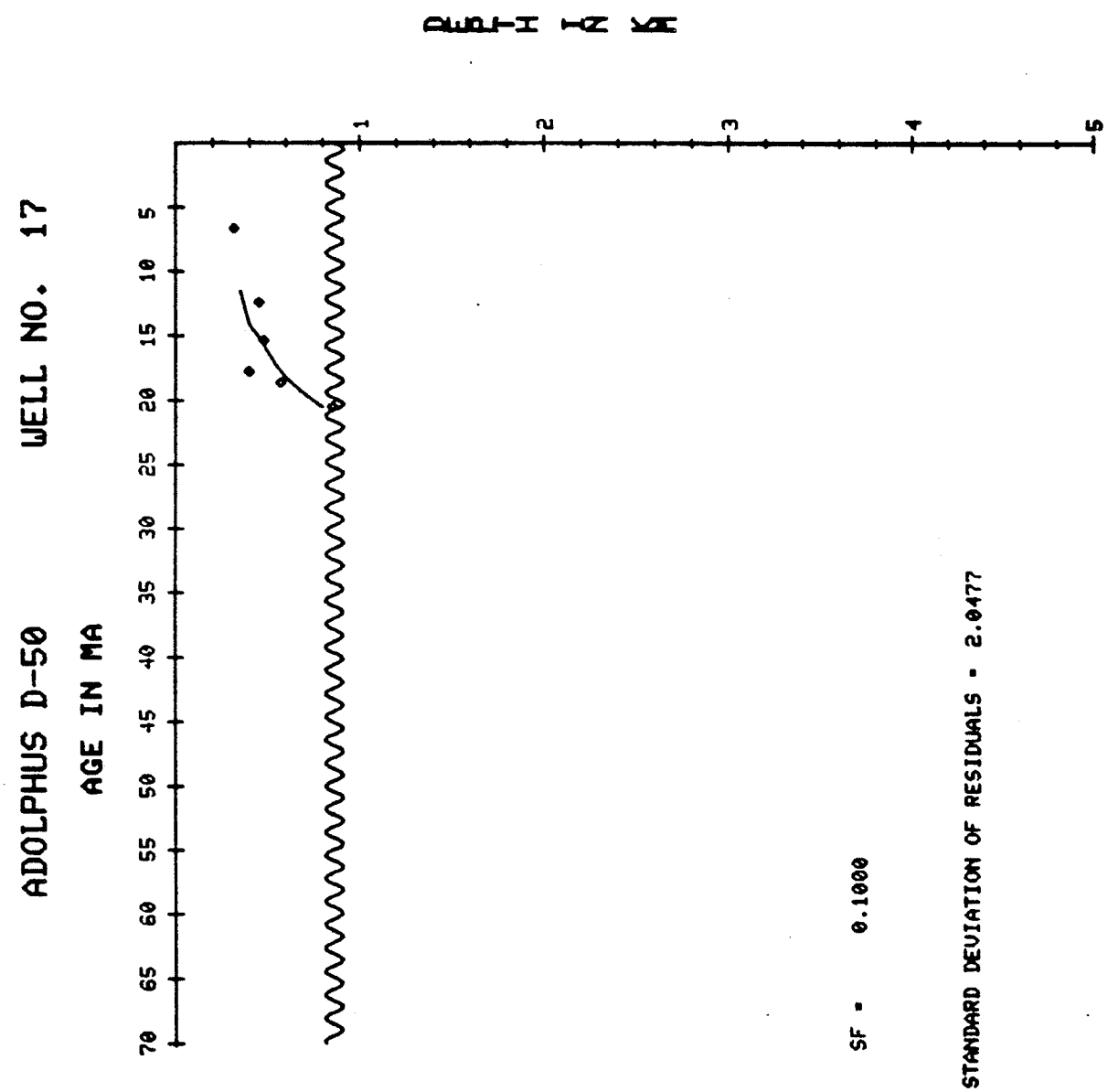
ADOLPHUS D-50
WELL NO. 17
AGE IN MA
5
10
15
20
25
30
35
40
45
50
55
60
65
70
1
2
3
4
5
SF = 0.1000
STANDARD DEVIATION OF RESIDUALS = 2.0477

Display 26

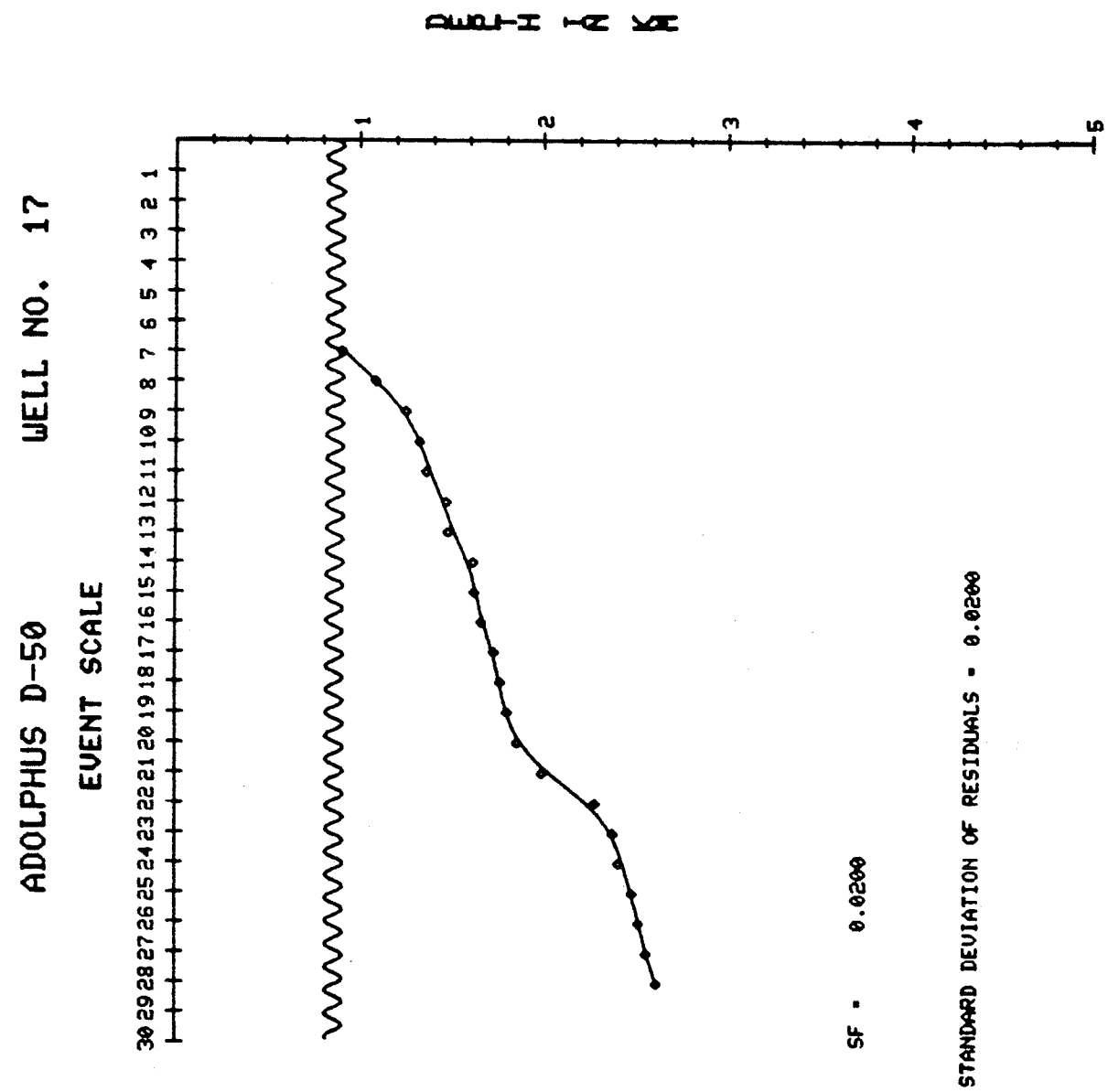
ADOLPHUS D-50
WELL NO. 17
EVENT SCALE
30 29 28 27 26 25 24 23 22 21 20 19 18 17 16 15 14 13 12 11 10 9 8 7 6 5 4 3 2 1
PERMEABILITY
1
2
3
4
5
SF = 0.0200
STANDARD DEVIATION OF RESIDUALS = 0.0200

Display 27

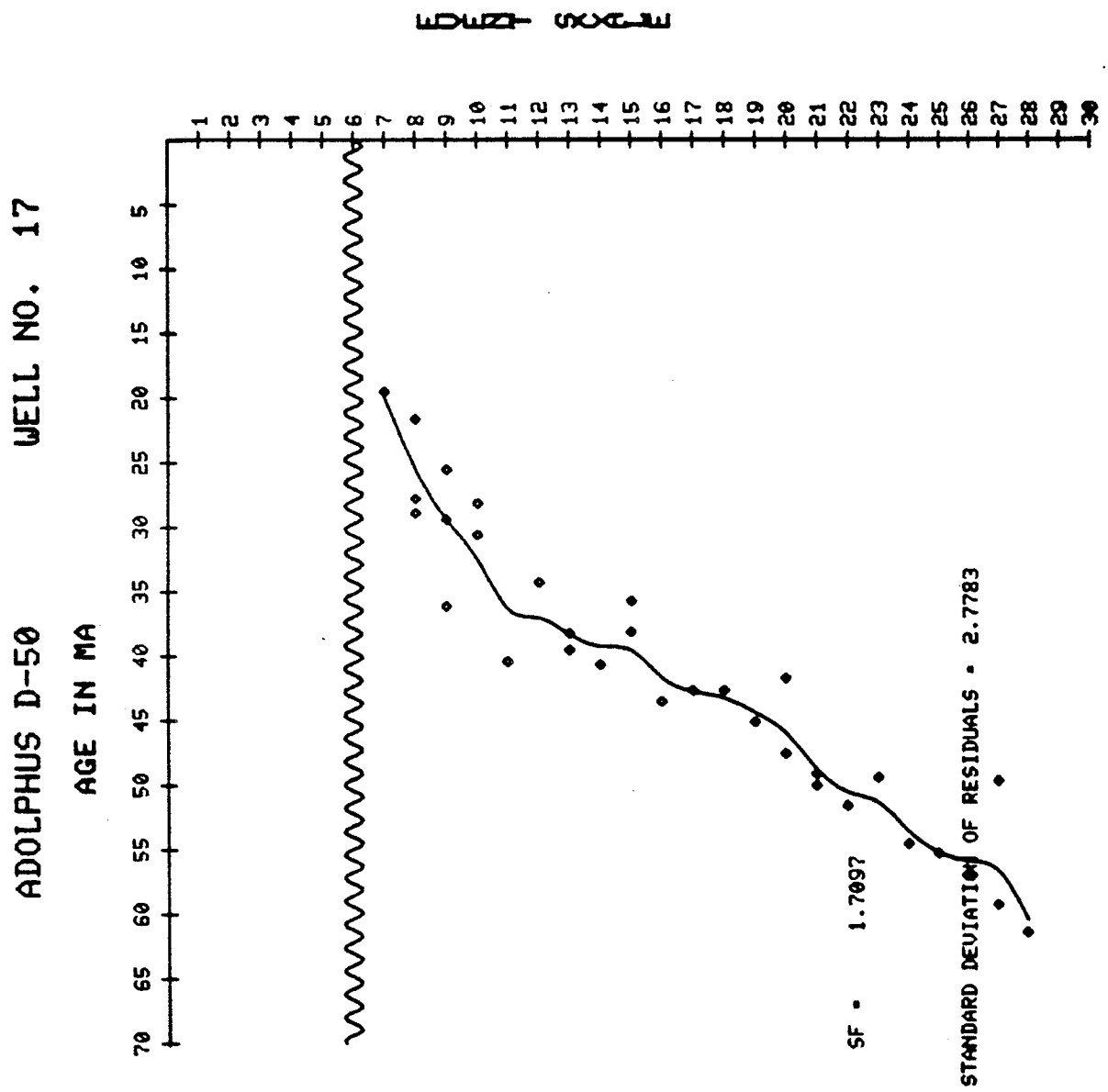
ADOLPHUS D-50
WELL NO. 17
AGE IN MA
70 65 60 55 50 45 40 35 30 25 20 15 10 5
1 2 3 4 5 6 7 8 9 10 11 12 13 14 15 16 17 18 19 20 21 22 23 24 25 26 27 28 29 30
SF = 1.7097
STANDARD DEVIATION OF RESIDUALS = 2.7783

Display 28

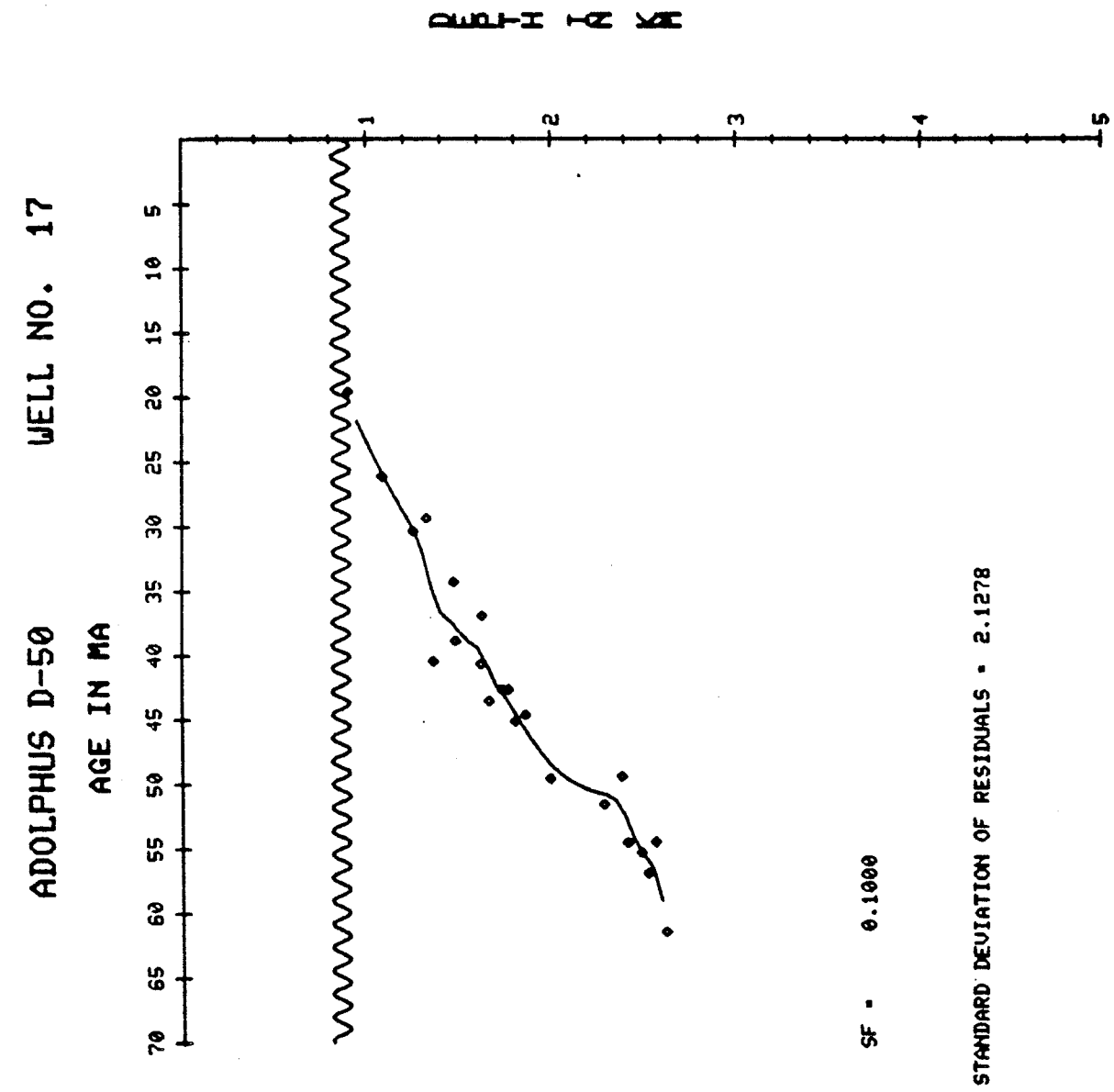
ADOLPHUS D-50
WELL NO. 17
AGE IN MA
70 65 60 55 50 45 40 35 30 25 20 15 10 5
DEPTH IN KM
1 2 3 4 5
SF = 0.1000
STANDARD DEVIATION OF RESIDUALS = 2.1278

Display 29

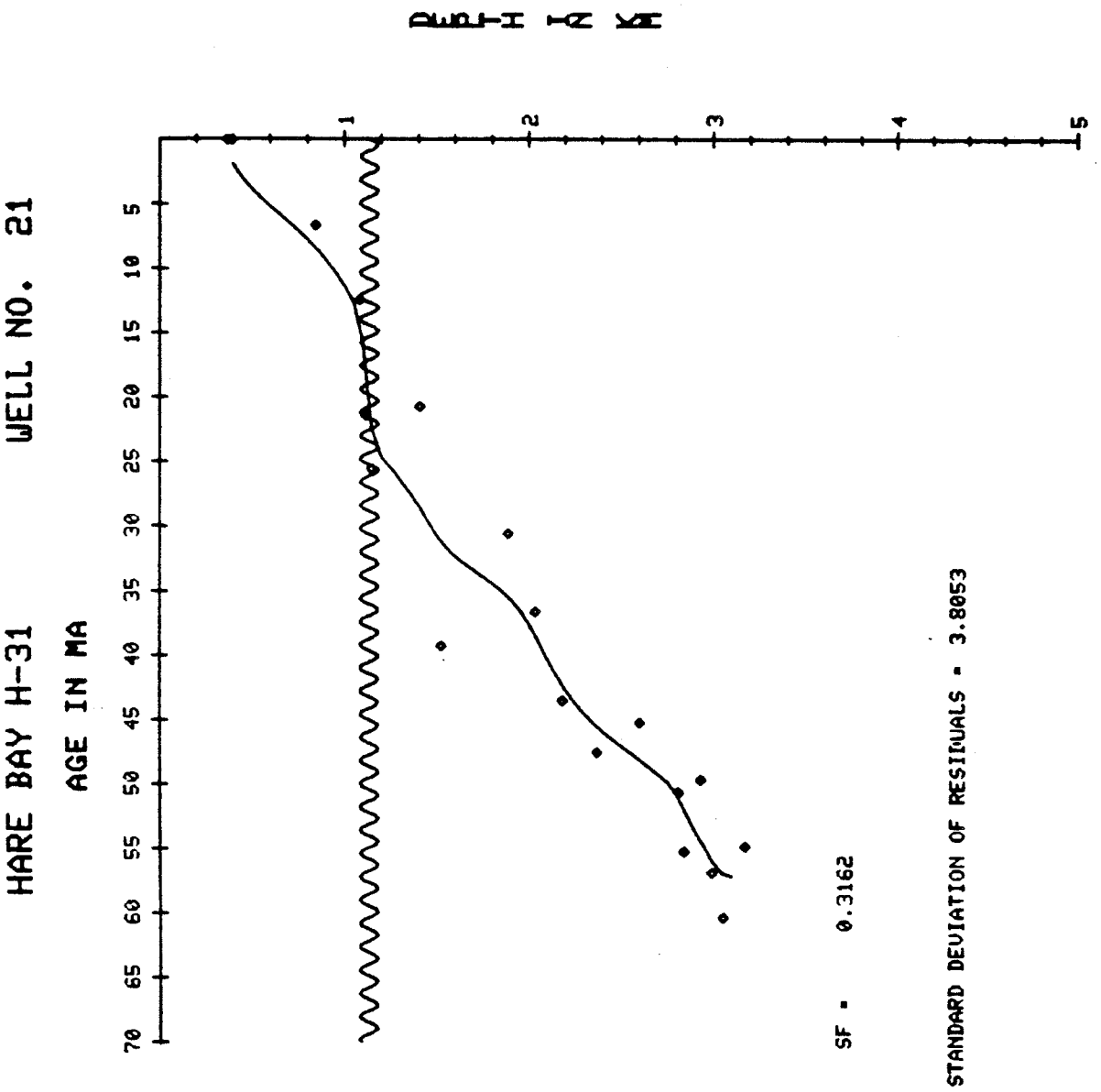
HARE BAY H-31
WELL NO. 21
AGE IN MA
5
10
15
20
25
30
35
40
45
50
55
60
65
70
1
2
3
4
5
SF = 0.3162
STANDARD DEVIATION OF RESIDUALS = 3.8053

Display 30

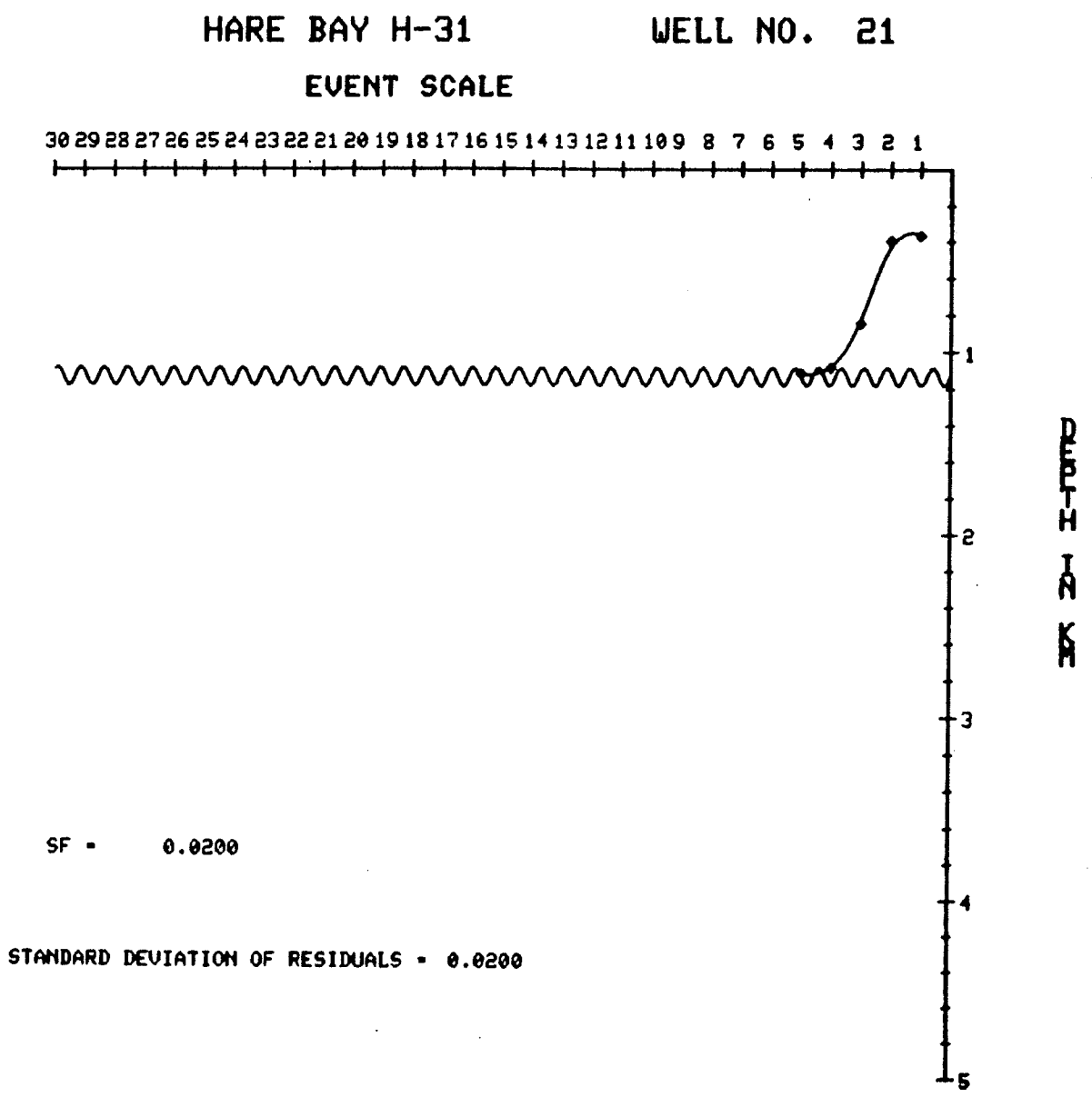
HARE BAY H-31
WELL NO. 21
EVENT SCALE
30 29 28 27 26 25 24 23 22 21 20 19 18 17 16 15 14 13 12 11 10 9 8 7 6 5 4 3 2 1
1
2
3
4
5
DEPTH IN KM
SF = 0.0200
STANDARD DEVIATION OF RESIDUALS = 0.0200

Display 31

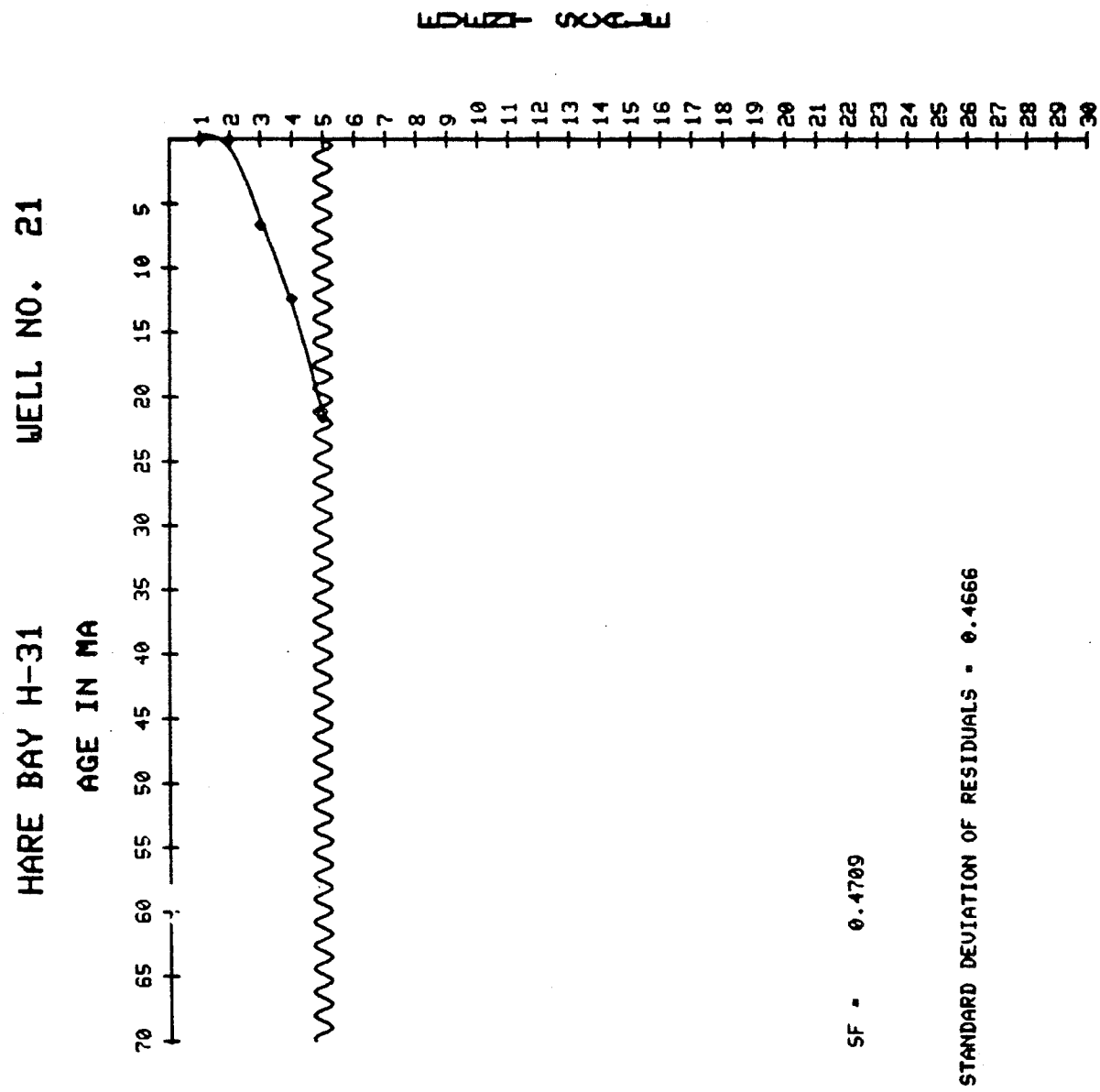
HARE BAY H-31
WELL NO. 21
AGE IN MA
70 65 60 55 50 45 40 35 30 25 20 15 10 5
1 2 3 4 5 6 7 8 9 10 11 12 13 14 15 16 17 18 19 20 21 22 23 24 25 26 27 28 29 30
REACH SCALE
SF = 0.4709
STANDARD DEVIATION OF RESIDUALS = 0.4666

Display 32

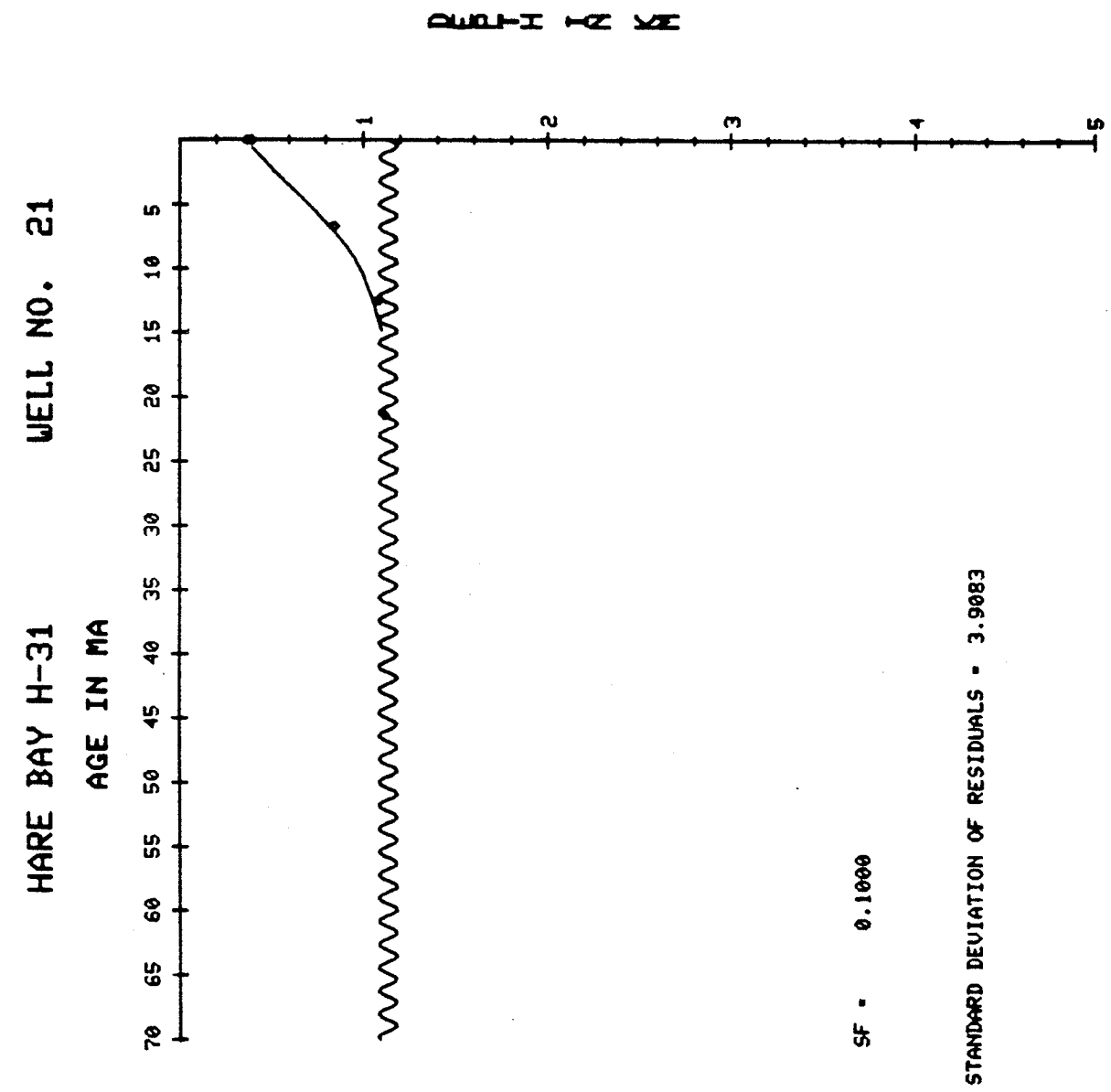
HARE BAY H-31
WELL NO. 21
AGE IN MA
70 65 60 55 50 45 40 35 30 25 20 15 10 5
1 2 3 4 5
DEPTH IN KM
SF = 0.1000
STANDARD DEVIATION OF RESIDUALS = 3.9083

Display 33

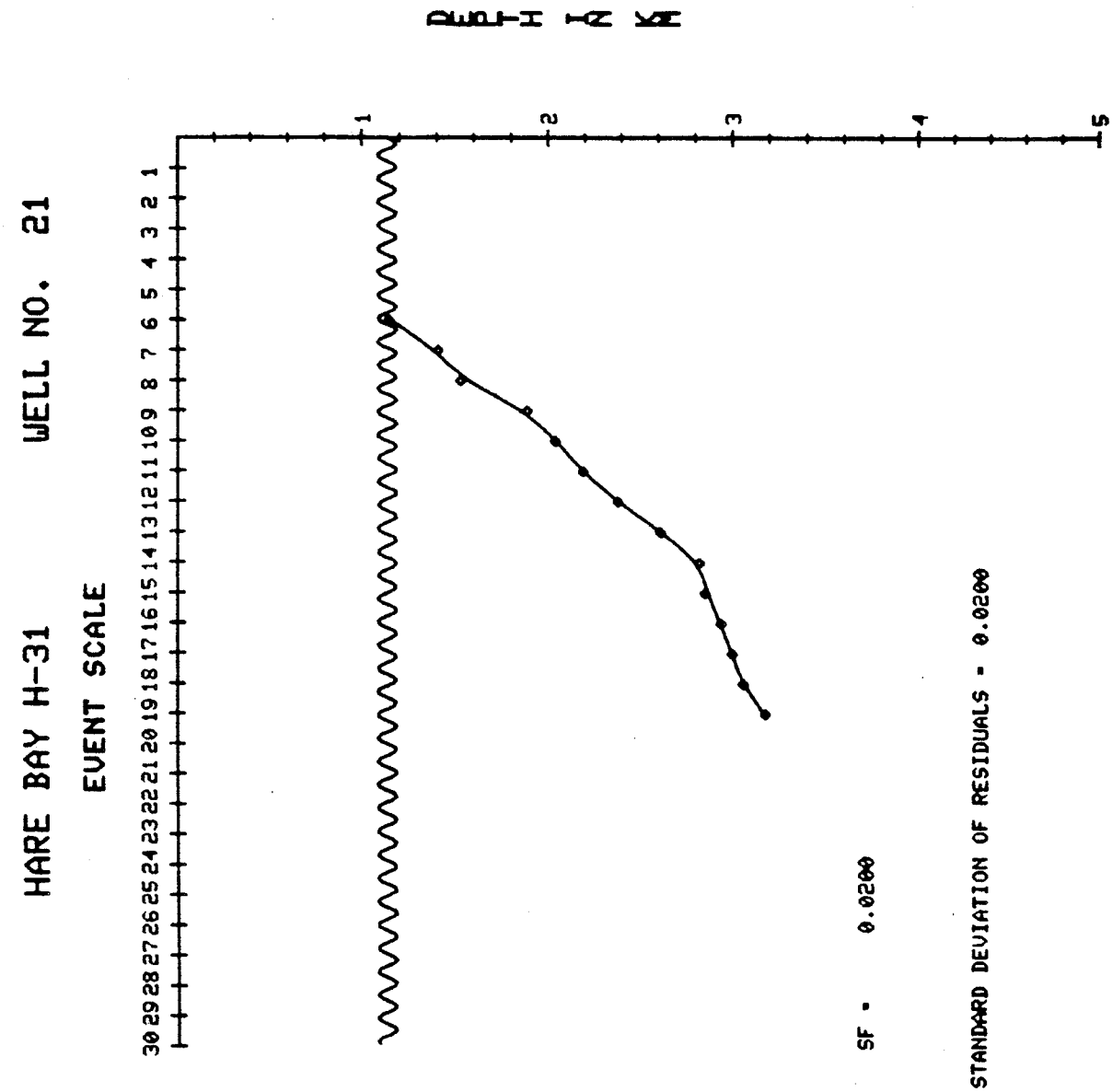
HARE BAY H-31
WELL NO. 21
EVENT SCALE
30 29 28 27 26 25 24 23 22 21 20 19 18 17 16 15 14 13 12 11 10 9 8 7 6 5 4 3 2 1
DEPTH IN KM
1
2
3
4
5
SF = 0.0200
STANDARD DEVIATION OF RESIDUALS = 0.0200

Display 34

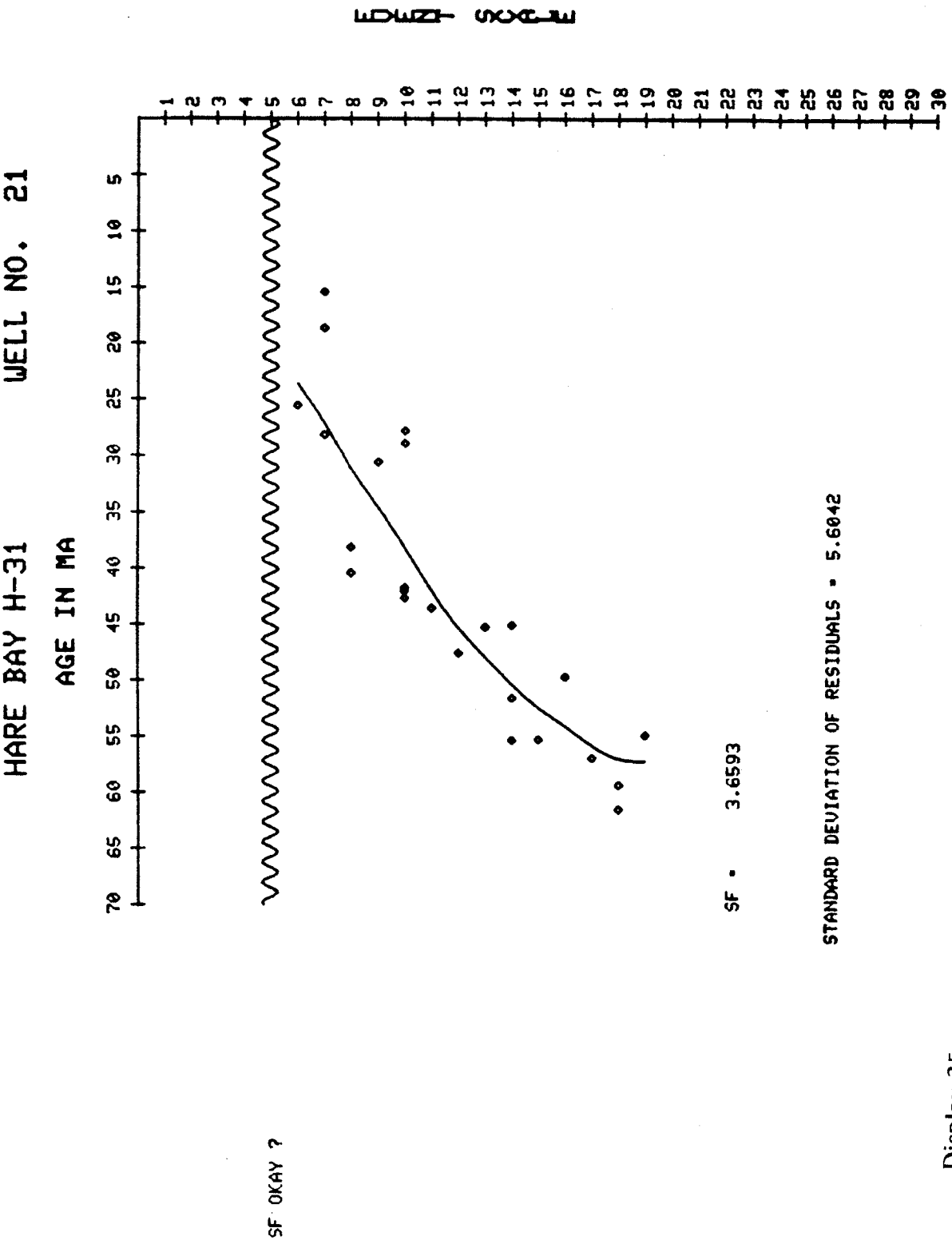
HARE BAY H-31
WELL NO. 21
AGE IN MA
70 65 60 55 50 45 40 35 30 25 20 15 10 5
1 2 3 4 5 6 7 8 9 10 11 12 13 14 15 16 17 18 19 20 21 22 23 24 25 26 27 28 29 30
REDUCED SCALE
SF OKAY ?
SF = 3.6593
STANDARD DEVIATION OF RESIDUALS = 5.6042

Display 35

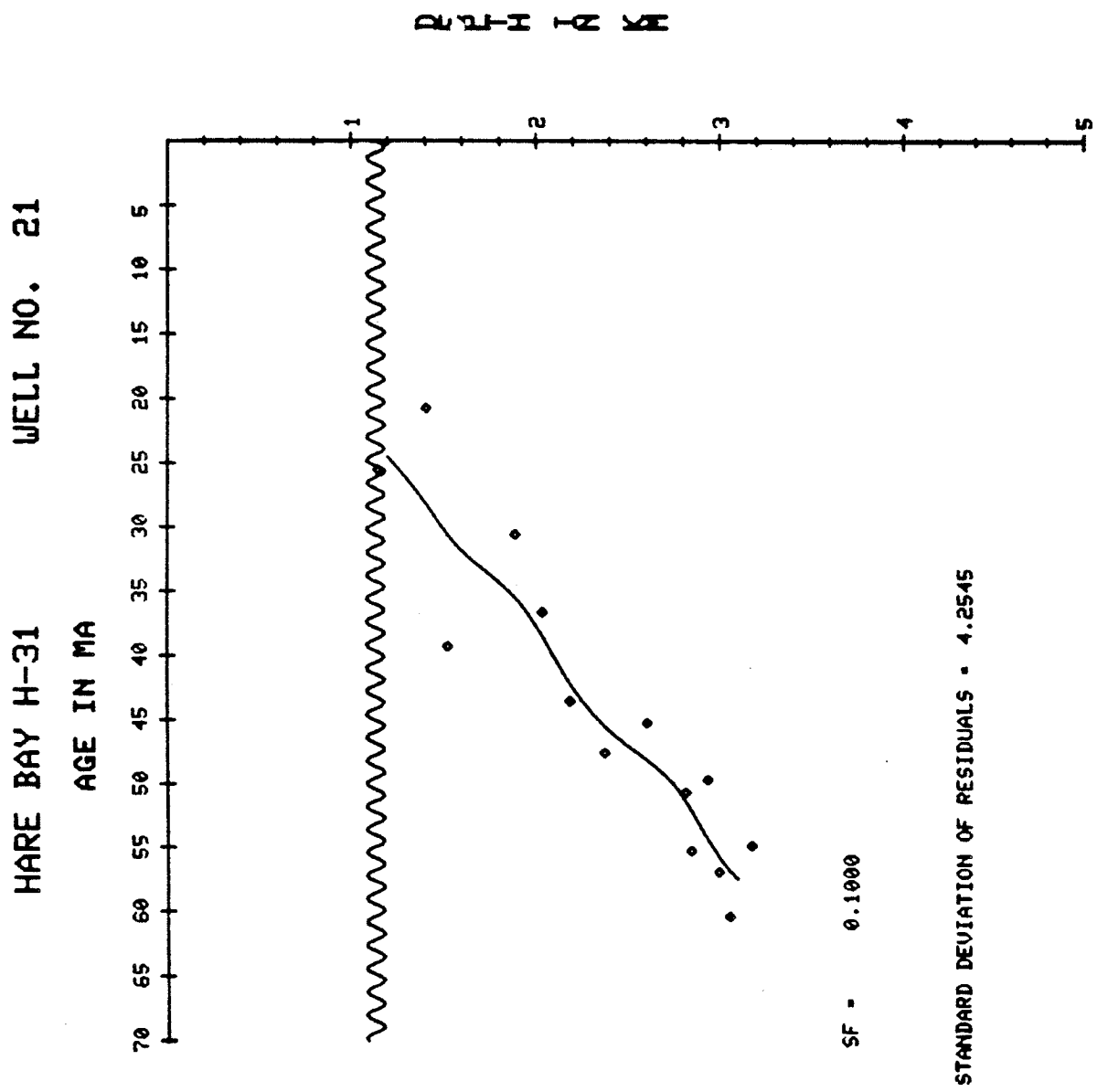
HARE BAY H-31
WELL NO. 21
AGE IN MA
70 65 60 55 50 45 40 35 30 25 20 15 10 5
1 2 3 4 5
DEPTH IN KM
SF = 0.1000
STANDARD DEVIATION OF RESIDUALS = 4.2545

Display 36

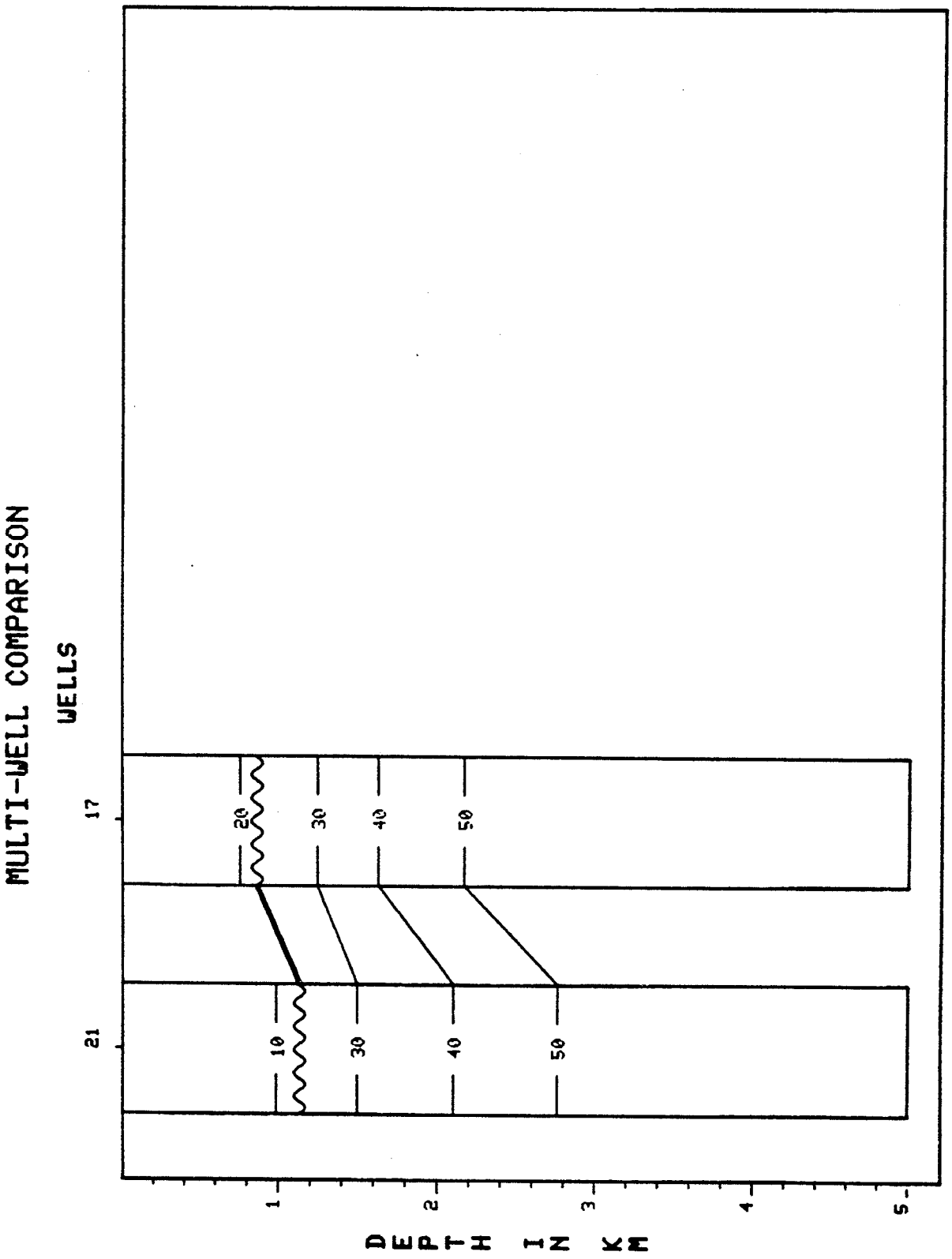
MULTI-WELL COMPARISON
WELLS
21
17
10
20
30
40
50
30
40
50
1
2
3
4
5
DEPTH IN KM

Display 37

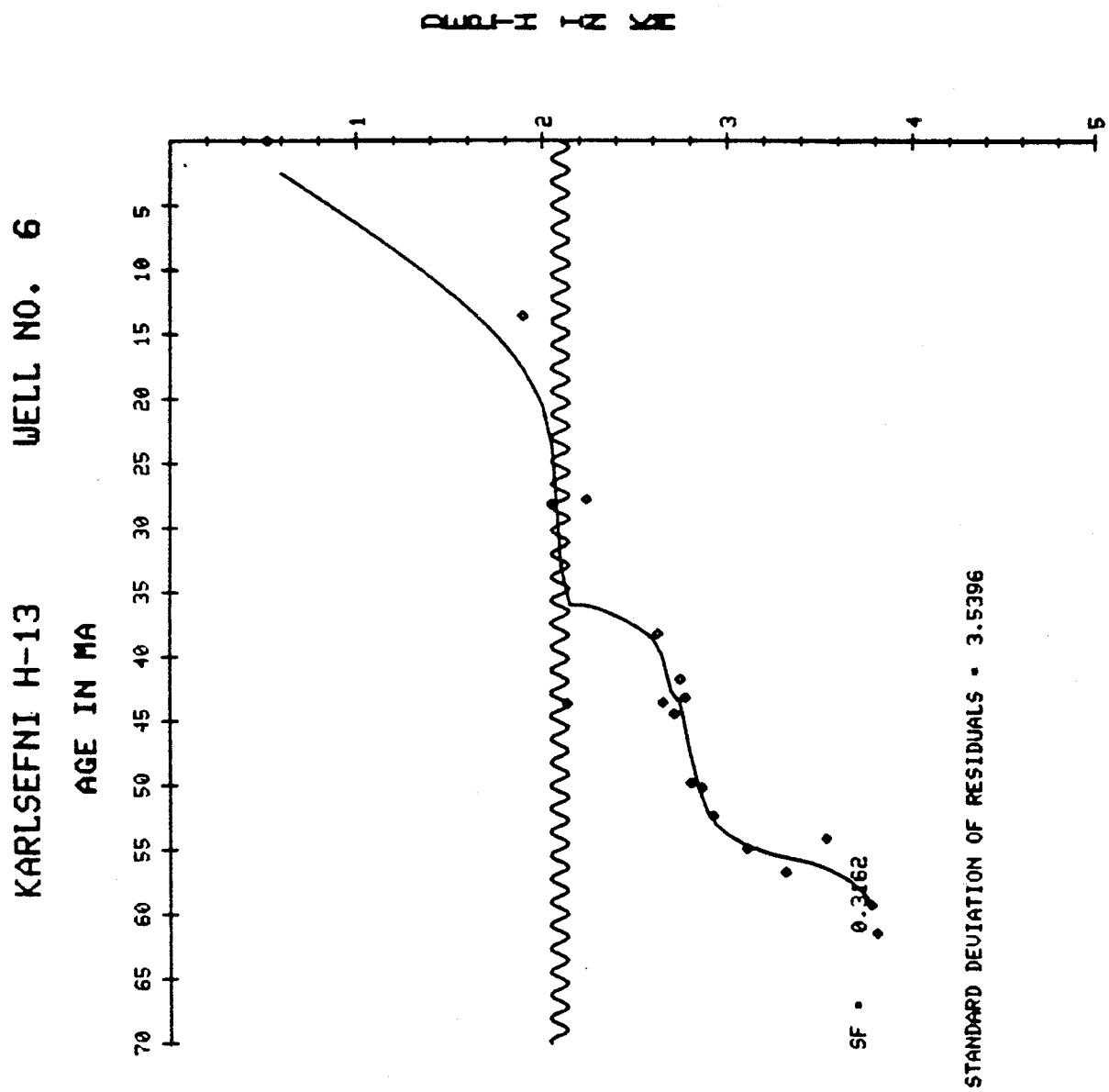
KARLSEFNI H-13
WELL NO. 6
AGE IN MA
DEPTH IN KM
1
2
3
4
5
5
10
15
20
25
30
35
40
45
50
55
60
65
70
SF = 0.3762
STANDARD DEVIATION OF RESIDUALS = 3.5396

Display 38

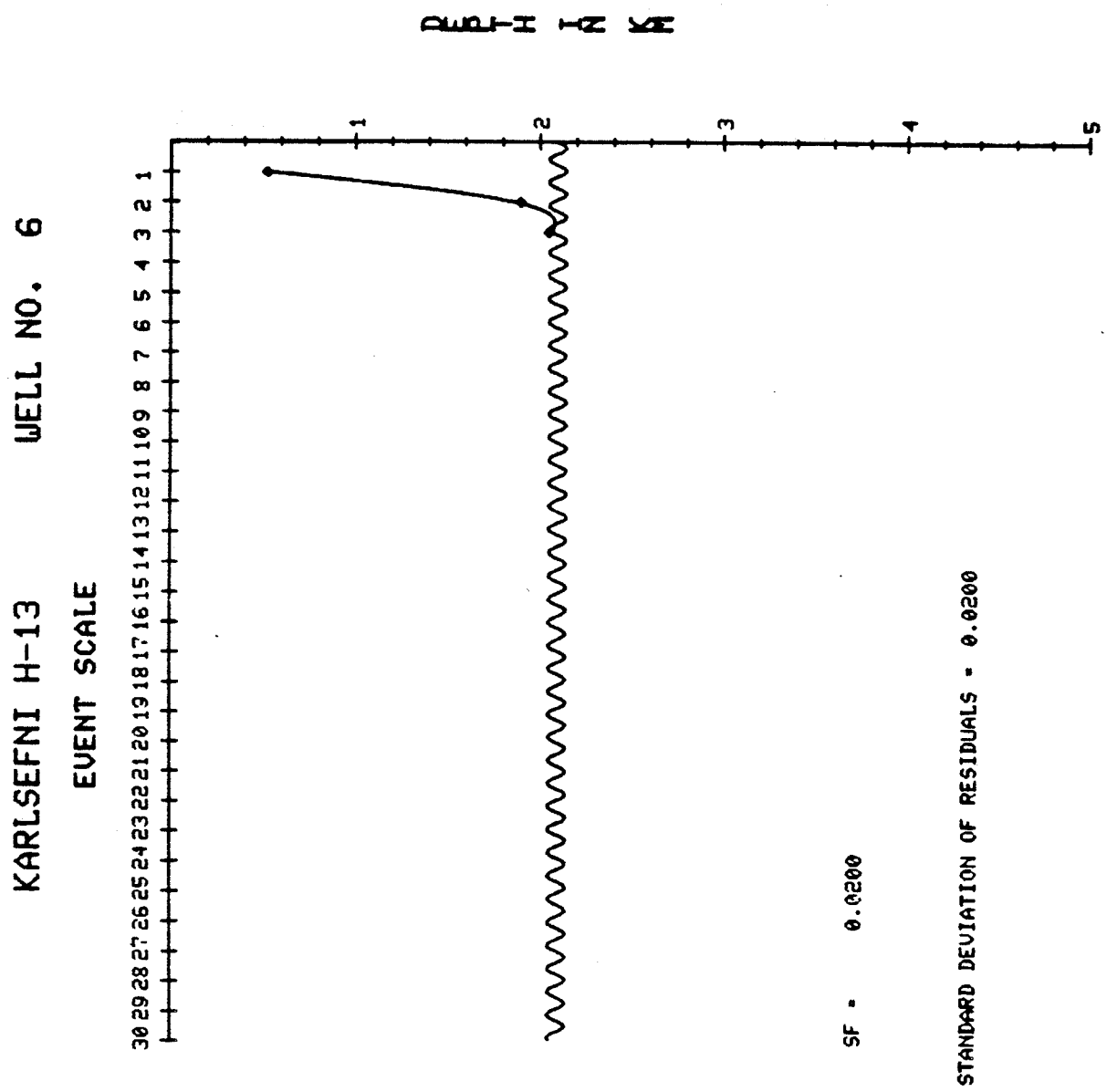
KARLSEFNI H-13
WELL NO. 6
EVENT SCALE
30 29 28 27 26 25 24 23 22 21 20 19 18 17 16 15 14 13 12 11 10 9 8 7 6 5 4 3 2 1
DEPTH IN KM
1
2
3
4
5
SF = 0.0200
STANDARD DEVIATION OF RESIDUALS = 0.0200

Display 39

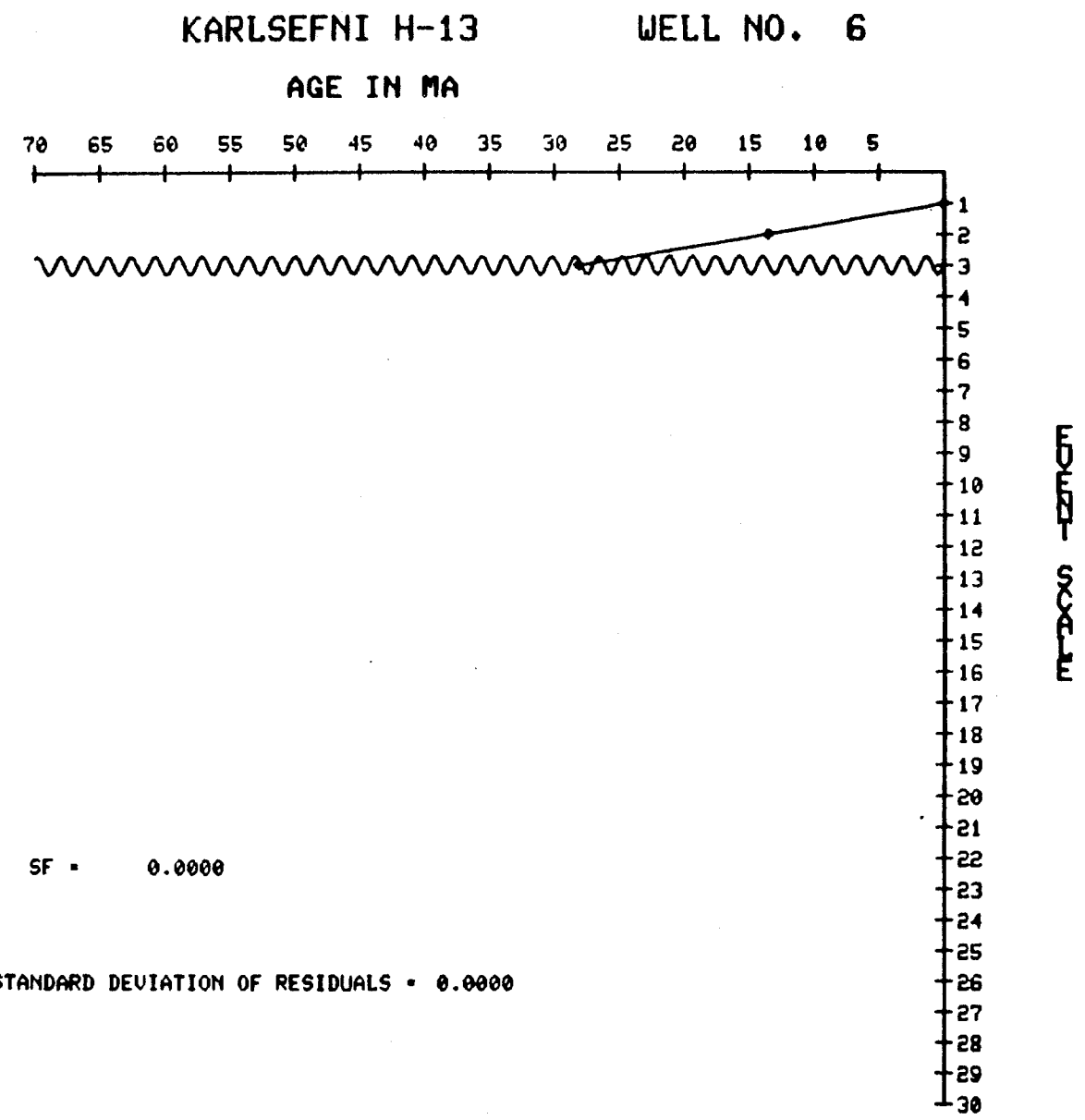
KARLSEFNI H-13 WELL NO. 6
AGE IN MA
70 65 60 55 50 45 40 35 30 25 20 15 10 5
1 2 3 4 5 6 7 8 9 10 11 12 13 14 15 16 17 18 19 20 21 22 23 24 25 26 27 28 29 30
EQUAL SCALE
SF = 0.0000
STANDARD DEVIATION OF RESIDUALS = 0.0000

Display 40

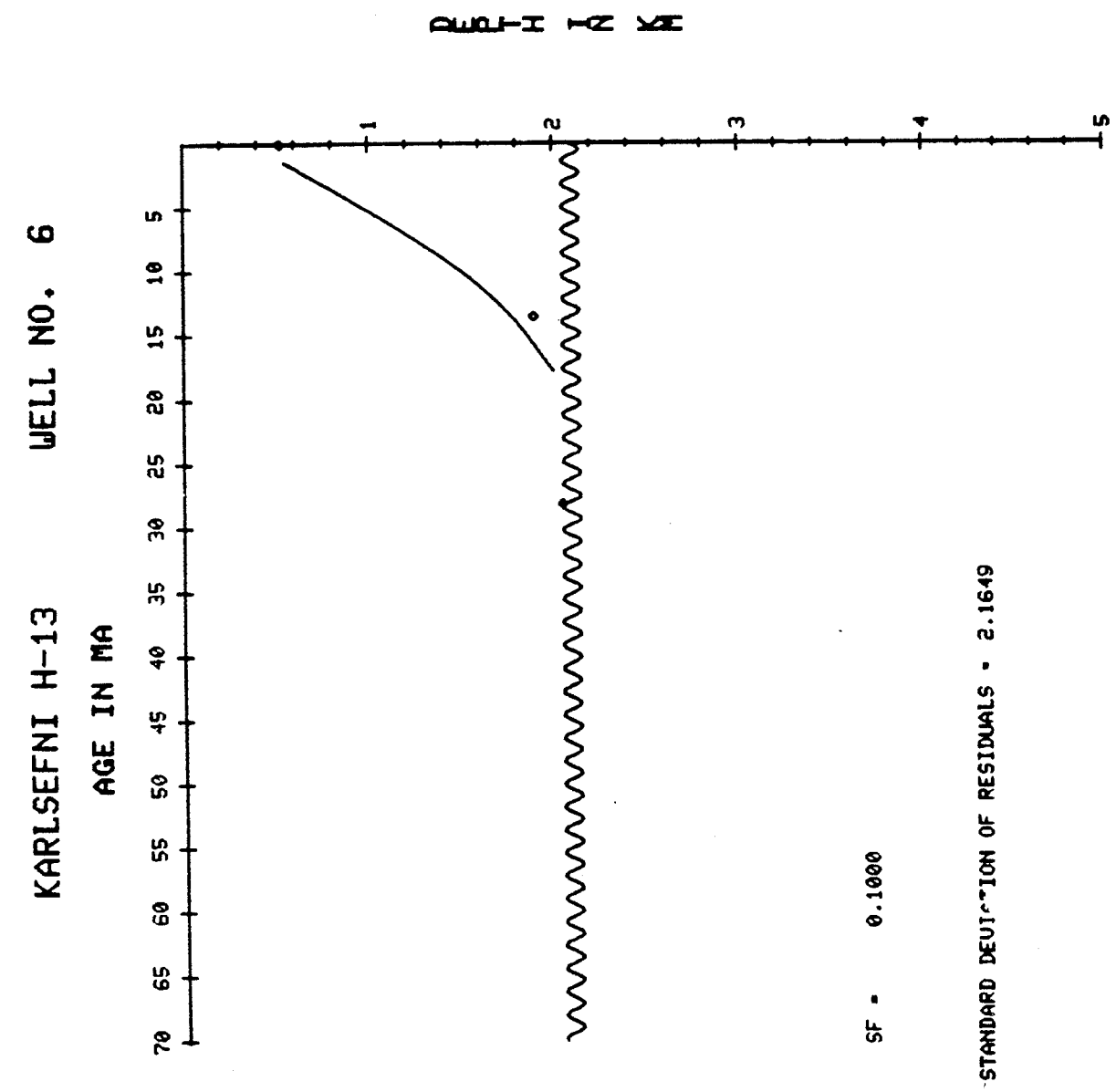
KARLSEFNI H-13
WELL NO. 6
AGE IN MA
5
10
15
20
25
30
35
40
45
50
55
60
65
70
1
2
3
4
5
DEPTH IN KM
SF = 0.1000
STANDARD DEVIATION OF RESIDUALS = 2.1649

Display 41

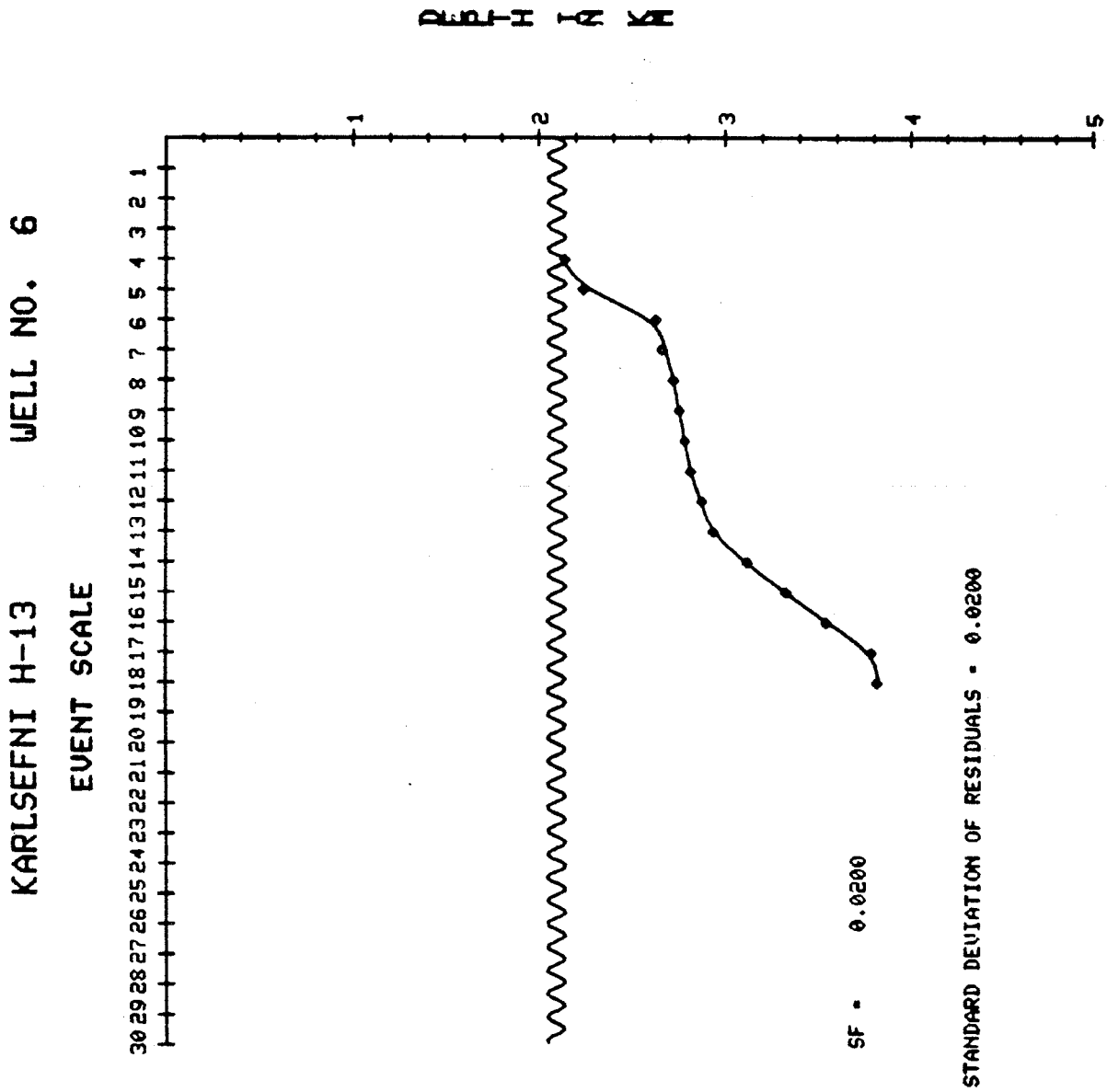
KARLSEFNI H-13
WELL NO. 6
EVENT SCALE
30 29 28 27 26 25 24 23 22 21 20 19 18 17 16 15 14 13 12 11 10 9 8 7 6 5 4 3 2 1
1
2
3
4
5
DEPTH KM
SF = 0.0200
STANDARD DEVIATION OF RESIDUALS = 0.0200

Display 42

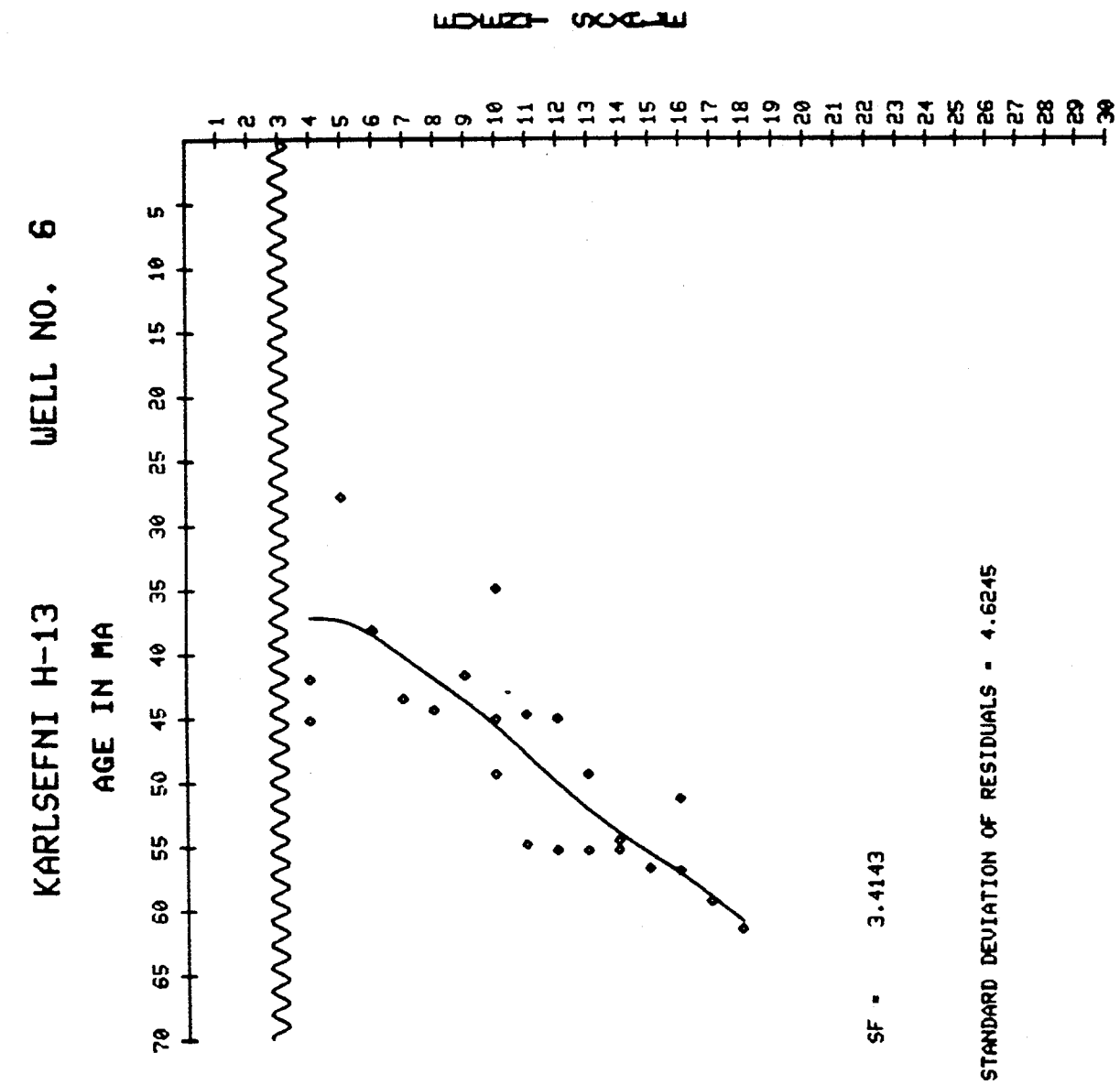
KARLSEFNI H-13
WELL NO. 6
AGE IN MA
70 65 60 55 50 45 40 35 30 25 20 15 10 5
1 2 3 4 5 6 7 8 9 10 11 12 13 14 15 16 17 18 19 20 21 22 23 24 25 26 27 28 29 30
DEP SCALE
SF = 3.4143
STANDARD DEVIATION OF RESIDUALS = 4.6245

Display 43

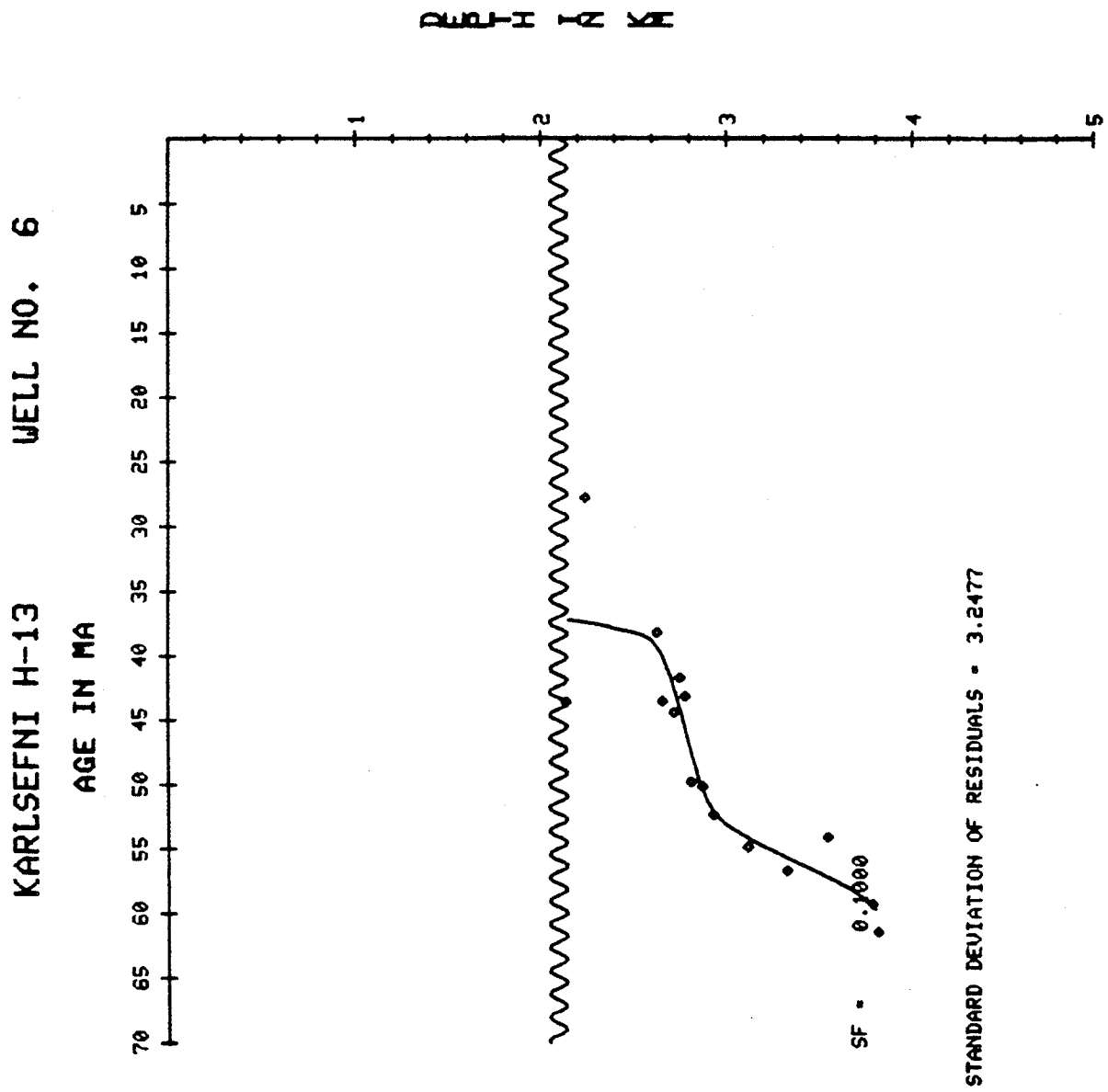
KARLSEFNI H-13 WELL NO. 6
AGE IN MA
5 10 15 20 25 30 35 40 45 50 55 60 65 70
DEPTH IN KM
1 2 3 4 5
SF = 0.1000
STANDARD DEVIATION OF RESIDUALS = 3.2477

Display 44

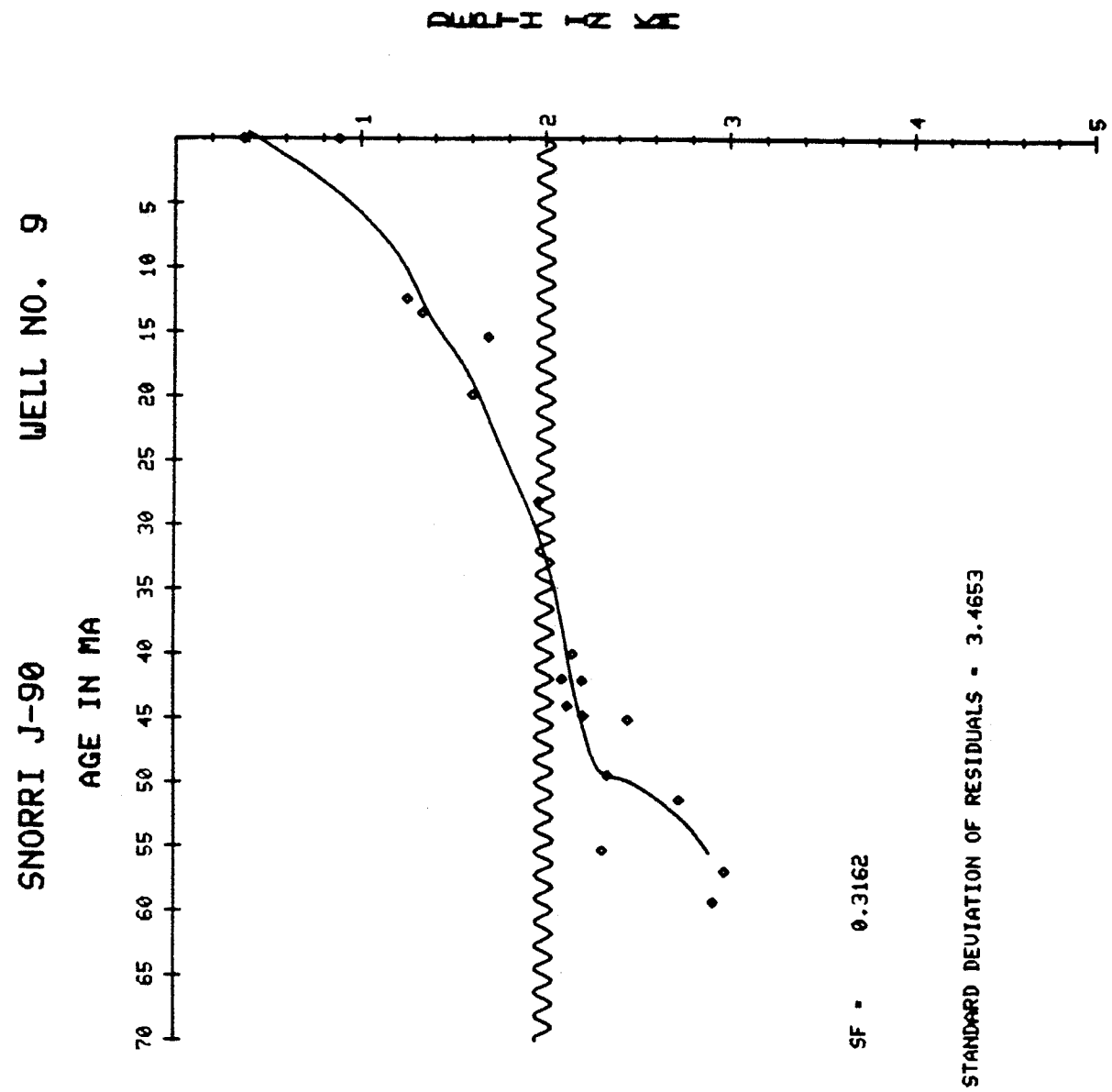
SNORRI J-90
WELL NO. 9
AGE IN MA
70 65 60 55 50 45 40 35 30 25 20 15 10 5
DEPTH IN KM
1 2 3 4 5
SF = 0.3162
STANDARD DEVIATION OF RESIDUALS = 3.4653

Display 45

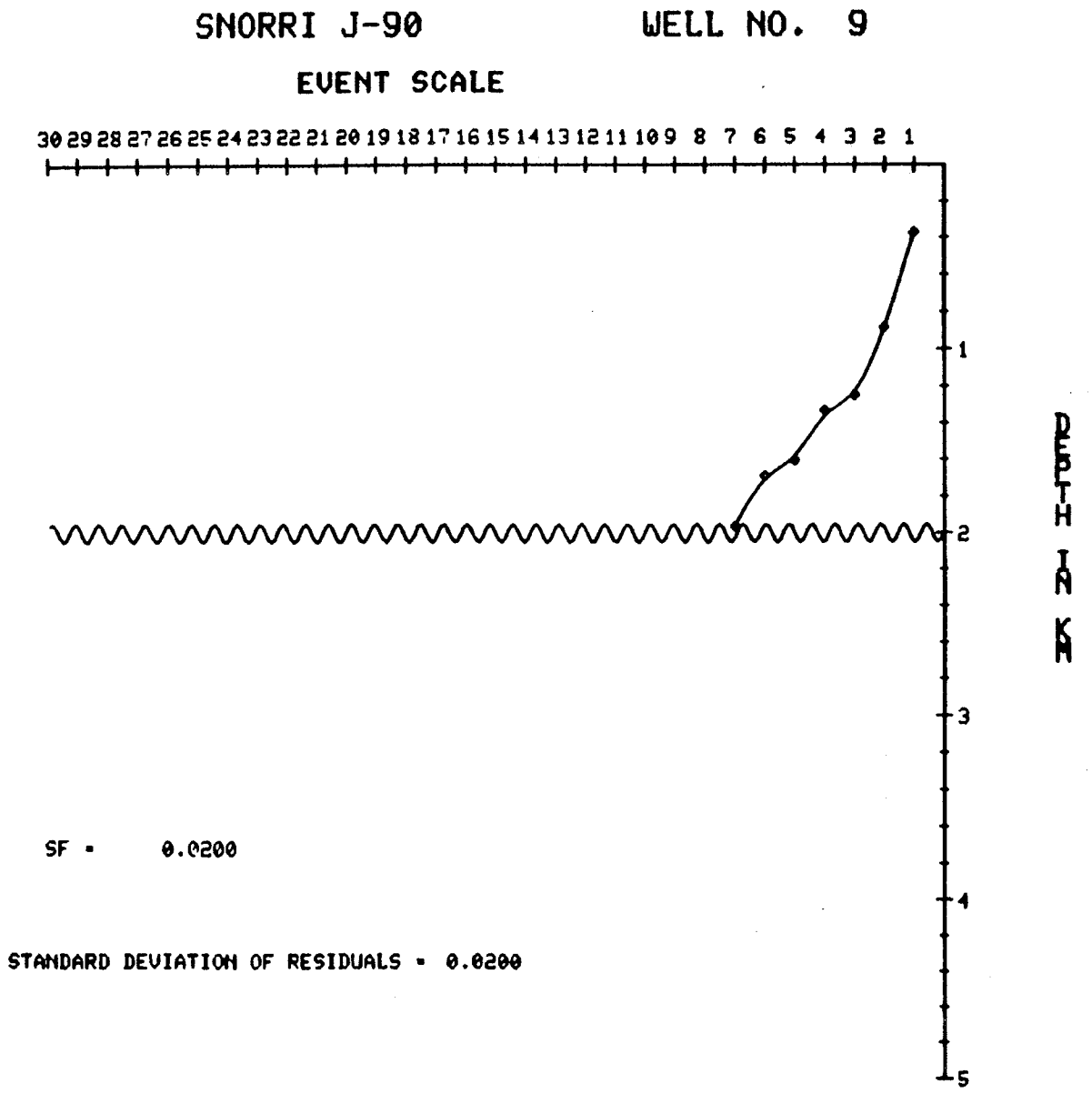
SNORRI J-90 WELL NO. 9
EVENT SCALE
30 29 28 27 26 25 24 23 22 21 20 19 18 17 16 15 14 13 12 11 10 9 8 7 6 5 4 3 2 1
1
2
3
4
5
DEPTH IN KM
SF = 0.0200
STANDARD DEVIATION OF RESIDUALS = 0.0200

Display 46

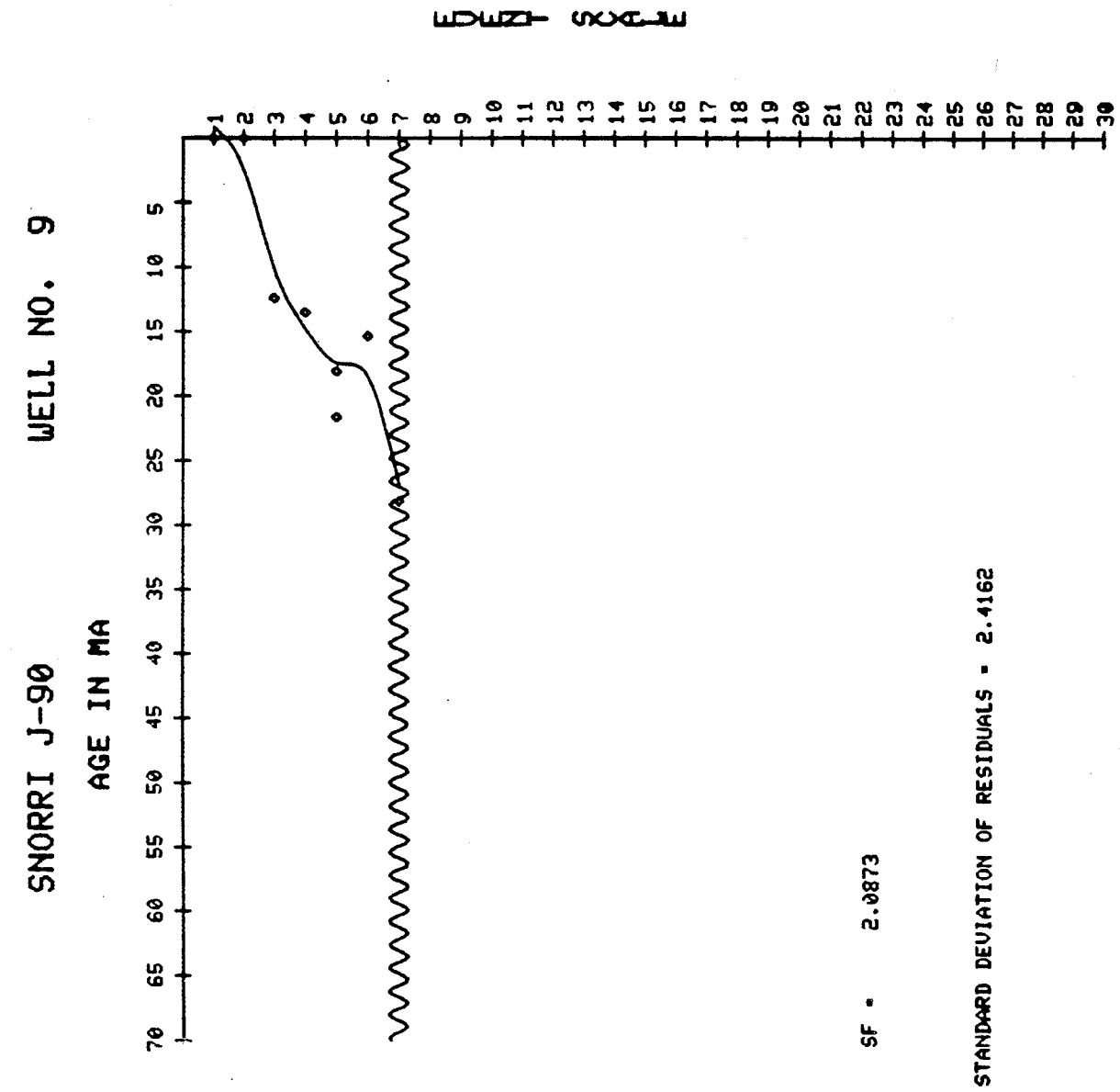
SNORRI J-90
WELL NO. 9
AGE IN MA
70 65 60 55 50 45 40 35 30 25 20 15 10 5
1 2 3 4 5 6 7 8 9 10 11 12 13 14 15 16 17 18 19 20 21 22 23 24 25 26 27 28 29 30
EDEN SCALE
SF = 2.0873
STANDARD DEVIATION OF RESIDUALS = 2.4162

Display 47

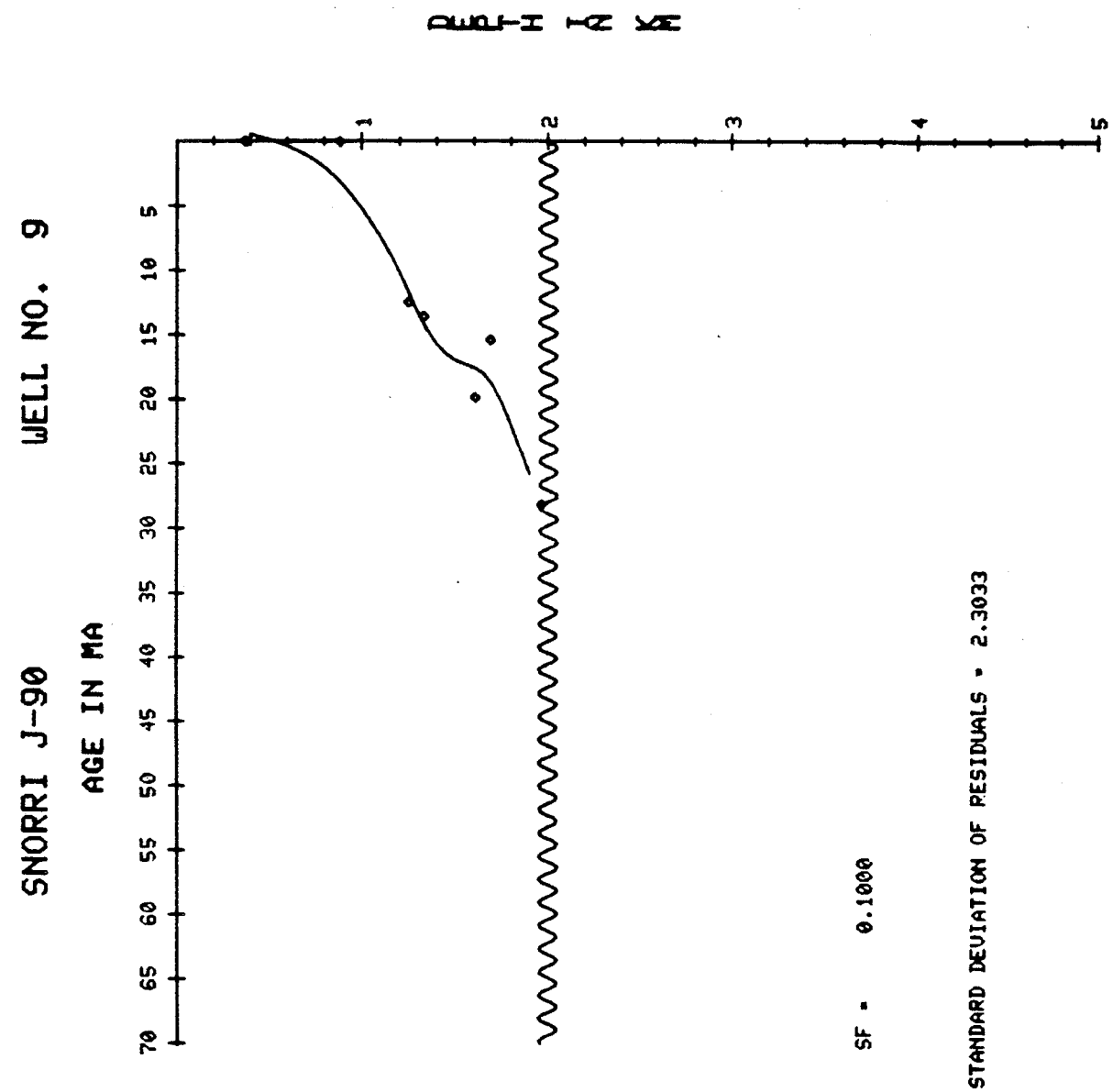
SNORRI J-90
WELL NO. 9
AGE IN MA
DEPTH IN KM
1
2
3
4
5
5
10
15
20
25
30
35
40
45
50
55
60
65
70
SF = 0.1000
STANDARD DEVIATION OF RESIDUALS = 2.3033

Display 48

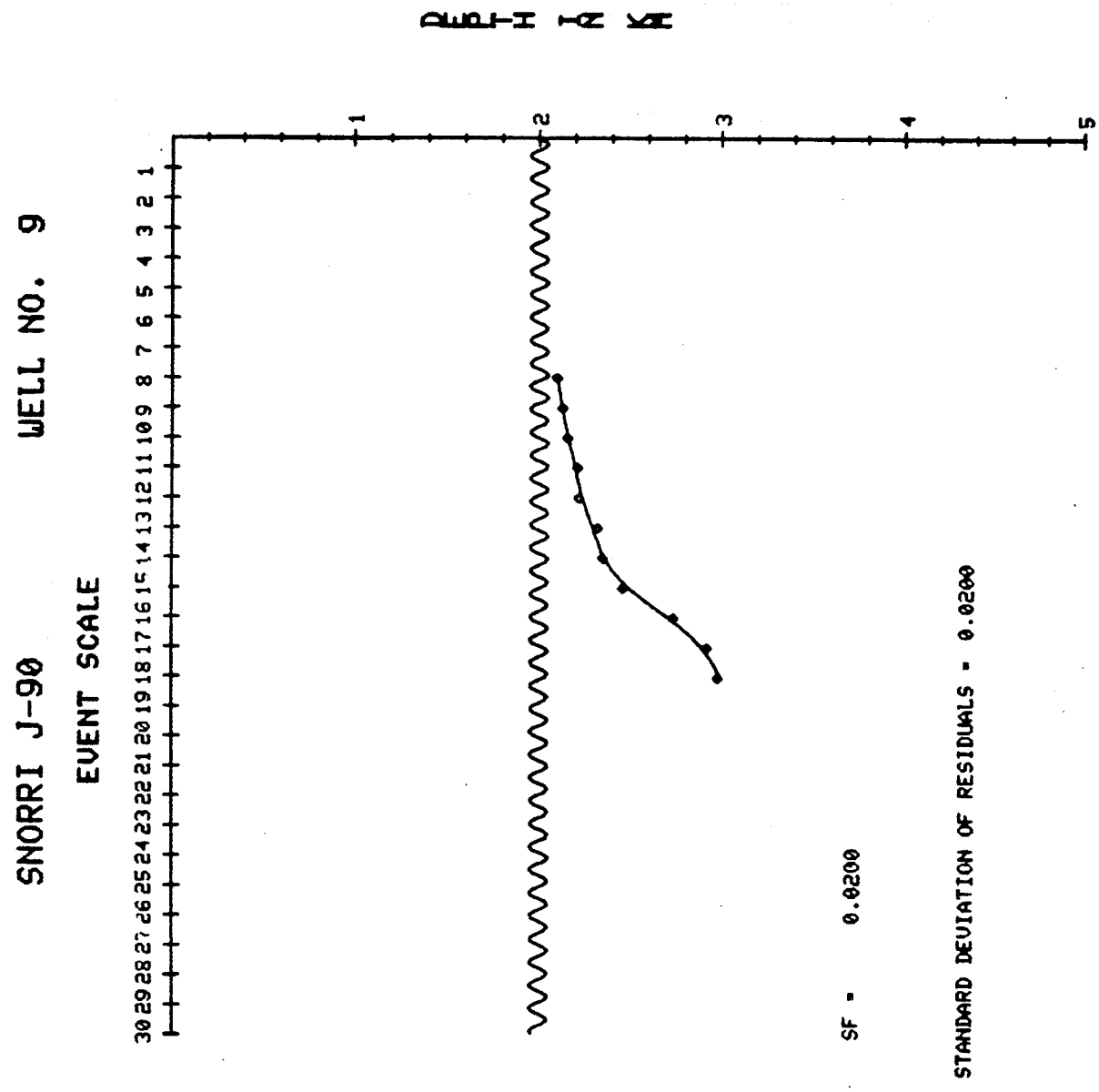
SNORRI J-90
WELL NO. 9
EVENT SCALE
30 29 28 27 26 25 24 23 22 21 20 19 18 17 16 15 14 13 12 11 10 9 8 7 6 5 4 3 2 1
PERM
1
2
3
4
5
SF = 0.0200
STANDARD DEVIATION OF RESIDUALS = 0.0200

Display 49

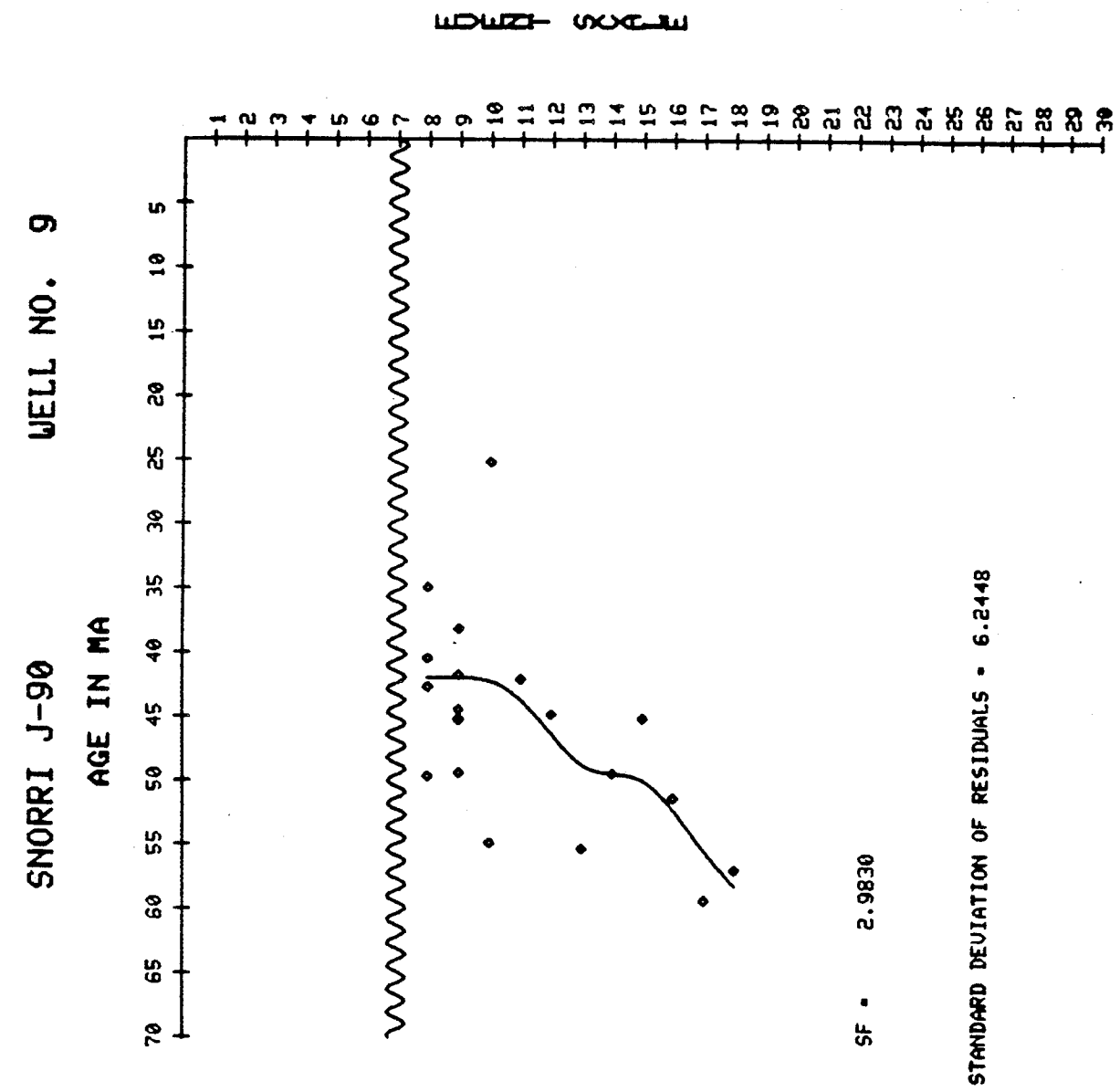
SNORRI J-90
WELL NO. 9
AGE IN MA
70 65 60 55 50 45 40 35 30 25 20 15 10 5
1 2 3 4 5 6 7 8 9 10 11 12 13 14 15 16 17 18 19 20 21 22 23 24 25 26 27 28 29 30
EDGE SCALE
SF = 2.9830
STANDARD DEVIATION OF RESIDUALS = 6.2448

Display 50

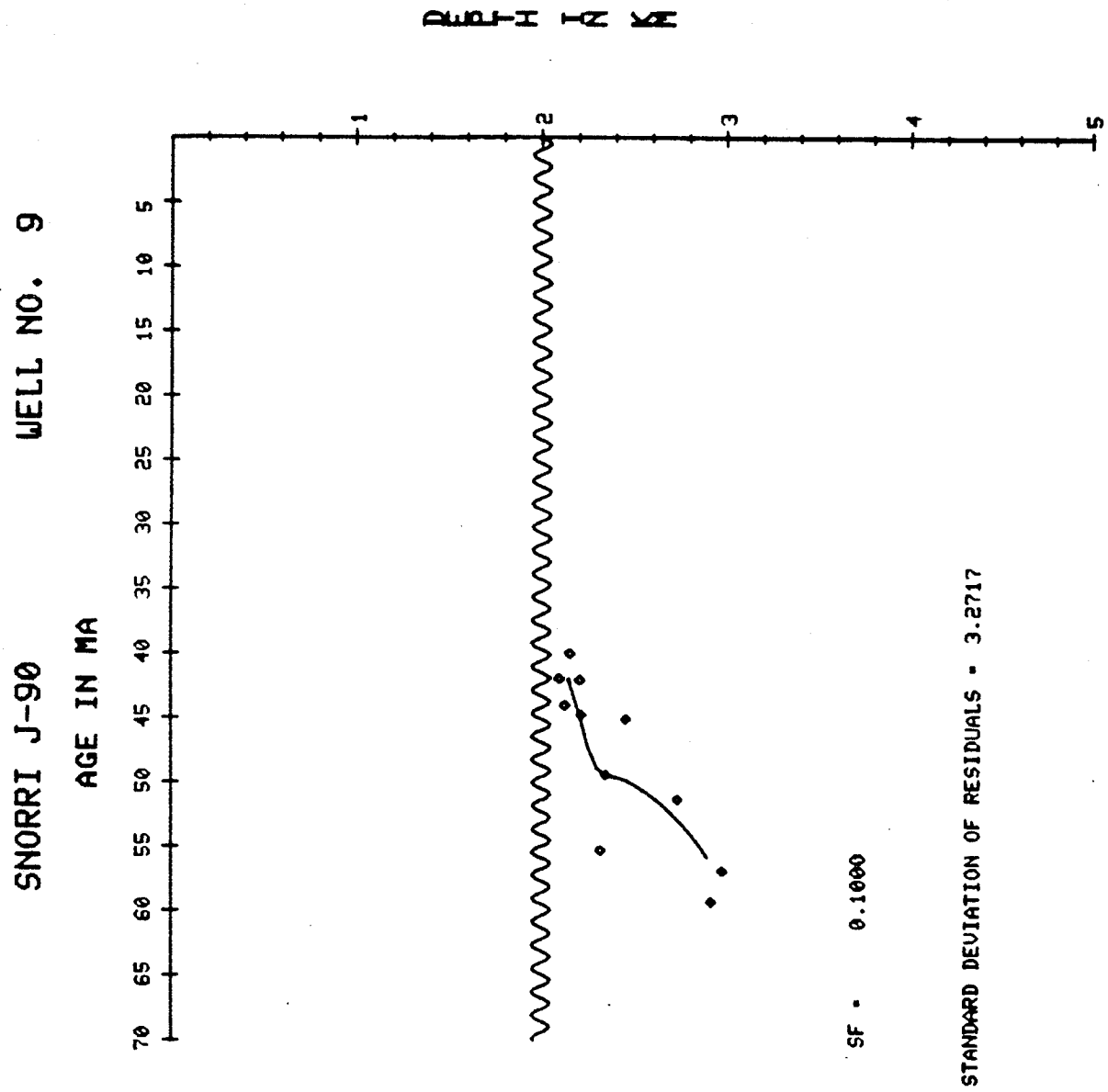
SNORRI J-90
WELL NO. 9
AGE IN MA
70 65 60 55 50 45 40 35 30 25 20 15 10 5
1 2 3 4 5
DEPTH IN KM
SF = 0.1000
STANDARD DEVIATION OF RESIDUALS = 3.2717

Display 51

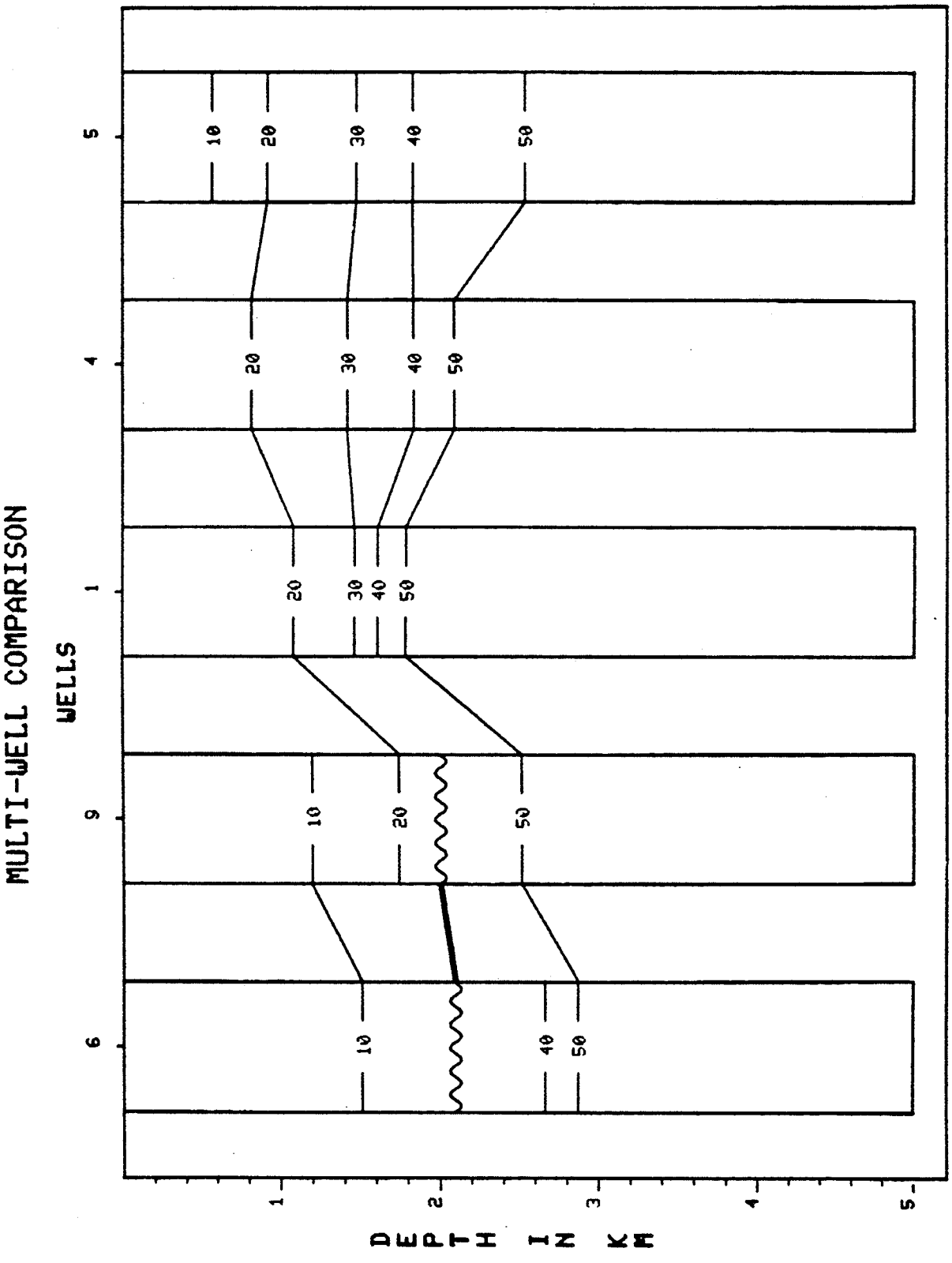
MULTI-WELL COMPARISON
WELLS
DEPTH IN KM
1
2
3
4
5
6
9
1
4
5
10
20
30
40
50

Display 52

APPENDIX 3

DOCUMENTATION OF SUBROUTINES

Subroutine AVERAGE

- finds the averaged values of CANDID for distinct values of DISTNCT
- updates DISTNCT values for averaged values of AVGED
- table of averaged values optional
- slightly different versions in Distancecasc and Optimumcasc

Subroutine AXIS

- draws the frame and the labels for the various plots
- two types of plots can be drawn:
  - origin at the bottom-lefthand corner of the screen
  - origin at upper-righthand corner of the screen
- makes use of Tektronix routines
- different versions in Distancecasc and Optimumcasc

Subroutine CIRCLE

- draws the observed points with symbols
- makes use of Tektronix and user-created routines
- versions the same in Distancecasc and Optimumcasc

Subroutine CONVERT

- draws a smooth curve by connecting the data points
- points are assumed to be already scaled into Tektronix screen points
- in general, the number of points drawn is:

$$(NUM - 1) * 10 + 1$$

- makes use of Tektronix routines
- slightly different versions in Distancecasc and Optimumcasc

Subroutine FINDSM

- finds the smallest smoothing factor that produces a non-decreasing spline fit when submitted to ICSSCU (an IMSL routine)
- makes use of a Tektronix routine, a FORTRAN function, and user-created routines
- calls FINDSM2 to try out various smoothing factors
- same version in Distancecasc and Optimumcasc

Subroutine FINDSM2

- returns yes or no to FINDSM, when asked if a smoothing factor will produce a non-decreasing spline
- performs a fine-check on the values using the first derivative
- uses IMSL and FORTRAN routines
- same version in Distancecasc and Optimumcasc

Subroutine FRAME

- draws the labels and frame background for the multi-well comparisons
- makes use of Tektronix routines
- is in the multi-well comparisons (PLOT A, PLOT B, PLOT C) of Distancecasc

Subroutine GLOBAL

- gives the global error estimation for a well
- interpolates the depth for a given age
- dependent on the first derivative of the spline
- is in multi-well comparisons in Distancecasc (PLOT A, PLOT B, PLOT C)

Subroutine LOCAL

- once the interval has been found, the interpolated depth is needed
- the interpolated point for the correct interval is computed linearly
- accumulates the information for the local error bar analysis
- is in the multi-well comparisons for Distancecasc

Subroutine INTVALS

- finds all the intervals containing the point to be interpolated, and then returns the indices for the first and last occurrence
- the correct interval is chosen in the following fashion:
  - if there are no intervals containing this point, then zeroes are returned
  - if there is only one interval containing this point, then this is the correct interval
  - if the point is found in an odd number of intervals, then the middle interval is chosen
  - for an even number of intervals, we return the indices of both the first and last interval; the calling subroutine will then use these to compute an average
  - is in the multi-well comparisons in Distancecasc

Subroutine PLOT1

- plots the optimum sequence against the event scale
- finds the positions of the fossils in the optimum sequence
- recodes the fossils, taking into account whether or not they are coeval
- uses the coeval events to average the optimum sequence
- the event scale is updated at the same time
- a cubic spline is fitted to the data by the IMSL routine ICSSCU
- computes the standard deviation of the residuals
- the graph is drawn with the points calculated from the co-efficient matrix and the fitted values generated by the subroutine ICSSCU
- this array is used to draw the smooth curve and contains:

$$(INCR - 1) * 10 + 1$$

  points

- unconformity is drawn as a sine curve if unconformity option previously chosen

- makes use of Tektronix, user-created, and mass storage routines, and indirectly uses IMSL routine ICSSCU
- is in Optimumcasc

Subroutine PLOT2

- plots RASC distances against the event scale
- recodes the fossils based upon whether they are coeval or not
- checks if any of the fossils are anomalous
- anomalies are excluded from any further manipulation in the programme and are indicated by a different symbol on the graph
- determination of anomaly is made upon inspection of the second order difference
- if its absolute value is greater than STANDEV (obtained from a special version of the RASC programme) it is declared to be anomalous
- the second-order difference is output from the special RASC
- upon removal of these events, the levels are updated to compensate for any gaps created
- the number of points computed from the spline routine used to draw the curve is:

$$(INCR - 1) * 10 + 1$$

- makes use of Tektronix, user-created, and mass storage routines
- indirectly uses ICSSCU by calling subroutine SPLINER
- is in Distancecasc
- has provisions for drawing the unconformity if one exists

Subroutine PLOT3

- plots the RASC distances against the age
- distances are averaged for distinct values of ages
- distances are sorted into ascending order for use in ICSSCU
- spline values are calculated from the C matrix and Y array of ICSSCU, yielding:

$$(INCR - 1) * 10 + 1$$

  points to be used for the curve
- makes use of Tektronix, user-created routines and indirectly uses ICSSCU
- is in Distancecasc

Subroutine PLOT4

- plots the depth scale in km against the event scale
- reads in the depths from the mass storage file (TAPE22)
- converts the depths from metres into kilometres
- fits a cubic spline to the data using ICSSCU
- obtains

$$(INCR - 1) * 10 + 1$$

  points for the curve
- computes the standard deviation of the residuals
- draws the graph and the curve
- makes use of Tektronix, user-created, mass storage routines and, indirectly, IMSL routine ICSSCU for the spline

- slight differences between Distancecasc and Optimumcasc versions
- mechanism for redrawing the plot immediately, if curve is unsatisfactory
- draws the unconformity if one exists

Subroutine PLOT5

- plots age against depth in km for Distancecasc
- plots optimum sequence against depth in km for Optimumcasc
- for regular increments of depths (0.05 km), an age or optimum sequence scale is obtained through interpolation (depending on which version of CASC is used)
- scaling is done on the user points to obtain Tektronix screen points
- the graph is drawn using the 150 points computed in the interpolation
- the technique is basically the same in Distancecasc and Optimumcasc with only small differences
- makes use of Tektronix and user-created routines
- draws unconformity if one exists

Subroutine PLOT6

- plots age against depth in km for Distancecasc
- plots optimum sequence against depth in km for Optimumcasc
- age values or optimum sequence values (depending on which CASC is used) are obtained at regular intervals of depth (Every 0.05 km)
- a cubic spline is fitted with 150 values
- the standard deviation of the residuals is computed
- the minimum and the maximum of the fitted values from ICSSCU are found
- information for the multi-well comparisons is stored at this point for both Distancecasc and Optimumcasc
- different versions in Distancecasc and Optimumcasc
- makes use of Tektronix, user-created, IMSL, and mass storage routines
- clusters may be defined and drawn, if this option is selected
- unconformity option available using three methods:
    - make an event the unconformity
    - put an unconformity between two events
    - choose unconformity with cursor

Subroutine PLOT7

- produces multi-well comparison for Optimumcasc
- the choice of wells and fossils is up to the user
- a maximum of five wells and ten fossils is permitted
- original dictionary numbers for the fossils are used
- the option for local error bar analysis is available
- if a fossil is chosen but not found in one of the wells requested, then that well is skipped and the next well is processed
- makes use of Tektronix and mass storage routines
- draws unconformities as sine curves
- is in Optimumcasc

Subroutine PLOT9

- plots age against the event scale
- converts RASC distances into ages in millions of years
- the ages are averaged
- a cubic spline is fitted yielding

$$(INCR - 1) * 10 + 1$$

  points for the curve
- the standard deviation of the residuals is computed
- mechanism available for doing the plot over immediately if the curve is unsatisfactory
- makes use of Tektronix routines, user-created routines, mass storage and indirectly IMSL routine ICSSCU
- is in Distancecasc

Subroutine PLOT10

- plots the inverse of the first derivative against the event scale
- the interpolation algorithm uses the co-efficients generated by ICSSCU in PLOT9
- 150 points are computed to draw the curve
- makes use of Tektronix and user-created routines
- this subroutine is an optional one
- is in Distancecasc

Subroutine PLOT13

- plots the rate of sedimentation
- 150 points are generated through the interpolation of the curve
- the depths increase regularly by 0.05 km against values of the first derivative
- if the value is greater than 10.0, it is set to 10.0
- makes use of Tektronix and user-created routines
- this subroutine is an optional one
- is in Distancecasc

Subroutine PLOTA

- plots multi-well comparison for Distancecasc
- the user can choose a maximum of five wells
- an age interval (in MA) is picked by the user
- two choices are then available to the user:
  - a plot if the age interval is at least 10 MA
  - a table of ages and depths for any age interval
- error analysis can be applied in one of three ways:
  - local estimation
  - local and global estimations
  - no error analysis
- the necessary data are read from the mass storage file
- for each chosen age interval, an interpolated depth is found

- unconformities, if present are represented by a sine curve if the graph option is chosen (Likewise for PLOTB and PLOTC)
- makes use of Tektronix, user-created, and mass storage routines

Subroutine PLOTB

- plots multi-well comparison for Distancecasc
- three kinds of error analysis (local, local and global, or none)
- reads from mass storage
- checks if ages are less than 70 MA
- finds a distance for each fossil, converts the distance to an age, and obtains an interpolated depth for the age
- writes a table of fossils, depths, and error estimates to TAPE23

Subroutine PLOTC

- plots multi-well comparisons for Distancecasc
- the user has a choice of wells and age boundaries
- a maximum of five wells and five ages is allowed
- ages must be entered in increasing order or else an error will be generated in the graph
- the following options are available:
    - local error bar analysis
    - local and global error bar analysis
    - no error bar analysis
    - pattern scheme
- the necessary information is read from the mass storage file
- the proper interval is found and the point is interpolated within the interval
- unconformities of various wells are represented by sine curves in wells
- makes use of Tektronix, user-created, and mass storage routines

Subroutine RECODE

- recodes events to another level
- if events are coeval, they are assigned to the same level
- a table of the events and their new levels is printed
- same versions in Distancecasc and Optimumcasc

Subroutine SCALE

- scales user-points into Tektronix screen units
- origins and lengths of graphs are constants
- the subroutine does not destroy the original values
- formula:

Tektronix co-ordinate = Tek. origin - ((Tek.axis length/number of subdivisions in axis) * user co-ordinate)

- different versions in Distancecasc and Optimumcasc

Subroutine SDEVER

- calculates the standard deviation of the residuals
- uses Tektronix routines
- same version in Distancecasc and Optimumcasc

Subroutine SHAPER

- prints out the shape or smoothing factor for the graph
- makes use of Tektronix routines
- same version in Distancecasc and Optimumcasc

Subroutine SMOOTH

- implements the smoothing factor option
- the shape entered overrides the default
- this value is squared to be in a usable form for ICSSCU; later, the square root of the value is printed
- same version in both Distancecasc and Optimumcasc

Subroutine SPLINER

- fits a cubic spline to the data points
- the spline routine is from the IMSL Library and is called ICSSCU
- if NX points are given, then

$$(NX - 1) * 10 + 1$$

  points are calculated from the co-efficient matrix and the fitted values
- this number of points seems to give a smooth curve in most cases
- a terminal error will be indicated if the independent values are not in ascending order
- the Y array (the fitted values) and the input values are very similar
- makes use of Tektronix routines
- same version in Distancecasc and Optimumcasc

Subroutine STORE

- this subroutine reads in all the input data and places them in the mass storage file if necessary
- the depths can be entered in feet or in metres
- if there are in feet, they are converted into metres
- the final value stored in mass storage for the depths is calculated as:

(depth in metres) - (rotary table height)

- makes use of mass storage routines and puts all the information needed into TAPE22
- slight differences between versions in Distancecasc and Optimumcasc

Subroutine TABLE

- prints a list of all well names, and numbers them sequentially starting at 1 (a well is always referred to by this number)
- reads from the mass storage file, TAPE22, to get the name of the well
- slightly different versions in Distancecasc and Optimumcasc

Energy, Mines and Resources Canada
Énergie, Mines et Ressources Canada